

FUNCTIONALIZED LUCIFERINS FOR APPLICATIONS IN SUPRAMOLECULAR  
CHEMISTRY: DEVELOPMENT TOWARDS *IN VIVO* LIGHT SWITCHES

A THESIS SUBMITTED ON THE 2ND DAY OF MAY 2017

TO THE DEPARTMENT OF CHEMISTRY  
IN PARTIAL FULFILLMENT OF THE REQUIREMENTS  
OF THE SCHOOL OF SCIENCE AND ENGINEERING  
OF TULANE UNIVERSITY

FOR THE DEGREE OF  
MASTERS OF SCIENCE IN CHEMISTRY

BY



Harrison Patrick Rahn

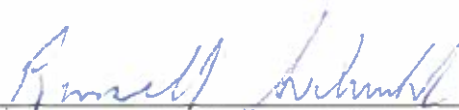
APPROVED BY:



Dr. Janarthanan Jayawickramarajah, PhD



Dr. Bruce C. Gibb, PhD



Dr. Russell H. Schmehl, PhD



## **Acknowledgements:**

Firstly, I would like to acknowledge the contribution of several of my mentors throughout my Tulane career, Bruno Ghersi, Gyan Aryal, Berk Atuk, Nick Ernst, Shane McGlynn and Cooper Battle. Dr. Battle inspired me to pursue the work in this thesis and a Master's degree. These graduate students and post-doctoral researchers trained, inspired, and befriended me in my short time at Tulane. For that I am very grateful.

Secondly, I would like to acknowledge the mentoring outside the classroom by Dr. Kyriakos Papadopoulos and his students in the realm of Karate. Karate has been one of the two things keeping me moderately sane throughout my Tulane experience alongside music, for which I would like to thank Mr. Mendel Lee for his support of the Tulane University Marching Band's many growing endeavors and my personal musical pursuits.

Thirdly, I would like to thank my friends, Andrew R. Crawford, Michael S. Hawke, and Nathan L. Sanders for their companionship through many sleepless nights, whether due to shenanigans or pressing academic work; through blissful ups and near terminal downs. These people have made my time at Tulane unforgettable and have filled my early adulthood with stories that I will remember for a lifetime. Along with these people, I must also acknowledge my family for their omnipresent support of my many pursuits in life.

Lastly and most importantly, I would like to thank Dr. Janarthanan Jayawickramarajah for both mentoring and advising me through my undergraduate career and into the start of my graduate career. His many letters of support and many "you should stop by my office" 's have been keys to not only my success at Tulane but also success proceeding forward as a graduate student and beyond. His initial offer to work with him was tempting and the prospect of something new and exciting enticed me into chemical research and later convinced me to join the major, beginning the first focused, long term, pursuit of knowledge in a specific field I have undertaken. And thus, to both my very first and very last professor at Tulane University, thank you.

## Table of Contents:

Chapter 1: Introduction .....	1
Chapter 2: Characterization of Luciferin-CB[7] Host-Guest Interaction	
2.1 Results and Discussion .....	11
2.2 Conclusions .....	21
2.3 Experimental.....	23
Chapter 3: Synthetically Functionalized Luciferins as Enzyme Substrates	
3.1 Luciferin Analogues as Substrates for Firefly Luciferase .....	25
3.2 Ether Functionalized Luciferin Analogues as <i>in vitro</i> Probes for Host-Guest Chemistry With CB[7].....	31
3.3 An Ester Functionalized Luciferin Analogue as <i>in vitro</i> Probes for Host-Guest Chemistry With CB[7].....	36
3.4 Experimental.....	46
References.....	50
Supporting Information	
SI.1 Synthesis of Functionalized Luciferins.....	SI-1
SI.2 NMR Spectra of Study Species.....	SI-11
SI.3 Absorbance Spectra Monitoring of Host-Guest Complexation .....	SI-33
SI.4 NMR Spectra of Study Species and CB[7].....	SI-40
SI.5 Enzyme assays .....	SI-43

## List of Figures, Schemes, and Tables

### *Figures*

CB[7] and Common Guests.....	2
------------------------------	---

Naturally Occurring Luciferins.....	3
Oxidation Mechanism of Firefly Luciferin.....	4
Production of firefly luciferase substrates from “caged” precursors.....	6
Labeled Carbon Positions of Luciferin.....	6
Luciferin analogues.....	7
Normalized Absorbance of luciferin and its derivatives.....	11
Structure of assay buffer components.....	12
Normalized Absorbance of Luciferin and Luciferin adamantanoate ( <b>XII</b> ).....	15
NMR Titration of Luciferin with CB[7] .....	18
NMR Titration of Luciferin-triazole-adamantane ( <b>VIII</b> ) with CB[7] .....	19
NMR Titration of Luciferin-adamantanoate ( <b>XII</b> ) with CB[7] .....	20
Crystal Structure of Luciferin and its active site.....	26
Determination of integrated bioluminescence and reaction velocity from the raw data kinetic curve.....	26
Bioluminescent output of Luciferin and Analogues.....	28
Bioluminescent spectra of Luciferin and Analogues.....	30
Bioluminescent output of Cationic Luciferins titrated with CB[7].....	33
Bioluminescent output of “Click” Luciferins titrated with CB[7].....	34
Absorbance and Fluorescence of Luciferin and Luciferin Adamantanoate ( <b>XII</b> ).....	37
Michaelis Menton Plot of Luciferin Adamantanoate ( <b>XII</b> ) and Porcine Liver Esterase....	38
Determination of reaction velocity from the raw data kinetic curve.....	39
Inhibition of Porcine Liver Esterase with CB[7].....	40
Porcine Liver Esterase Cleavage of <i>p</i> -Nitrophenol acetate.....	40

Reactivation of Bound complex by addition of Adamantyl Trimethylammonium.....	41
Bioluminescent Monitoring of Luciferin-adamantanoate ( <b>XII</b> ):CB[7] complex.....	42
Reactivation of Bound complex by addition of Adamantyl Trimethylammonium.....	43

*Schemes*

General Supramolecular Caging of Luciferins.....	9
Summary Synthetic Scheme .....	10
Supramolecular Caging of Ether Luciferins.....	31
Supramolecular Caging of Ester Luciferins.....	36
Synthesis of Cationic Luciferins .....	SI-1
Synthesis of “Click” Luciferins.....	SI-1
Synthesis of Luciferin-adamantanoate ( <b>XII</b> ) .....	SI-2

*Tables*

Binding constants as determined by UV-vis spectrometry .....	16
Luminescent output of Luciferin and Analogues.....	29

## Chapter 1: Introduction

Supramolecular chemistry is the study of how molecules interact non-covalently with each other. The field started in non-polar solvents with low dielectric constants such as chloroform, but the most important solvent to medicine and life is water. Because of the interactions of dipoles and small molecules characteristic to polar solvents, supramolecular chemistry in nonpolar solvents and in water is very different.<sup>[1]</sup> In particular, supramolecular interaction in water is governed by the poorly understood but very useful Hydrophobic Effect. The Hydrophobic Effect is observed when hydrocarbon containing moieties such as adamantyl or lipid groups assemble in ways that exclude water, resulting in an energetically favorable arrangement.<sup>[1][2]</sup> This is well documented in the formation of micelles, liposomes, and guest-host complexes with cavity containing molecules such as cucurbit[7]uril.<sup>[1][2][3]</sup> In the special case of cucurbit[n]urils (and similar molecules), the hydrophobic moieties are driven to associate within the non-polar cavities of the water soluble hosts, reversibly linking the host and guest.

In this series of studies, the candidate investigated the binding of several relatively inert, aliphatic, polycyclic moieties and their binding to cucurbit[7]uril, hereto referred to as CB[7] (See Figure 1.1B). Cucurbit[n]urils are synthesized from the acid-catalyzed condensation reaction of glycouril and formaldehyde.<sup>[1][4]</sup> Different *n*-mers, containing different numbers of glycourils, have different cavity sizes by increasing the diameter of the portals while maintaining a consistent depth of  $\sim 9.1$  Å. In particular CB[7] and CB[8] have volumes of  $279$  Å<sup>3</sup> and  $479$  Å<sup>3</sup>, respectively.<sup>[1][2][5]</sup> Cucurbiturils of  $n \leq 7$  can form 1:1 complexes with one host per one guest moiety (Figure 1.1A), but larger cucurbiturils of  $n \geq 8$  have potential to form ternary complexes in a well-designed system.<sup>[1][5]</sup>

Typically, host-guest complexation is characterized by changes in enthalpy, entropy, and Gibb's free energy. Furthermore, Gibb's free energy is directly related to the binding constant,  $K_a$ , the proportion of host-guest complex with respect to free guest and free host at equilibrium.<sup>[1][3]</sup> From standard binding assays in pure water, the binding interaction of CB[7] to guests shown in figure 1.1C has been determined to vary from  $K_a \approx 10^{14} \text{ M}^{-1}$  in adamantyl ammonium chloride to  $K_a \approx 10^5 \text{ M}^{-1}$  for *N,N*-dimethyl-DABCO. *N*-methyl Quinuclidinium is known to have a  $K_a \approx 10^9 \text{ M}^{-1}$ .<sup>[3]</sup> Some of the best guests contain a positive charge away from their aliphatic region which has a favorable enthalpic interaction with the electronegative carbonyls at the cucurbituril portals.

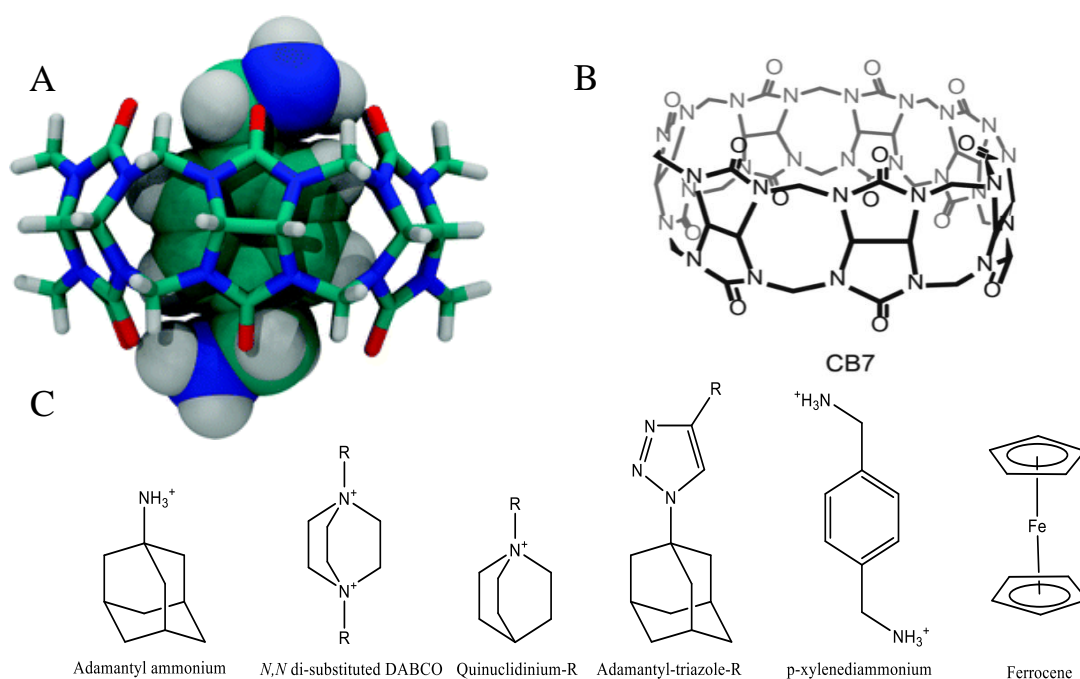


Figure 1.1: A) Structures of CB[7] para-xylenediammonium encapsulation complex.<sup>[27]</sup> There is favorable electrostatic interaction between the carbonyl-ringed portals of CB[7] and the positively charged ammoniums of the guest. B) Structure of CB[7]. C) Structure of common CB[7] guests. Often these guests have large, conformationally restricted, aliphatic regions and electropositive moieties.<sup>[3][4]</sup>

Cucurbiturils and their derivatives have been used for applications requiring strong host-guest affinity such as solubilizing pharmaceuticals and assembly of functionalized nanoparticles.<sup>[2][4]</sup> With respect to pharmaceuticals, a CB[7] derivative was used to enhance



the stability and activity of insulin. To solubilize insulin, a CB[7] derivative containing an azide was “clicked” to a strained alkyne containing a polyethyleneglycol (peg) substituent. The CB[7] conjugate has a strong affinity for the N-terminal non-polar amino acids so when mixed with insulin in solution GPC and MALDI-MS showed the formation of the protein:CB[7]-peg complex which had enhanced stability with respect to aggregation and showed better regulation of blood sugar in diabetic mice.<sup>[2]</sup> Membrane fishing using CB[7] was performed using CB[7] immobilized on sepharose beads. To fish membrane bound proteins, the bead was added to a complex mixture of ferrocene functionalized proteins from fetal bovine serum. The formation of the CB[7]:ferrocene complex bound the proteins of interest to the beads. Release from the beads was performed using a strong CB[7] binding guest and the proteins were release for analysis.<sup>[2]</sup> These are two example of the many applications CB[7] has found in biologically relevant research though many more exist.<sup>[2][4]</sup>

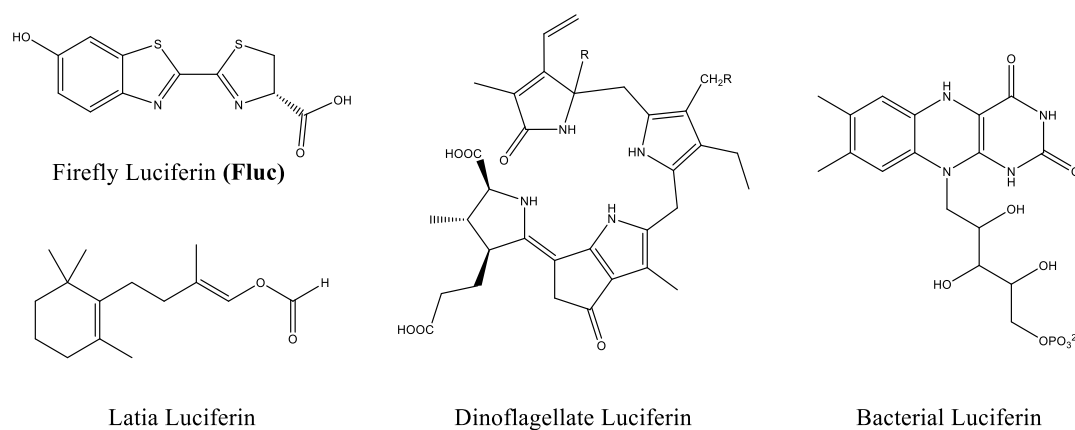


Figure 1.2: Naturally occurring luciferins.

Luciferins (Figure 1.2) are a wide class of substrates for luciferase enzymes that, upon undergoing a reaction, emit a photon to transition from an excited state to a ground state. In nature, luciferin-luciferase systems are found in a wide variety of organisms,

ranging from annelids, cnidarians, chordates, crustaceans, bacteria, dinoflagellates, and insects.<sup>[6]</sup> Luciferases from these groups rarely share sequence or structural homology, suggesting an independent origin of these enzymes. Often this form of bioluminescence is oxidative and facilitated by a cofactor such as  $\text{Ca}^{2+}$  or adenosine triphosphate (ATP). These reactions serve diverse purposes such as defense, predatory lures, or signaling.<sup>[5]</sup>

This study will focus on firefly luciferin, further referenced as simply “luciferin”, because of its prolific use in cellular assays, and ease of synthesis. Luciferin produced by the family of insects Lampyridae, is a heterocyclic molecule and is most well-known because of its use by fireflies to give their signature periodic glow <sup>[6][7][8][9]</sup>. The luciferin molecule undergoes peroxidation and radical rearrangement to yield excited oxyluciferin after reacting with magnesium, ATP, and of course luciferase (see Figure 1.3). The oxyluciferin then decays to a non-excited state by emission of a photon with a color in the range of red to yellow green. The mechanism for this reaction is depicted in Figure 1.3. <sup>[10]</sup>

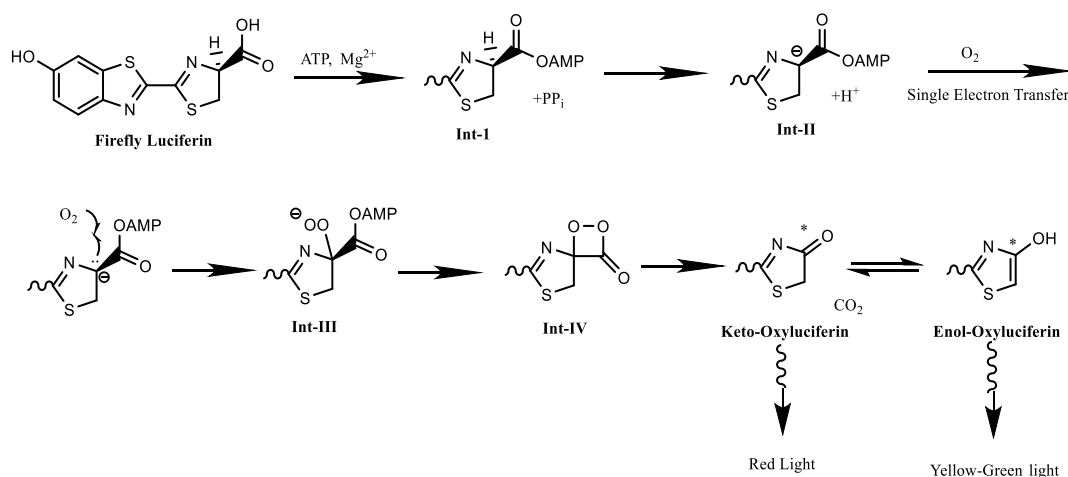
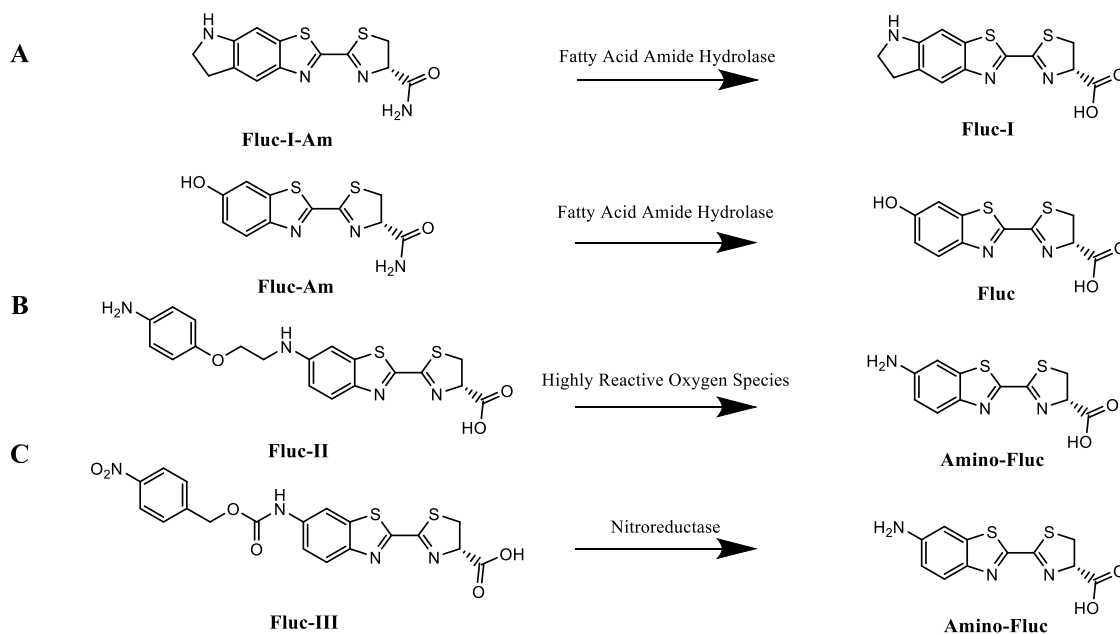
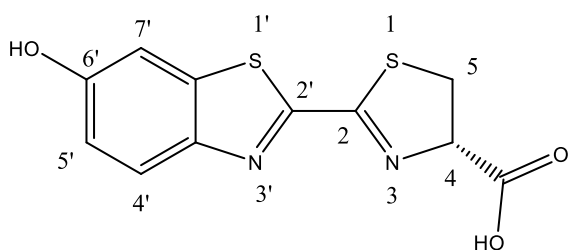


Figure 1.3 (Reproduced from Close et. al.)<sup>[28]</sup>: Mechanism for firefly luciferin oxidation and photon emission: Luciferin’s carboxylic acid displaces a pyrophosphate from ATP to yield **Int-I**. **Int-I** is then deprotonated  $\alpha$  to the carbonyl by a general base to yield **Int-II**. Molecular oxygen and the carbanion undergo a single electron transfer resulting in a four-member ringed intermediate (**Int-IV**). A rearrangement to lose  $\text{CO}_2$  gives the excited oxyluciferin which can relax from the keto-form to give a lower energy red photon, or from the enol form to give a yellow-green photon, which is the predominant emission.

Because the luciferin-luciferase system is highly specific with regard to substrates and reagents, and has a high quantum yield, it has been used in many biomedical applications. For instance, because of the necessity of both ATP and  $Mg^{2+}$  for oxidation of luciferin, the luciferase assay can be used to detect these cofactors.<sup>[6][7][8]</sup> In a recent study, modified D-luciferin was used to demonstrate *in vivo* activity of fatty acid amide hydrolase (FAAH), by replacing the carboxylic acid functionality with an amide, rendering it inert to luciferase. Rendering a luciferin-analogue inert to luciferase is the concept of “caging.”<sup>[11]</sup> Upon reacting with FAAH, the amide is converted to a carboxylic acid and the luciferin becomes a substrate for luciferase (Figure 1.4A). The subsequent emission of light allows for the system to be used as a reporter for FAAH activity. This type of caging contributes to selectivity of the reporting because both luciferin localization and the enzyme activity are limiting to a signal release.<sup>[12]</sup> Another way to cage luciferin is by electron withdrawing functionalization of the 6'-hydroxyl unit. Functionalization of the 6'-hydroxyl with a labile linker creates a luminescent reporter for the cleavage of the O-R linkage.<sup>[11]</sup> When a reaction occurs that releases free luciferin, it becomes a substrate for luciferase, resulting in photon emission, which can be used to study both reaction rates and localization.<sup>[11][12]</sup>



*Figure 1.4* : Production of firefly luciferase substrates from “caged” precursors. A) amides are hydrolyzed by FAAH to produce carboxylic acids on the thiazole ring. This produces a cyclic aminoluciferin (top) and firefly luciferin (bottom) as reporters. B) A highly reactive oxygen species oxidizes the 6' amine of **Fluc-II** to release aminoluciferin (**Amino-Fluc**) as a reporter. C) Nitroreductase reduces the aromatic nitro group of **Fluc-III** to an amine. This results in a rearrangement to cleave the “caged” luciferin into 4-methylenecyclohexa-2,5-diene-1-imine and **Amino-Fluc** as a reporter.<sup>[9][11][17]</sup>



*Figure 1.5: Labeled carbon positions of luciferin*

Luciferin modifications have focused

on changing the aromatic structure to alter its emission frequency (Figure 1.6C). However, these analogues are often poor substrates with greatly reduced affinity for the native firefly

luciferase enzyme. To circumvent this issue some commercially available engineered luciferase enzymes have been evolved with higher affinities for luciferin analogues.

<sup>[11][12][13]</sup> A recent study functionalized the 5' position to yield an alkyne functional group that is conjugated into the benzothiazole aromatic region.<sup>[14]</sup> This analogue's emission spectrum was red-shifted, preserved the electron donating hydroxyl, and had an emission intensity comparable to many commercially available analogues (albeit about 1% that of

native firefly luciferin; Figure 1.6). Furthermore, this luciferin analogue has potential to be “clicked” to other molecules via Copper Catalyzed Alkyne-Azide Cycloaddition (CuAAC).<sup>[14]</sup> The functionalization at the 6'-hydroxyl or 5'-alkyne allows for conjugation to cellular targeting molecules, antibodies, steroids, or molecules facilitating cellular uptake and thus enhance localization in the cell or at specific cell types.

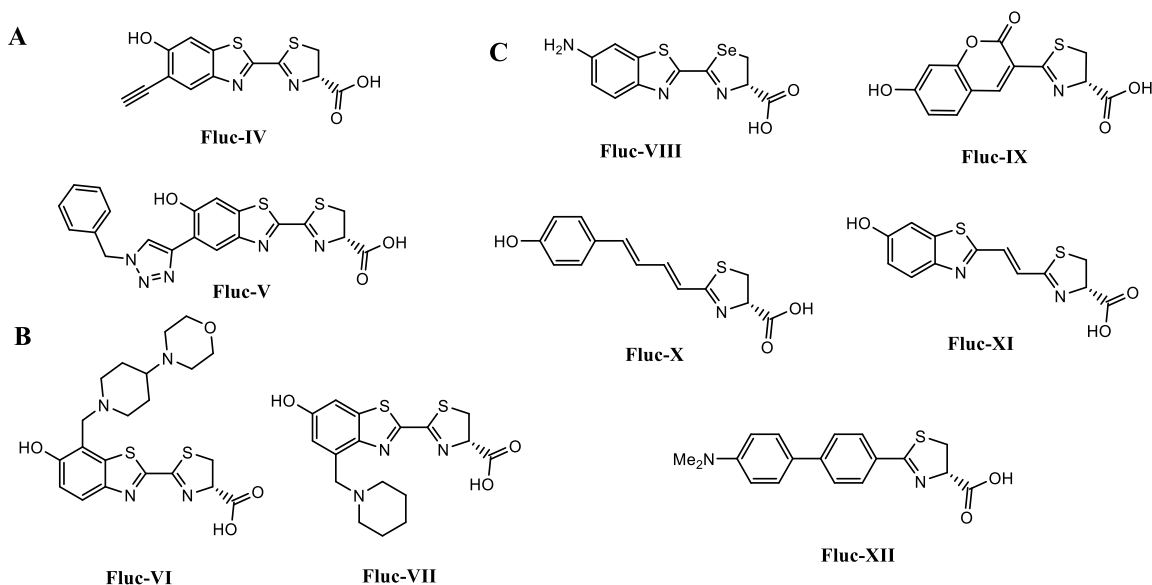


*Figure 1.6:* Luciferin analogues: A) luciferin with an alkyne functionality at the 5' position of the aromatic ring (**Fluc-IV**) was used to click-couple benzyl azide to yield the **Fluc-V**.<sup>[14]</sup> B) **Fluc-VI** and **Fluc-VII** are sterically modified luciferin analogues for applications as orthogonal luciferin-luciferase pairs.<sup>[15]</sup> The left is modified at the 7' position; the right is modified at the 4' position. C) several luciferins with modified aromatic structures to change the wavelength of emission from deep red (**Fluc VIII**) to violet in (**Fluc-X** to **Fluc-XII**).<sup>[16]</sup>

A 2017 study demonstrated the synthesis of orthogonal luciferin-luciferase pairs to expand the tool kit used for bioluminescent imaging. The luciferins were functionalized off the 4' and 7' positions with sterically bulky substituents (Figure 1.6B). The best luciferin analogue developed had a bioluminescent output with wildtype luciferase ~1% of native luciferin with wildtype luciferase. These substrates were then used as targets for evolving mutant luciferases that selectively oxidized 4' or 7' functionalized luciferins. The novel luciferin-luciferase pairs showed substrate selectivity but with an even greater

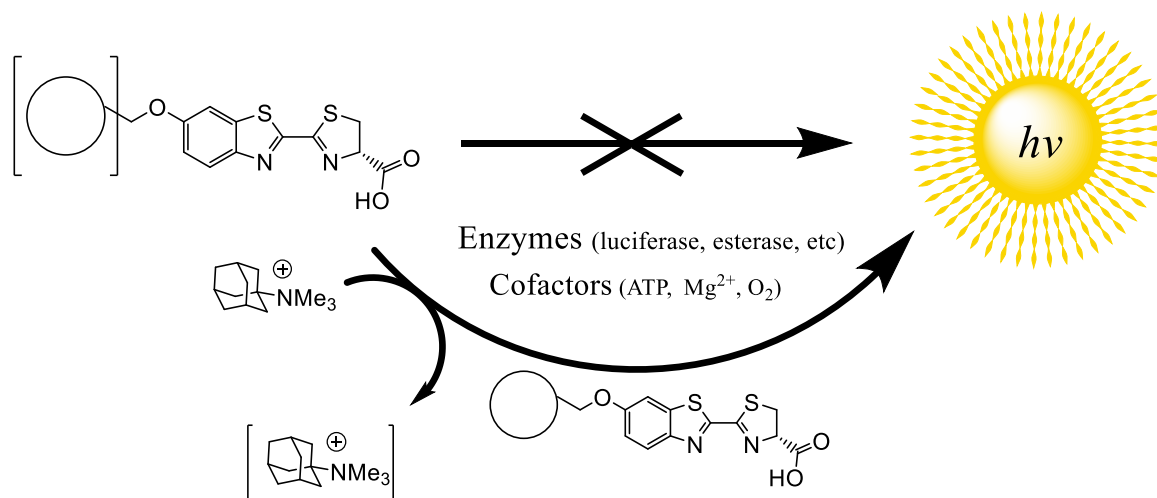
reduction in bioluminescence. While the signal is detectable, it highlights a major hurdle in bioluminescent imaging using modified luciferins, that is the significant loss of signal when deviating from the wildtype luciferin-luciferase pair.<sup>[11][14][15]</sup>

In this thesis, I detail the application of luciferin derivatives to study a novel caging method that harnesses host-guest chemistry. In particular, the 6'-hydroxyl is used to tether guests with both sturdy (ether) and labile (ester) linkers (Scheme 1.2). The system is designed such that upon complexation with CB[7], the modified luciferin becomes non-covalently caged from interacting with enzymes thus it cannot be oxidized to an oxyluciferin and give off light. However, in the presence of a strong competitive guest for CB[7], the modified luciferin can be oxidized by luciferase and will be bioluminescent (Scheme 1.1). If this hypothesis is true, this will demonstrate a novel caging method for a luciferin-luciferase pair.

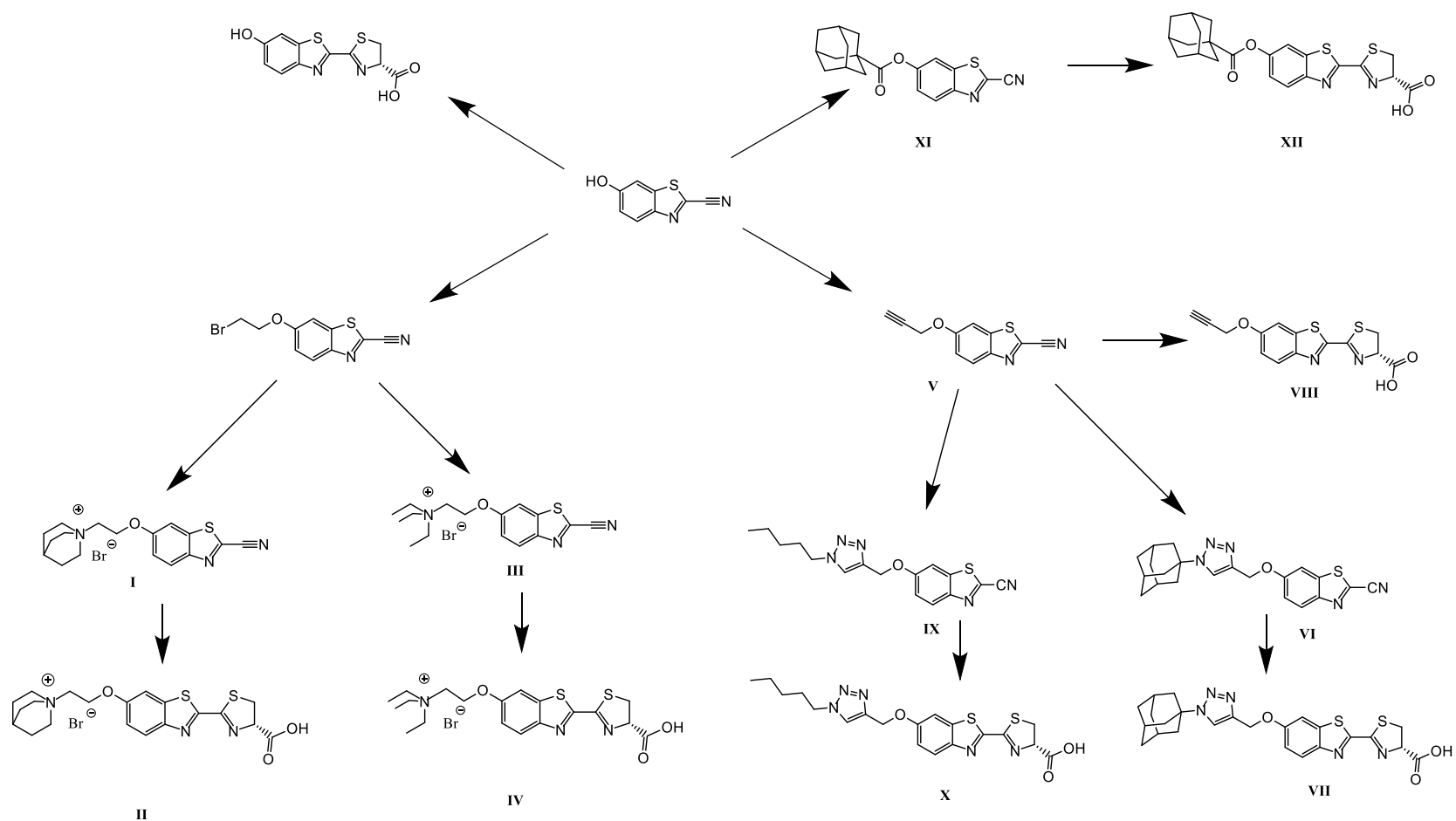
Non-polar guests, quinuclidinium and adamantane, were chosen as binding sites for the host CB[7], and thus these “head-groups” were ligated to luciferin.<sup>[1][3][18]</sup> Additionally, three control luciferin analogues were developed to understand the effect of functionalization of the 6' hydroxyl, addition of a quaternary ammonium unit, and a triazole unit (Scheme 1.3). Most of the synthetic work was carried out by the candidate to satisfy the Honor's Thesis requirement for his Bachelor's Degree. This thesis focuses on the characterization of the host-guest interaction, caging from enzyme catalysis, and bioluminescent studies.

Specifically, Chapter 3 focuses on the use of these novel molecules and their host-guest complexes with CB[7] as enzyme substrates in both fluorescent and bioluminescent assays to test the hypotheses of this study. Chapter 2 discusses the use of UV-vis and NMR

spectroscopy to characterize the binding of CB[7] to luciferin and the functionalized analogues required to understand the data collected for Chapter 3.



*Scheme 1.1:* Proposed mechanism for supramolecular caging of novel luciferin analogues. The functionalized luciferin:CB[7] complex is not a viable substrate for an enzyme of interest due to the position of the host (square brackets) on the non-polar group, thus the complex is in an inert form until a strong CB[7] binder (adamantyl trimethylammonium) is added. This frees the luciferin analogue and it can be substrate for the enzymes catalytic process. The product luciferin is oxidized in the presence of ATP, magnesium cation, and molecular oxygen to give light. Thus, in the presence of a host, signal and kinetics of the reaction are expected to decrease. In the presence of a strong competitive binder, signal should increase greatly.



*Scheme 1.2: Scheme for Synthesis of Luciferin and six 6'-hydroxy functionalized derivatives; (Left to right) luciferin-oxylethyl-quinuclidinium bromide (II), luciferin-oxylethyl-triethylammonium bromide (IV), luciferin triazole-pentane (X), luciferin-triazole-adamantane (VII), luciferin-alkyne (VIII), and Luciferin-Adamantanoate (XII)*



## Chapter 2: Characterization of Luciferin-CB[7] Host-Guest Interaction

### Section 2.1: Results and Discussion

#### *Characterization by UV-vis Spectroscopy*

Binding of luciferin and its analogues with CB[7] was first interrogated by UV-vis spectroscopy which yielded modest results. CB[7] was not purified, but was calibrated using a cobaltocenium titration. Native luciferin had a peak absorbance at  $\lambda = 332$  nm, and  $\lambda = 266$  nm. The peak at 332 nm absorbed about twice as much light than the peak at 266 nm. All functionalized luciferins showed a small blue shifting of their peak near 332 nm while the peak at 266 nm did not show significant change in position between analogues (Figure 2.1).<sup>[19]</sup>

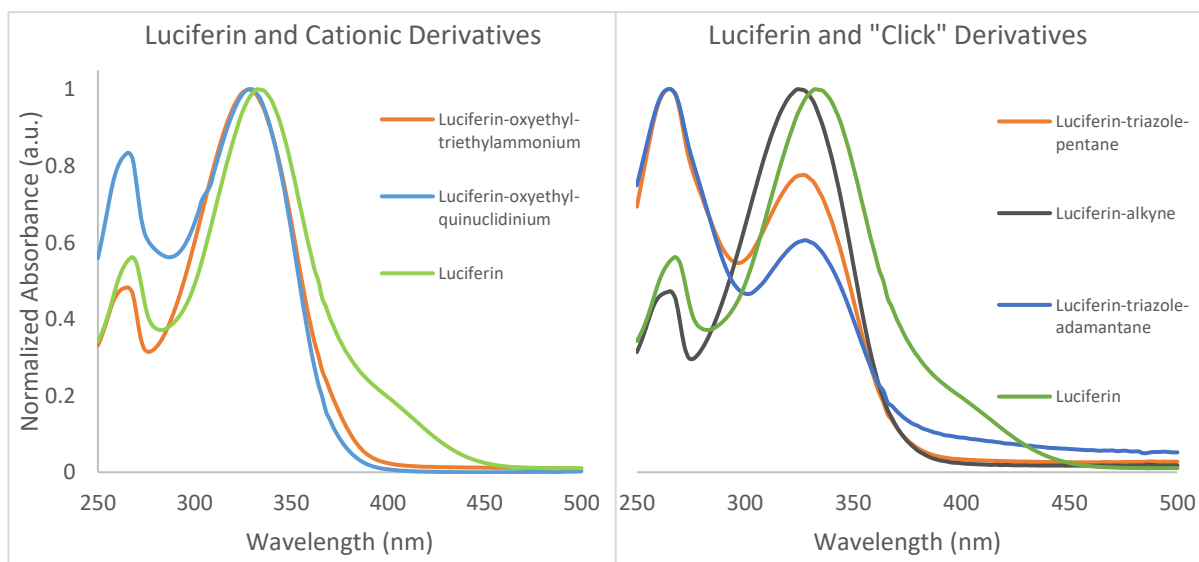


*Figure 2.1:* Normalized Absorbance of Luciferin and its derivatives. All 6'-hydroxyl functionalized luciferins have a blue shift of both peaks found in native luciferin. Cationic luciferins show a very similar spectrum, whereas "click" luciferins have a decreased absorbance near 330 nm and a greatly increased absorbance near 266 nm.

The triazole functionalized luciferins (**VII**) (**X**) and quinuclidinium functionalized luciferin (**II**) had a significantly larger absorbance at 266 nm than native luciferin. The

propargyl (**VIII**) and triethylammonium functionalized luciferins (**IV**) do not show this increase and thus most closely resemble a blue shifted native luciferin. Both cationic luciferins had their largest peak at 330 nm, and a smaller peak at 266 nm. Triazole functionalized luciferins' (**VII**) (**X**) peak at 330 nm was comparable in position to the other functionalized luciferins.

Titration of CB[7] to native luciferin showed a decrease in absorbance at both peaks and it was best fitted with a 1:1 type binding and  $K_a = 1.1 \times 10^3 \pm 5\% \text{ M}^{-1}$  was determined (see SI-32).<sup>[20]</sup> The value is close that of a recent paper which determined the binding of CB[7] to luciferin in its ionic form in pure water to be  $541 \pm 125 \text{ M}^{-1}$  using fluorescence.<sup>[19]</sup> The difference in the result of the binding assay could be due to the different buffer conditions. The buffer in this thesis' study was at pH 8 resulting in the formation of some dianionic luciferin (30 mM HEPES, 5 mM  $\text{MgSO}_4$ , pH 8; Figure 2.2).

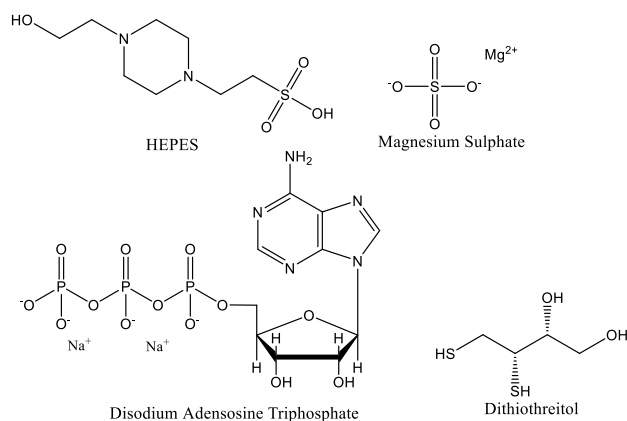


Figure 2.2: Structure of assay buffer components.

Furthermore, the buffer in this study contained magnesium salts and HEPES which would also effect host-guest interactions when compared to the same interacting in ultra-pure water. Counter-cations have the ability to interact with the carbonyl portal of CB[7] which could significantly change the electronic interactions of complexes with smaller guests. Potentially, the magnesium is forming an ion pair with the luciferin in solution which could attenuate the electrostatic repulsion one would expect from an anion and an electronegative portal. Titration with CB[7] to the propargylated luciferin showed a similar trend but with

a slightly increased affinity of  $1.4 \times 10^3 \text{ M}^{-1}$  (See SI-33). This can be reconciled because the guest molecule is monoionic at pH 8, rather than a dianion thus there would be less electrostatic repulsion between the 6'-hydroxyl and the carbonyl portal.<sup>[1][4]</sup> Both of these substrates show 1:1 binding, but interestingly, all other compounds showed a 2:1 binding of host (CB[7]) to guest (luciferin analogue).

The quinuclidinium functionalized luciferin (**II**) yields the best fitting from this data because it shows an initial increase in absorbance at 354 nm, no change at 332 nm, and a decrease at 266 nm from 0-1 equivalents followed by a gradual decrease in absorbance at all three wavelengths from 1-13 equivalents. Using this data all three curves were fit simultaneously giving a large initial binding of  $1.8 \times 10^6 \text{ M}^{-1} \pm 27\%$  and a modest secondary binding at  $1.5 \times 10^3 \text{ M}^{-1} \pm 1\%$  at another site (See SI-34). From this data, it is postulated that the first binding site is the quinuclidinium and the second site is the luciferin core. The first binding constant is reasonable knowing that in ultrapure solution quinuclidinium has a binding constant to CB[7] on the order of  $1 \times 10^9 \text{ M}^{-1}$  and the buffer in our study contains magnesium which would compete for electrostatic interactions at the portal.<sup>[3]</sup> The second binding is comparable to that of the propargylated luciferin as it is a luciferin with an alkyl ether linkage in both cases. The large error in the first constant is most likely due to the high affinity for quinuclidinium and CB[7] combined with the reduced sensitivity of UV-vis spectroscopy as compared to NMR and fluorescence spectroscopy when observing a binding event away from the aromatic region.<sup>[3][20]</sup>

The triethylammonium functionalized luciferin (**IV**) failed to fit a 2:1 binding isotherm because there was no significant change in absorbance at any wavelengths between 250 nm and 600 nm followed by a precipitous drop from 1 equivalent onward.

Because there was no major change between 0 and 1 equivalents, but a large change from 1 to 13 equivalents the algorithm failed to properly fit the curve. There are two binding modes being observed but the first did not result in a large change in absorbance thus it was difficult to characterize. (See SI-35). Based on past research one would expect the first binding to be to the triethylammonium with a  $K_a \sim 10^6 \text{ M}^{-1}$  in ultrapure aqueous conditions.<sup>[16]</sup> In the buffer conditions used in this study, there seems to be a consistent drop by about two to three orders of magnitude in binding constant due to the salts present, thus in this buffer one would expect to see a binding affinity of CB[7] to the triethylammonium moiety of  $K_a \sim 10^4 \text{ M}^{-1}$ . Secondly, based on the fitting of the second binding events of other luciferin synthesized for this research, the second binding event should be near  $K_a \sim 1400 \text{ M}^{-1}$ . A potential reason for the small change in absorbance between 0 and 1 equivalents of CB[7] is the distance of the charged portion of the moiety from the aromatic region of the molecule. The quinuclidinium (**II**) could have a greater change in its absorbance because as CB[7] is titrated into the solution and binds to the hydrophobic moiety there is a decrease in aggregation. Based on previous research into binding of quaternary amines to CB[7] and the research conducted for this thesis, it can be expected that luciferin-oxyethyl-triethylammonium (**IV**) is a relatively weak binder for CB[7] thus can act as control for the placement of a positive charge three atoms from the luciferin's 6' hydroxyl.

Both triazole functionalized luciferins were also fit from UV-vis data, and gave reasonable values for the binding process. The triazole pentane (**X**) showed an initial binding of about  $K_a = 6.8 \times 10^4 \text{ M}^{-1} \pm 10\%$  and is thus a weak binding control for the triazole adamantane analogue at  $2.3 \times 10^3 \pm 1\%$  (See SI-36). I have low confidence in the

determination of binding affinity for luciferin-triazole-adamantane (**VII**) and CB[7],  $K_a = 1.2 \times 10^5 \text{ M}^{-1} \pm 10\%$  (the first binding), because it is 1 or 2 orders of magnitude lower than would be expected for the interaction of adamantane and CB[7] even in buffer conditions (See SI-37).<sup>[1][3][20]</sup> The reason for this could result from it being a large, uncharged moiety attached at the position 4 atoms off the 6' hydroxyl. This means binding at the adamantyl position may not have a significant effect on the electronics of the luciferin aromatic core, aside from the effects expected from deaggregation. Though this implies a low reliability in these measurements in the case of the click functionalized analogues, it does not negate the use as a strong and weak binding pair for their use in for probing host guest interactions.

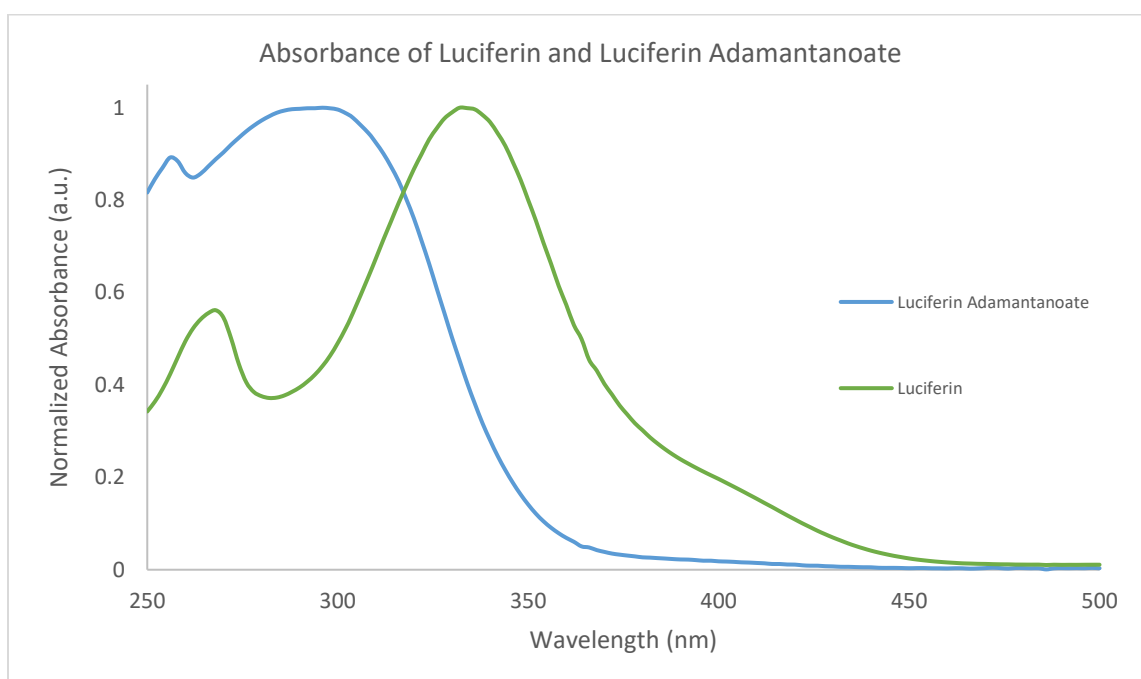


*Figure 2.3:* Normalized absorbance of luciferin and luciferin adamantanoate (**XII**). Luciferin adamantanoate shows a strong blue shift from  $\lambda_{\text{max}} = 332 \text{ nm}$  to  $296 \text{ nm}$ . The absorbance is also much broader than native luciferin.

The binding of CB[7] to luciferin adamantanoate (**XII**) was surprisingly low. There was a modest binding of  $7.4 \times 10^5 \text{ M}^{-1} \pm 26\%$  to the adamantyl functionalization and a

second weaker binding to the aromatic region (See SI-38). The binding to the aromatic region was within the bounds of values observed for other analogues, on the order of  $10^3 \text{ M}^{-1}$ . The initial binding is weaker than one would expect for an adamantyl moiety, but this may be due to the 1% DMSO used to dissolve the substrate, and by the high concentrations of buffer cations competing for binding to the CB[7]. Nevertheless, luciferin adamantanoate (**XII**) should be a strong candidate for binding by CB[7] in a complex environment to inhibit activity with an esterase.

Species	Structure	CB[7]:Guest	$K_1 \text{ (M}^{-1}\text{)}$	$K_2 \text{ (M}^{-1}\text{; if applicable)}$
Luciferin ( <b>Fluc</b> )		1:1	$1.1 \times 10^3 \pm 5\%$	N/A
Luciferin Alkyne ( <b>VIII</b> )		1:1	$1.4 \times 10^3 \pm 5\%$	N/A
Luciferin-oxyethyl-quinuclidinium bromide ( <b>II</b> )		2:1	$1.8 \times 10^6 \pm 27\%$	$1.5 \times 10^3 \pm 1\%$
Luciferin-oxyethyl-triethylammonium bromide ( <b>IV</b> )		2:1	—	—
Luciferin-triazole-adamantane ( <b>VII</b> )		2:1	$1.2 \times 10^5 \pm 10\%$	$2.2 \times 10^3 \pm 2\%$
Luciferin-triazole-pentane ( <b>X</b> )		2:1	$6.8 \times 10^4 \pm 10\%$	$2.3 \times 10^3 \pm 1\%$
Luciferin adamantanoate ( <b>XII</b> )		2:1	$7.4 \times 10^5 \pm 26\%$	$1.6 \times 10^3 \pm 4\%$

Table 2.1: Binding constants as determined by UV-vis spectroscopy: Luciferin and luciferin-alkyne showed binding consistent with 1:1 type binding, while all others showed a 2:1 type binding stoichiometry.

*Characterization by NMR Spectroscopy*

NMR titration of native luciferin showed no significant shift changes as CB[7] was added to the solution (Figure 2.4). Overall, binding to this molecule is very weak and significant shifts would not be observed in a biologically relevant regime.

NMR titration of luciferin-triazole-adamantane (**VII**) showed the presence of new adamantyl peaks which are shifted up-field after 1 equivalent is added and do not experience any further changes at higher equivalents (Figure 2.5). This implies it is a strong binding event even with DMSO in solution. Along with the adamantyl hydrogens, the triazole ring's hydrogen is also shifted up-field with respect to all other aromatic peaks which experience a downfield shift after 1 equivalent is added. This downfield shift is ascribed to deaggregation of the luciferin-adamantanoate (**XII**). At 10 equivalents the aromatic hydrogens experience a broadening which imply a fast exchange rate on the NMR timescale. This could be an artifact of the low concentrations and poor signal to noise ratio. Taken together this data is indicative of 1:2 binding as expected from changes in absorbance spectra of the CB[7] complexes with the analogue.

NMR titration of luciferin-adamantanoate (**XII**) showed an expected shift in the adamantyl region then aromatic region (Figure 2.6). At 1 equivalent of CB[7] there was an up-field shift in the adamantyl region, as expected from CB[7] complexation. Also at 1 equivalent there was a slight down-field shift in the aromatic region. Both of these shifts are expected because the CB[7] tends to induce an up-field shift upon binding. The shift in the aromatic structure is associated with deaggregation which is also reflected in UV-vis spectroscopy. At higher equivalencies there are small up-field shifts in the aromatic region which is expected knowing the 1:2 binding mode of luciferin-adamantanoate (**XII**) to CB[7].

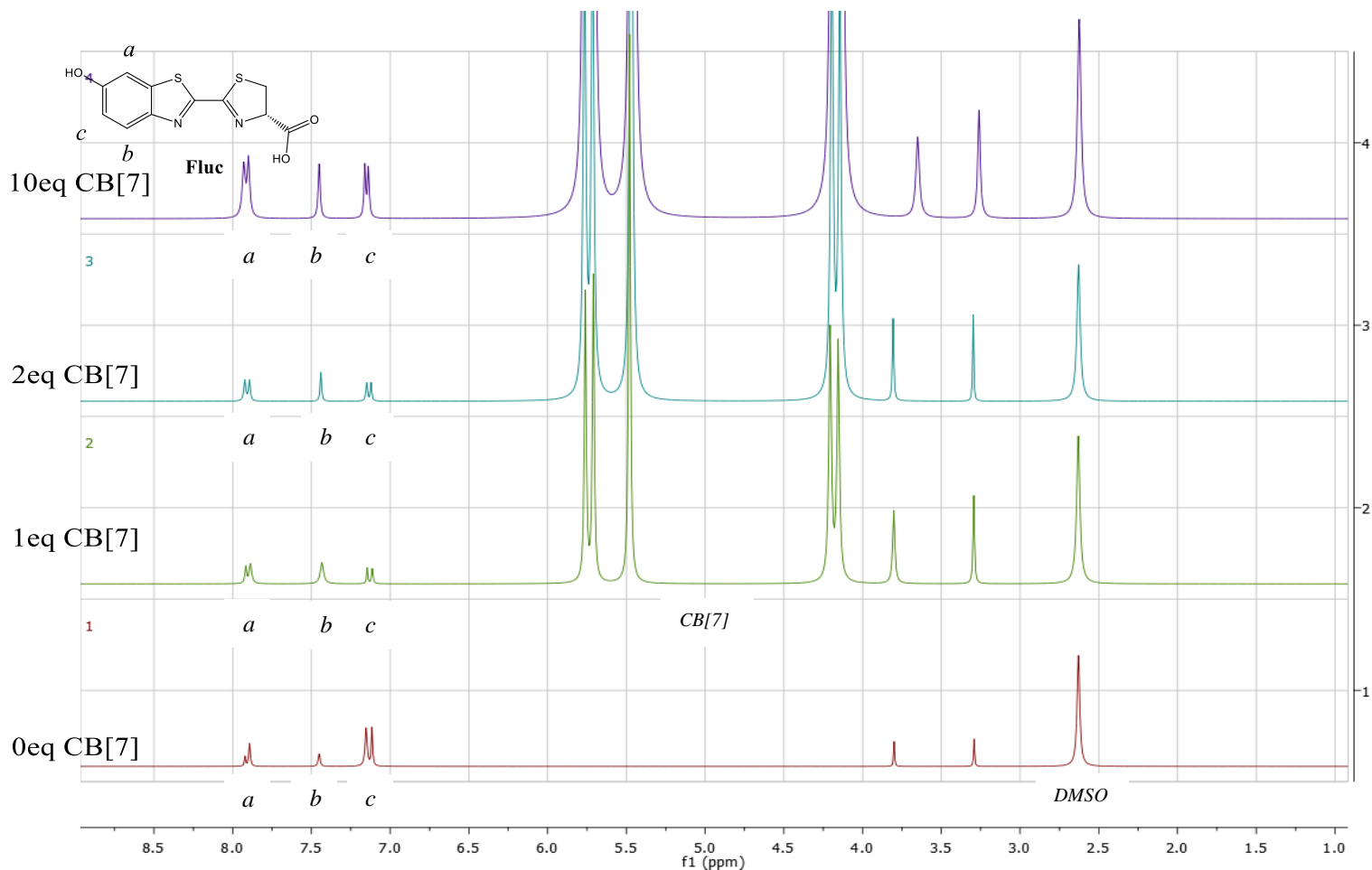


Figure 2.4: NMR of luciferin in  $D_2O$ : 1%  $d_6$ -DMSO titrated with 0, 1, 2, 10 equivalents of CB[7] (increasing vertical displacement in the figure). Concentration of luciferin is 0.167 mmol. **A** represents aromatic hydrogen peaks, **CB[7]** represents peaks from the CB[7] hydrogens.



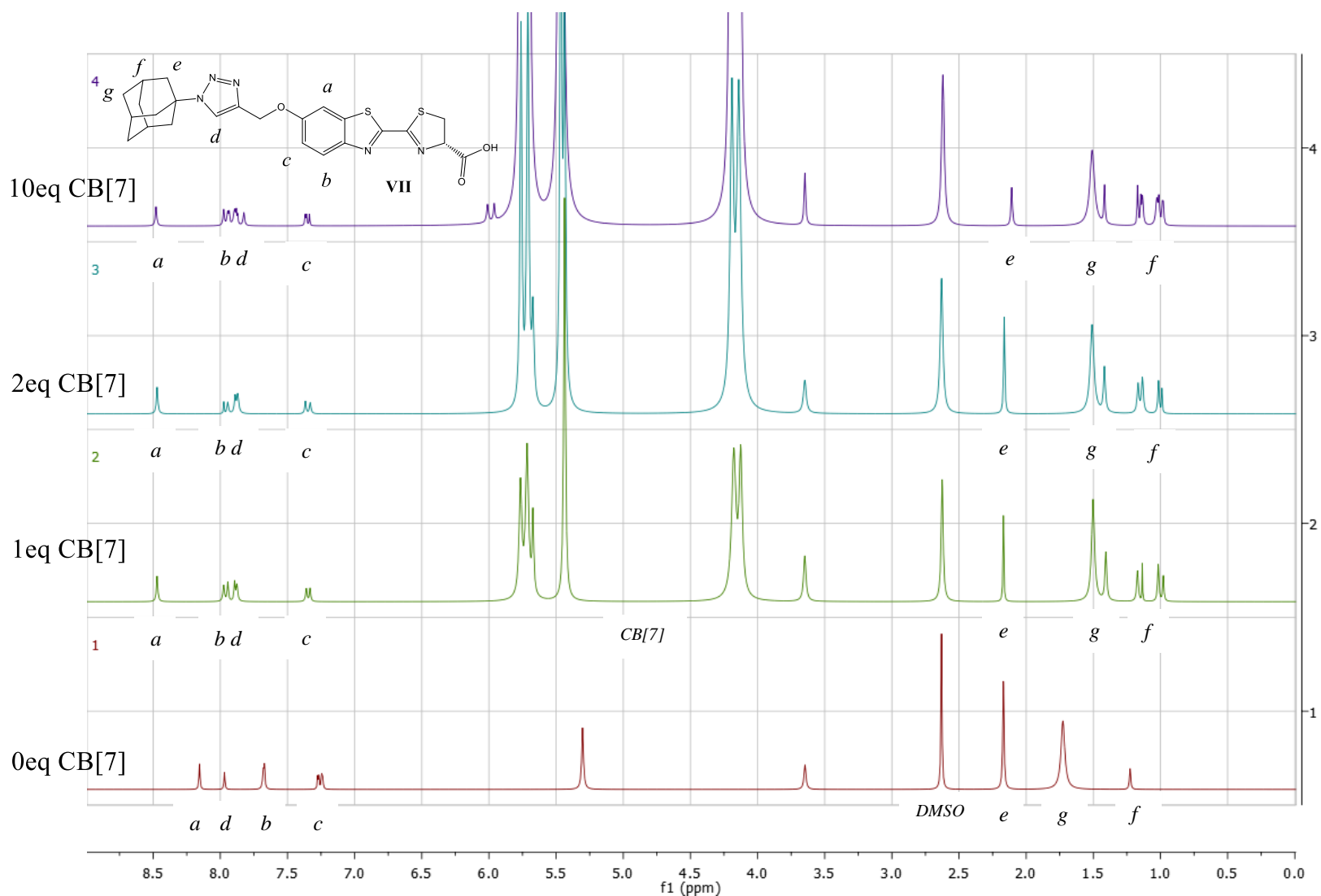


Figure 2.5: NMR of luciferin-triazole-adamantane in D<sub>2</sub>O: 1% d<sub>6</sub>-DMSO titrated with 0, 1, 2, 10 equivalents of CB[7] (increasing vertical displacement in the figure). Concentration of luciferin-triazole-adamantane is 0.167 mmol. **A** represents aromatic peaks, **B** represents adamantyl hydrogen, **C** represents the triazole hydrogen peak. **CB[7]** represents peaks from the CB[7] protons.

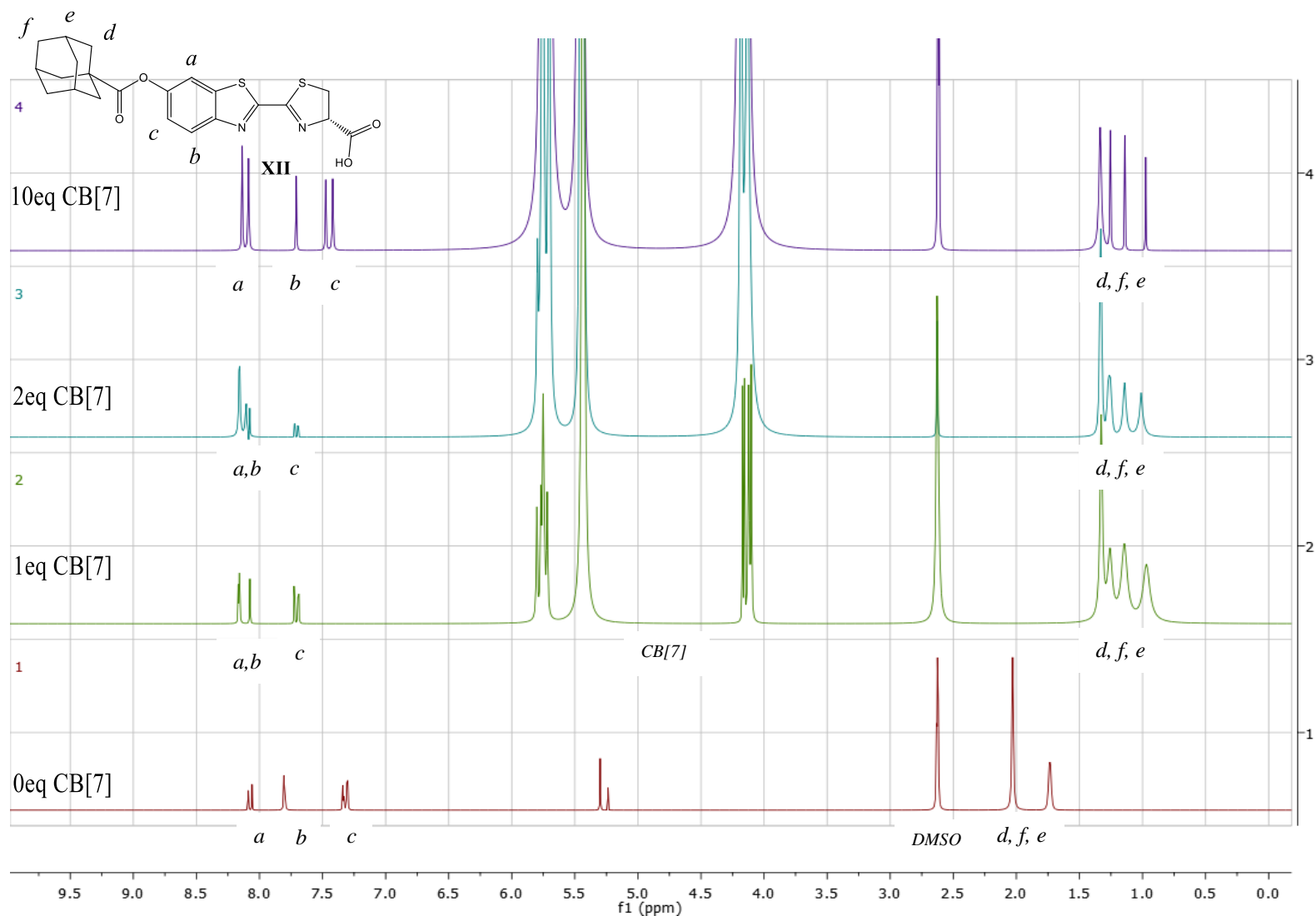


Figure 2.6: NMR of luciferin-adamantanoate in D<sub>2</sub>O: 1% d<sub>6</sub>-DMSO titrated with 0, 1, 2, 10 equivalents of CB[7] (increasing vertical displacement in the figure). Concentration of luciferin-adamantanoate (XII) is 0.167 mmol. **A** represents aromatic peaks, **B** represents adamantyl hydrogen, **CB[7]** represents peaks from the CB[7] protons.

## Section 2.2: Conclusions

UV-vis gave the first insight into the type of binding that was occurring in the CB[7]:Luciferin complex and revealed the 2:1 binding in most functionalized species. This technique also revealed luciferin-oxyethyl-quinuclidinium (**II**) and luciferin-triazole-adamantane (**VII**) are strong binders of CB[7] and luciferin-oxyethyl-triethylammonium (**IV**) and luciferin-triazole-pentane (**X**) are weaker binders of CB[7]. Secondly the binding to the aromatic core is relatively weak in comparison and should not have a significant effect in the inhibition of a luciferin-luciferase system as it would likely have a rapid on-off rate which would favor association with luciferase rather than CB[7]. UV-vis had its limitations when observing neutral luciferin species, and species where a charge is distant from the aromatic region. This is because these modifications may not have resulted in a large change in the electronics of the aromatic region. Fluorescence was deemed not a viable technique for measuring binding constants because as the substrates were titrated with CB[7] they did not show an isobestic point. Thus, the fluorescence data was not usable and not reported in this thesis.

<sup>1</sup>H-NMR showed the first binding event in all 2:1 host guest complexes was to the hydrophobic functionalization and the second binding event was to the aromatic region. The saturation at 1 equivalent for the strong binders confirms that they are in fact strong binders even in competitive environments with DMSO present. Binding to native luciferin was small and only occurred at the aromatic region, and was not saturated at 10 equivalent. Thus this binding event would not contribute significantly to any effects in biological conditions. Taken together these binding studies give a rationale for the effects that are

expected to be observed in the next chapter where host-guest chemistry will be the driving force of observables in enzyme catalyzed systems.

## Section 2.3: Experimental

### *Calibration of CB[7]*

The following calibration method is modified from Yi and Kaifer (2011) and was performed by Ryan S. Vik. Five cobaltocenium solutions, 10  $\mu\text{M}$ , 15  $\mu\text{M}$ , 20  $\mu\text{M}$ , 25  $\mu\text{M}$ , and 100  $\mu\text{M}$  were made from a 100  $\mu\text{M}$  stock solution and calibrated using beers law with the molar absorptivity of cobaltocenium at 261 nm. To the calibrated 15  $\mu\text{M}$  solution of cobaltocenium, titrate with a 150  $\mu\text{M}$  solution of CB[7] (dried, uncalibrated) and monitor absorbance at 261 nm. Monitoring this absorbance versus concentration of CB[7] will yield the effective concentration of CB[7] so allow for calibration of the stock.

### *Observation of Host-Guest interaction by UV-vis*

In general, a QS High Precision Cell (10 mm Pathlength, Hellma Analytics) with 1mL enzyme substrate solution (30 mM HEPES, 5 mM  $\text{MgSO}_4$ , 50  $\mu\text{M}$  Luciferin/analogue) was scanned for absorbance from 250-500 nm in a spectrophotometer (HP Hewlett Packard 8452A Diode Array spectrophotometer). To this solution was titrated aqueous 1 mM CB[7] solution such that the addition of 20 aliquots gave final concentration of 0 to 10 equivalents of CB[7] to luciferin analogue. Up to 10 points were taken between 0 and 1 equivalent at 0.1 equivalent intervals (0-50  $\mu\text{L}$  titrant). The remaining points were spread out to a maximum of 13 equivalents. After each addition the vial was mixed by inverting multiple times and allowed to rest for 2-5 minutes. The blank was taken as the general buffer solution (30 mM HEPES, 5 mM  $\text{MgSO}_4$ ) and automatically subtracted.

*Observation of Host-Guest interaction by NMR*

NMR titrations were performed on Bruker 300. 500  $\mu\text{L}$  of 1mM solution of each luciferin were prepared. Luciferin, luciferin-adamantanoate, and luciferin-triazole-adamantane were prepared in 6%  $d_6$ -DMSO: 94%  $\text{D}_2\text{O}$ . These solutions were mixed with 2 mM CB[7] in  $\text{D}_2\text{O}$  to a give 600  $\mu\text{L}$  at the desired equivalency. Mixtures were allowed to sit for 1 day to ensure equilibrium had been reached.

(Final concentrations: 167  $\mu\text{M}$  luciferin analogue, 0-1.67mM CB[7], 1%  $d_6$ -DMSO)

## Chapter 3: Synthetically Functionalized Luciferins as Enzyme Substrates

### Section 3.1: Luciferin Analogues as Substrates for Firefly Luciferase

All luciferin analogues were initially shown to be viable substrates for firefly luciferase, though their luminescence was between 10 and 1000 times lower than the native Luciferin. A workable Luciferin analogue for wildtype luciferase often has a 2-3 order of magnitude decrease in luminescent output rendering it still detectable in many assays for both cellular imaging and deep tissue imaging. In our studies, two interesting trends are observed. 1) The cationic luciferin analogues show a greatly reduced activity with luciferase even in the less hydrophobic, triethylammonium analogue. 2) The “click” analogues show exceptional activity compared to all other species (Figure 3.2).

This first trend was a surprise because the cationic species were much more water soluble, and thus less likely to aggregate in solution compared to the “click” species. Investigation into the crystal structure of luciferin reveals there are two arginine residues at the portal of the enzyme which would be in close proximity to the benzothiazole moiety’s hydroxyl (Figure 3.1).<sup>[21][22]</sup> This gives potential for a favorable coulombic interaction in which the positive charge of the arginine is attracted to the electron rich hydroxyl of luciferin thus increasing the affinity of the enzyme’s active site for native luciferin.<sup>[21]</sup> In our set of molecules there is a positive formal charge on the nitrogen which is two atoms away from the oxygen. The formal charge is located on the nitrogen, but is more accurately represented as being spread around the surrounding carbons and is thus relatively diffuse, but would still result in an unfavorable coulombic interaction with the luciferase active site.<sup>[16]</sup> This could potentially explain the reduction in luminescence from this set of luciferins.

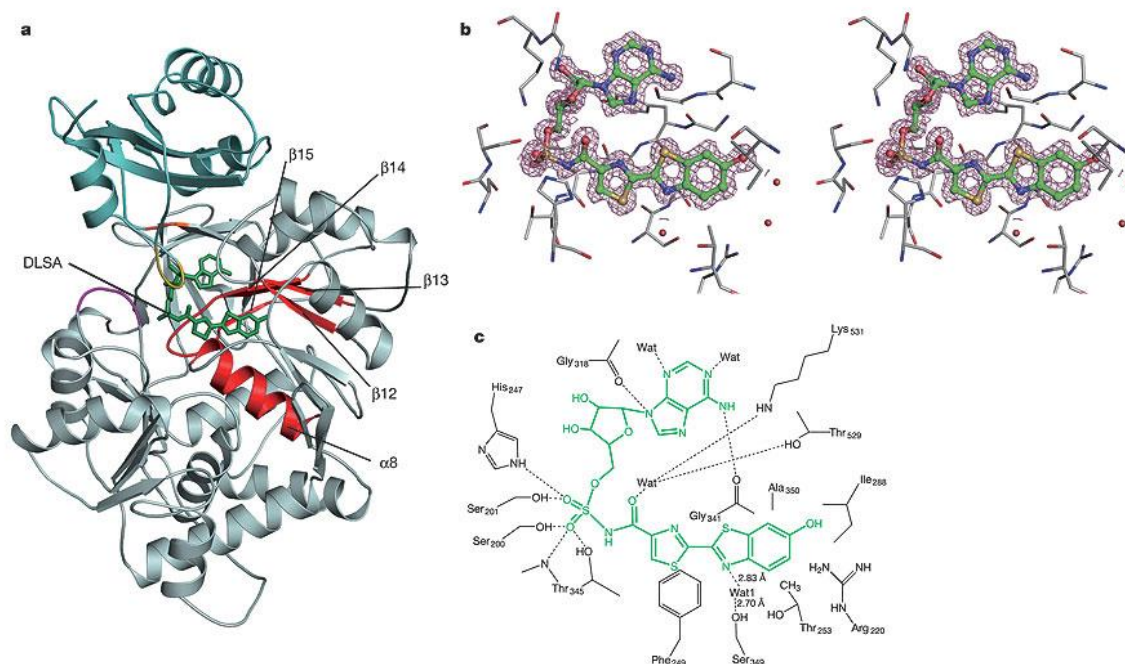


Figure 3.1 (Reproduced with permission from Nakatsu et. al): The luciferase active site with a bound luciferin analogue. (a) shows a ribbon diagram of wildtype luciferase complexed with the analogue (green). (b) shows a stereo view of residues in the active site and the electron density map of the bound luciferin analogue. (c) shows a schematic drawing of the active site. Dashed lines represent polar interactions between the residues and the substrate.

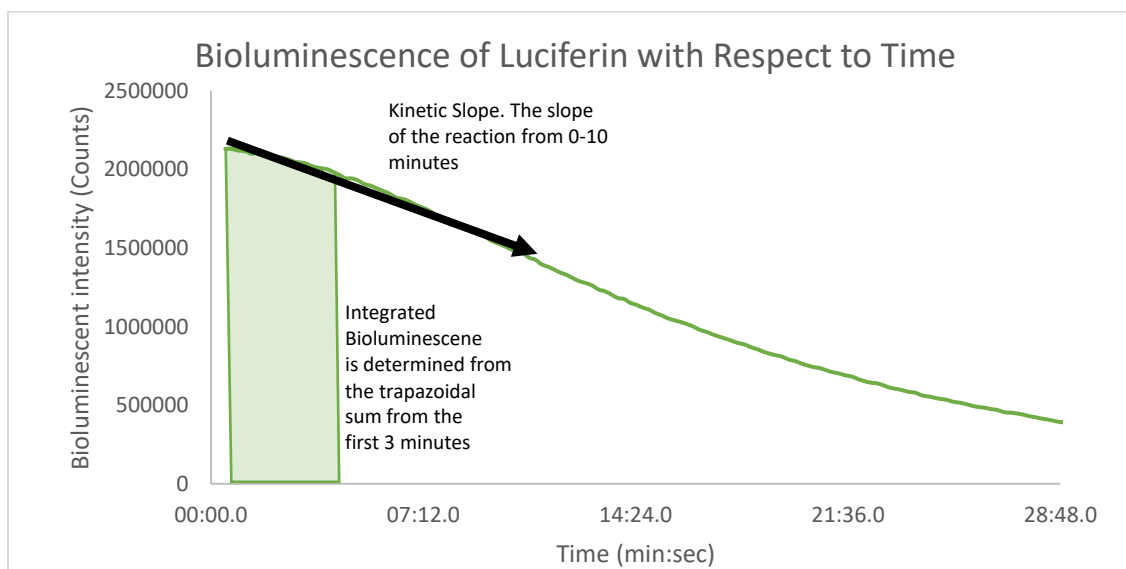


Figure 3.2: Determination of integrated bioluminescence and reaction velocity from the raw data kinetic curve. Integrated bioluminescence is determined from the trapezoidal sum over the first 2-3 minutes of the reaction this provides a consistent measure of the photon flux over the first three minutes. The following equation was used:  $\Phi = \int_{t_i}^{t_f} y dt \approx \sum_0^n \left[ \left( \frac{1}{2} \right) (y_{t+1} + y_t) * (t_{t+1} - t_t) \right]$  The reaction velocity is taken over the first 10 minutes because it is a relatively linear regime after the delay time to compensate for burst type kinetics typically observed in luciferin-luciferase reactions. Because reaction rate is measured by a decrease in luminescence, a more negative kinetic slope means a faster reaction.



The second interesting trend is the high bioluminescence for the “click” luciferins. Following the argument based on electrostatic interaction in cationic luciferins, the highly electronegative triazole moiety could have a minor role in compensating for the loss of the negative charge from native luciferin resulting in a viable substrate for native luciferase. The 3-fold increase in luminescence from luciferin-triazole-adamantane (**VII**) to luciferin-triazole-pentane (**X**) is likely to be a function of sterics, as both species are nearly identical electronically. The adamantane functionality has two factors reducing its viability as a substrate. The first is its bulkiness and the second is its aggregation potential. An aggregated luciferin would be less accessible and harder to diffuse into an active site. Though luciferin-triazole-pentane has an aliphatic region that can facilitate aggregation, there is more freedom of movement in the chain so it is less sterically hindering than adamantane.

Luciferin-alkyne (**VIII**) failed to show significant bioluminescence in many trials. This shows there is a significant deactivation of the luciferin luciferase system following functionalization of the 6' hydroxyl with an alkyne. This substrate is not viable and was thus not tested for its responsivity to CB[7] because in addition to its lack of bioluminescence the binding to CB[7] is also very weak.

The luciferin adamantanoate (**XII**) shows a highly reduced luminescence which is most likely due to reduced electron donation at the 6' position compared to a hydroxyl or ether functionality at the same position. Given solvolysis is a possible decay pathway for a phenolic ester, it is possible that some luminescence observed in this assay originated from background native luciferin rather than the enzymatic conversion of luciferin adamantanoate to an oxyluciferin adamantanoate.

When comparing spectra of firefly luciferin and the other compounds in this study there is little difference (Figure 3.3). A shift of 1 nm or 2 nm in the peak emission occurred but this followed no distinct trend. All substrates had a very strong emission near 555 nm. In past literature, some analogues with changes to the aromatic structure have shown red or blue shifting but functionalization at the 6' hydroxyl shows little effect on the emission energy of the photon because of its distance from the thiazole moiety. This finding emphasized the importance of the binding pocket chemistry of luciferase in determining the wavelength of the emitted photon.<sup>[19][22]</sup>

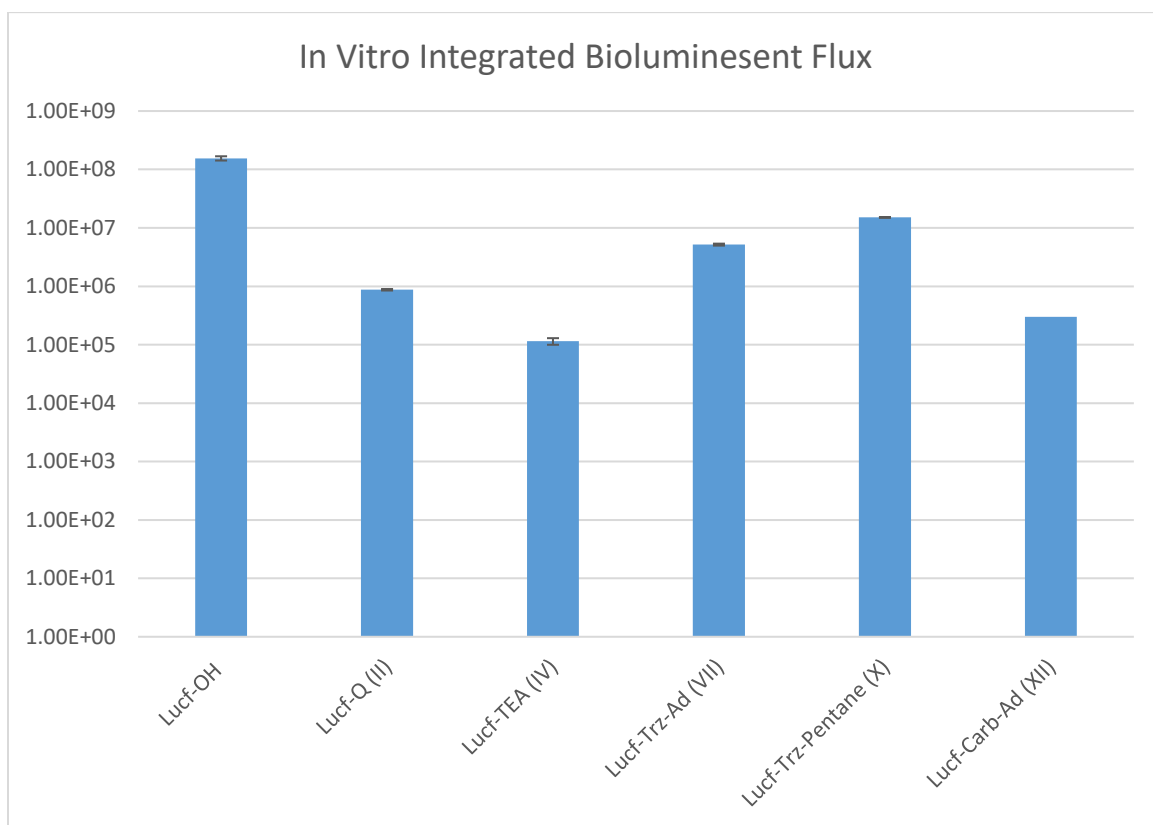


*Figure 3.2:* Luminescent output over the first 180 seconds after addition of ATP. Each species was at 5  $\mu$ M in a 200  $\mu$ L well. Derivation of these values is explained in figure 3.2. Note Log base 10 scale

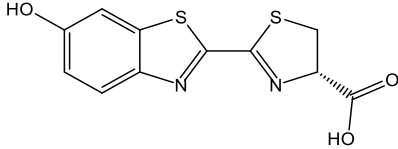
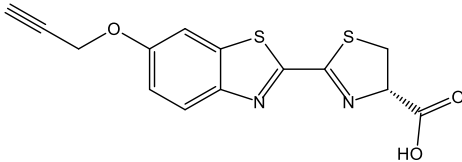
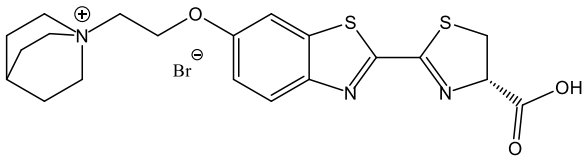
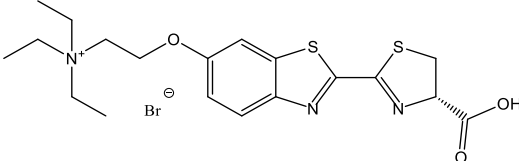
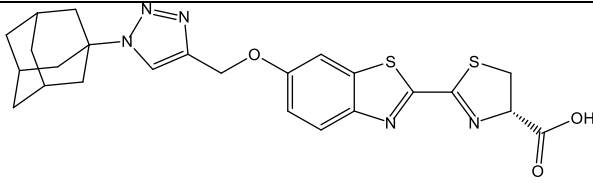
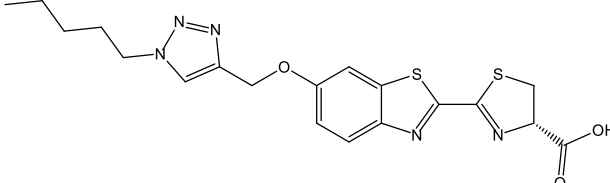
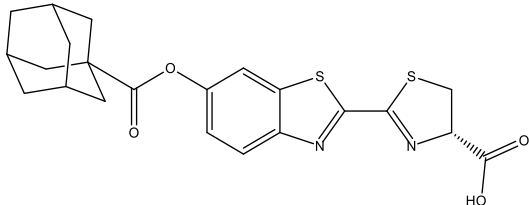
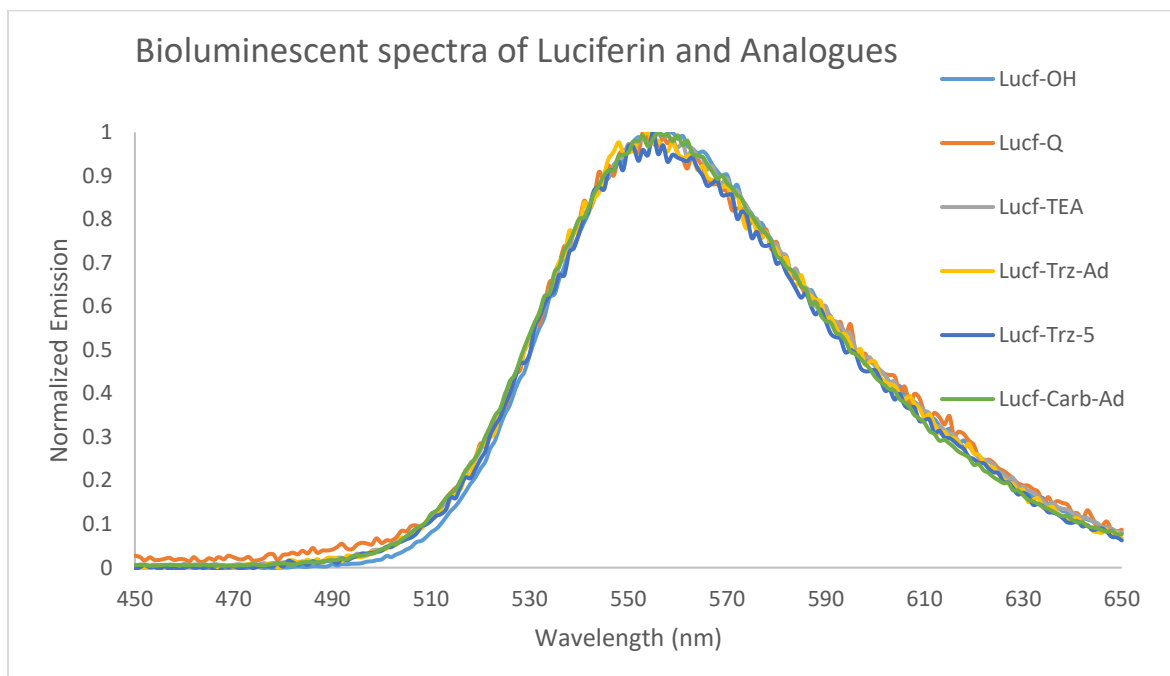
Species	Structure	Integrated Luminescence (count*s)	Relative to Luciferin
Luciferin		$1.55 \times 10^8 \pm 8.4\%$	100%
Luciferin Alkyne (VIII)		---	----
Luciferin-oxyethyl-quinuclidinium bromide (II)		$8.72 \times 10^5 \pm 3.0\%$	0.56%
Luciferin-oxyethyl-triethylammonium bromide (IV)		$1.15 \times 10^5 \pm 12.9\%$	0.07%
Luciferin-triazole-adamantane (VII)		$5.17 \times 10^6 \pm 3.9\%$	3.33%
Luciferin-triazole-pentane (X)		$1.51 \times 10^7 \pm 0.56\%$	9.73%
Luciferin adamantanoate (XII)		$3.00 \times 10^5$	0.19%

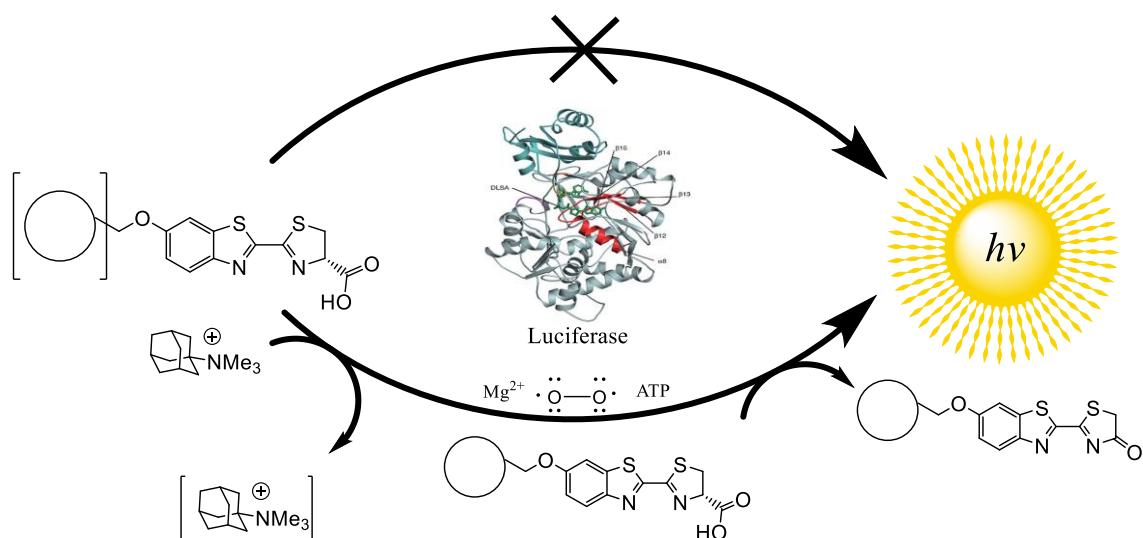
Table 3.1: Integrated bioluminescent output over the first 180 seconds after addition of ATP. Each species was at 5  $\mu\text{M}$  in a 200  $\mu\text{L}$  well. Derivation of these values is explained in figure 3.2.



*Figure 3.3:* Normalized Bioluminescent flux in general buffer solution of luciferin analogue, luciferase, and ATP. Emission spectra are all nearly identical when normalized, but the unnormalized data showed firefly luciferin was a significantly stronger emitter than other compounds.

### Section 3.2: Ether Functionalized Luciferin Analogues as *in vitro* Probes for Host-Guest Chemistry With CB[7]

The use of ether linked luciferin analogues has a significant draw back. As shown previously there is a decrease in the bioluminescence associated with functionalizing the 6'-oxygen, but this modification is necessary to reversibly cage our luciferin using host-guest interactions. We expected the modified luciferin to be caged from luciferase in the presence of CB[7] due to sterics, but in the presence of a strong competitive guest molecule, the modified luciferin should be a viable substrate for luciferase. This reactivation will be detectable using bioluminescence (Scheme 3.1).



*Scheme 3.1:* Proposed mechanism for supramolecular caging of novel ether linked luciferin substrates. Modified luciferin enters the deep enzyme pocket and is converted to modified oxyluciferin giving off light when relaxing from the excited state. Upon binding of CB[7] (square brackets) to a hydrophobic moiety (attached circle) of the modified luciferin, the binding of a modified luciferin to luciferase will be less favorable than native luciferin's binding to luciferase. Thus, in the presence of a host, signal and kinetics of the reaction are expected to decrease. Upon addition of a strong competitive binder, bioluminescent signal from oxidation of the substrate should increase again.

As the concentration of luciferin-analogue:CB[7] complex increased different effects were observed on the reaction rate as determined by bioluminescence. Firstly, native luciferin showed no clear trend in kinetic slope as CB[7] was added (SI-43). This is expected because luciferin is a weak binder of CB[7] and the system has several other

potential guest and cationic salts which would outcompete luciferin as a binder. Furthermore, there is no increase in bioluminescent output which would be the most useful quantity in an optimized system for applications into biological systems (SI-43).

Cationic species are poor substrates for wildtype luciferase, but there is still a general decrease in the kinetic slope of luciferin-oxyethyl-quinuclidinium's (**II**) oxidation by luciferase as CB[7] is added to the reaction from between 0 and 1 equivalents (SI-44). At 0 equivalents of CB[7] the kinetic slope is  $-434 \pm 13$  counts/second, at 1 equivalent, the kinetic slope fell to  $-319 \pm 52$  counts/second. At greater concentrations of CB[7] there is an increase in the kinetic slope  $-388 \pm 71$  counts/second to but there is a high standard of error thus it is not clear if there is a secondary effect of the CB[7] binding to the aromatic region or if this effect is an artifact of error (SI-44). The triethylammonium functionalized luciferin (**IV**) showed no change when CB[7] was titrated. This can be a function of its already very low activity with luciferase thus minor changes in kinetics would not be visible within error. When comparing the two cationic luciferins, the quinuclidinium functionalized luciferin (**II**) had approximately an order of magnitude greater bioluminescent output than the triethylammonium functionalized luciferin (**IV**, Figure 3.2). It also showed an initial decrease in bioluminescent output as CB[7] is added while the triethylammonium shows no change. This is to be expected given triethylammonium is a much weaker binder to CB[7] than quinuclidinium in aqueous conditions. These results directly mimic the kinetic slope measurements. (See SI-44)<sup>[18]</sup>

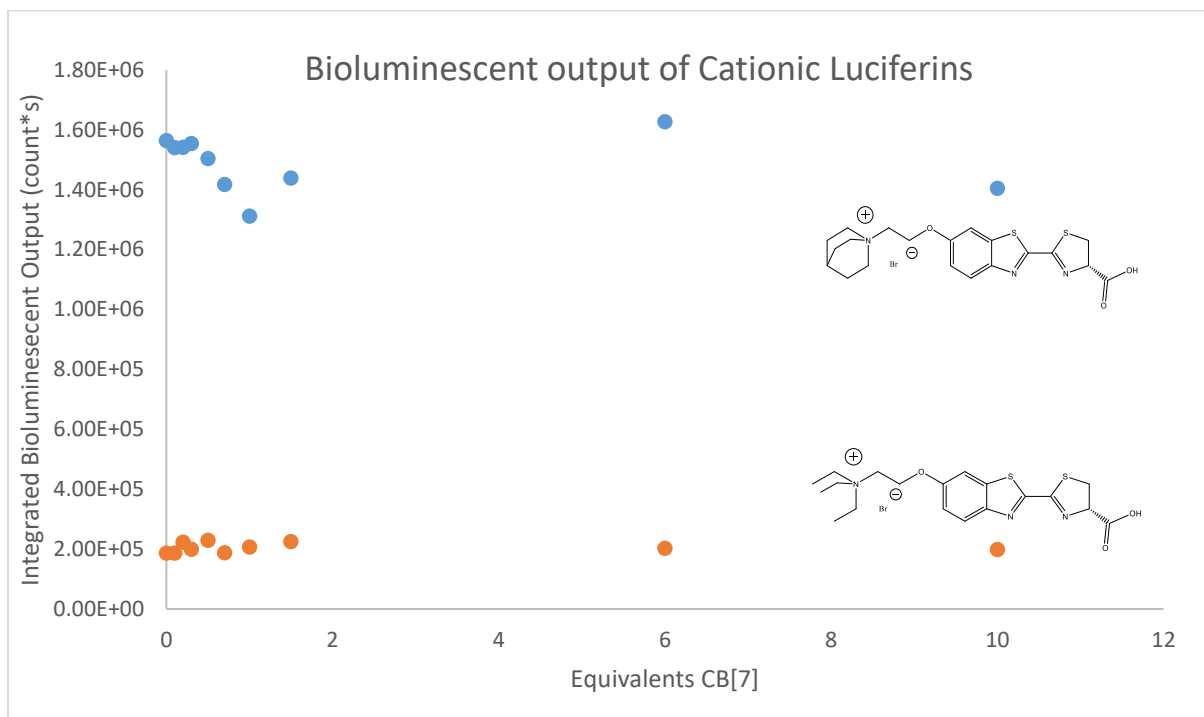


Figure 3.4: Bioluminescent output of cationic luciferin analogues over the first 2 minutes of reaction time. There is no significant trend from the titration with CB[7] in the case of luciferin-oxetyl-triethylammonium (IV). The quinuclidinium functionalized luciferin (II) shows an initial decrease followed by an increase.

The “click” luciferins were much better substrates for luciferase thus they gave greater kinetic rates (SI-45) and bioluminescent outputs (Figure 3.2). The adamantane functionalized click luciferin showed a general increase in reaction rate as determined by both kinetic slope and integrated bioluminescent output. The pentane functionalized click luciferin showed no change in kinetic slope or bioluminescent output as CB[7] was added, thus the change must be a function of CB[7] binding to the hydrophobic region of the luciferin analogue (Figure 3.5). While sterics would suggest that as CB[7] binds to the hydrophobic region of luciferin-triazole-adamantane (VII) it should be a less viable substrate for the deep binding pocket of luciferase, the opposite effect is observed. This can be explained by the deaggregation of the amphiphilic molecule making it more available for luciferase. This is supported by a visibly increased solubility of luciferin-triazole-adamantane as CB[7] is added to a solution. In solutions containing both luciferin-

triazole-adamantane and CB[7] there is no sign of undissolved solute. While in solutions of only luciferin-triazole-adamantane, precipitate is observed after the solution is left unagitated for several hours. The distance between the hydrophobic moiety and the aromatic region might explain the lack of steric effect on the enzymatic reaction thus the deaggregation becomes the dominating factor in the observables.

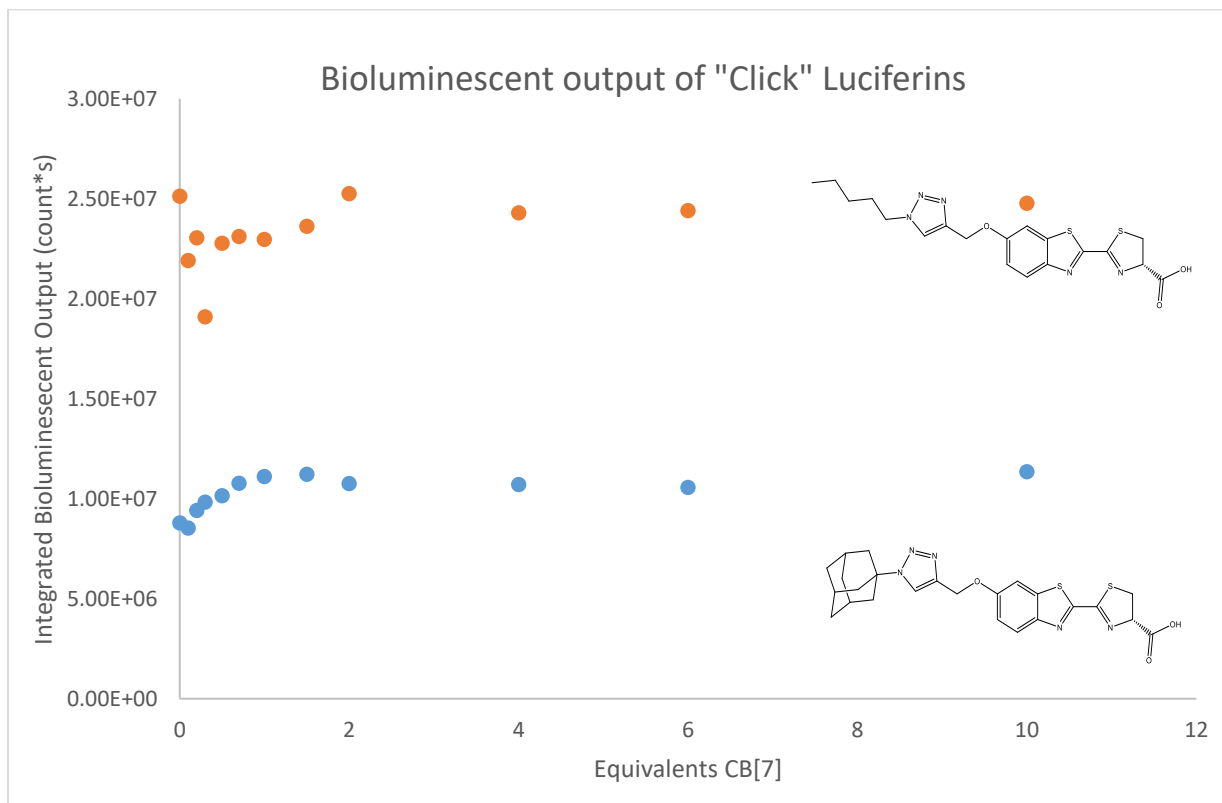


Figure 3.5: Bioluminescent output of “click” luciferin analogues over the first 2 minutes of reaction time. There is no significant trend from the titration with CB[7] in the case of luciferin-triazole-pentane (**X**). The triazole-adamantane functionalized luciferin (**VII**) shows an increase in output as the concentration of CB[7] increases.

In conclusion, luciferin-oxyethyl-quinuclidinium (**II**) showed a negative correlation between reaction rate and increasing CB[7]. This implies there is a strong binding of CB[7] to the quinuclidine moiety which sterically hinders the interaction with the enzyme. Future applications using cationic luciferin analogues would require an increase in its affinity for luciferase, and potential removal of the 2-carbon linker to



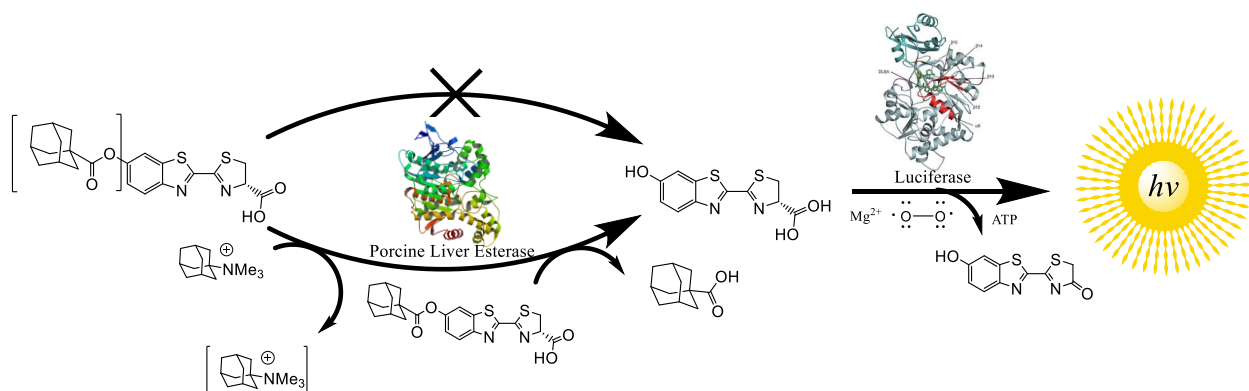
increase the effects of sterics. Removal of the 2 arginine residues at the portal of wildtype luciferase and replacement with 2 anionic residues could also greatly increase affinity of luciferin-oxyethyl-quinuclidinium (**II**) to luciferase thus increasing bioluminescent signal. In the synthesis and development of orthogonal luciferin-luciferase pairs, directed evolution procedures were used to engineer luciferases with selectivity for a single modified luciferin over other luciferins.<sup>[15]</sup> This same mechanism could be employed for similar applications with the cationic or “click” luciferins.

The “click” luciferins had a decreased activity with luciferase compared to native luciferin but showed amazing viability as wildtype luciferase substrates. With only a reduction by 90% and 97% in luciferin-triazole-pentane (**X**) and luciferin-triazole-adamantane (**VII**), respectively. This ligation method could be expanded to create a large library of readily available luciferin conjugate with great affinity for wildtype luciferase. Furthermore, luciferin-triazole-adamantane showed an increase in reaction rate which means there are competing factors for changes in bioluminescence, including but not limited to sterics, electrostatics, and aggregation.

In general, the addition of CB[7] to these substrates did not have a large effect on their bioluminescent outputs, but they were still viable substrates for luciferase. These substrates were also poor light emitters compared to native luciferin, so a new mechanism was developed for monitoring host-guest chemistry by a supramolecular caging. This strategy uses of an adamantyl ester functionalized luciferin, and is discussed in the next section.

### Section 3.3: An Ester Functionalized Luciferin Analogue as an *in vitro* Probe for Host-Guest Chemistry With CB[7]

The caging mechanism using luciferin adamantanoate is like that used in section 3.2 (Scheme 3.1), but will take advantage of the low bioluminescent flux observed with 6' functionalized luciferins. In this mechanism, the host-guest complex is caged from interacting with an esterase, rather than luciferase, preventing the ester modified luciferin's cleavage to native luciferin and 1-adamantylcarboxylic acid. The native luciferin has a 500-fold increase in bioluminescence so a large change in signal should be observed upon the addition of a strong competitive guest (Scheme 3.2).



*Scheme 3.2:* Proposed mechanism for supramolecular caging of novel ester linked luciferin substrate. Luciferin adamantanoate:CB[7] complex is not a viable substrate for porcine liver esterase due to the position of the host (square brackets) on the hydrophobic group, thus the complex is in an inert form until a strong CB[7] binder (adamantyl trimethylammonium) is added. This frees the luciferin adamantanoate (**XII**) and it can be cleaved into firefly luciferin and 1-adamantylcarboxylic acid. Firefly luciferin is oxidized in the presence of ATP, magnesium cation, and molecular oxygen to give oxyluciferin and light. Thus, in the presence of a host, signal and kinetics of the reaction are expected to decrease. In the presence of a strong competitive binder, signal should increase greatly.

#### *Enzymatic hydrolysis of Luciferin Adamantanoate*

Using the difference in the fluorescence spectra of luciferin adamantanoate (**XII**), and native luciferin, the hydrolysis of luciferin adamantanoate to luciferin by porcine liver esterase could be monitored. Luciferin adamantanoate has a weak absorbance at 330 nm, and a weak emission at 533 nm following excitation at 330 nm. Luciferin, has a strong

absorbance at 330 nm and a strong emission at 533 nm (Figure 3.6). Thus, the catalysis can be monitored by the increase in signal at 533 nm which will correspond to the production of luciferin and not be effected by luciferin adamantanoate. This finding is used to determine the Michaelis-Menton parameters for this catalysis, and to determine inhibition of this reaction by addition of CB[7] to form the host-guest complex.

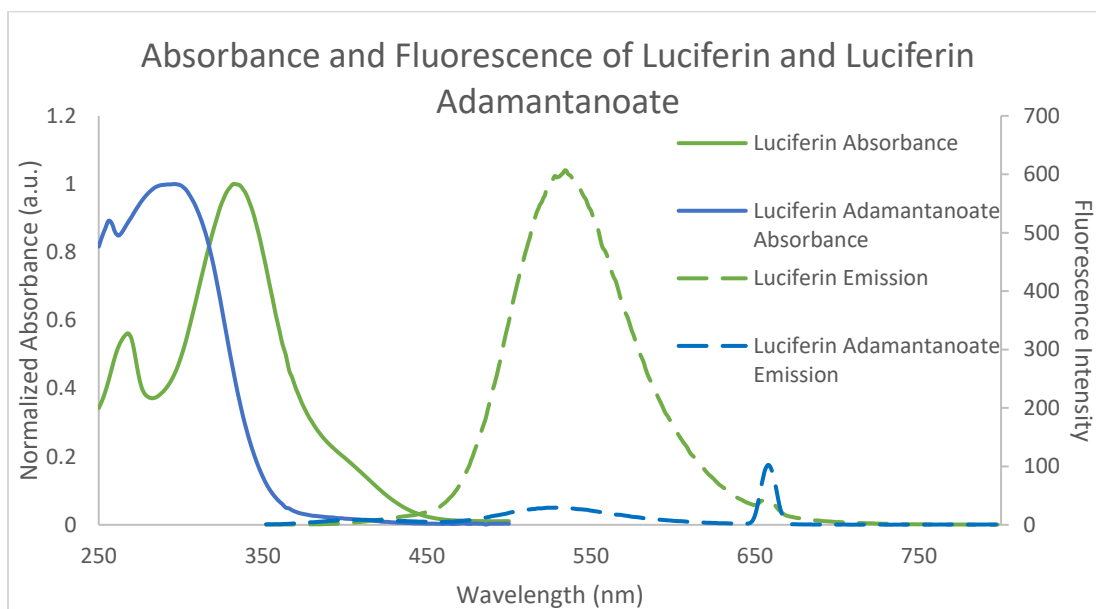


*Figure 3.6:* Luciferin and luciferin-adamantanoate (**XII**) have very different absorbance and emission spectra. Luciferin's peak absorbance is 330 nm, its corresponding emission peak is 535 nm. The adamantanoate has a peak absorbance at 296 nm. When excited at 330 nm there is a small peak at 408 nm with a very small value corresponding to luciferin adamantanoate and another at 535 nm that is slightly larger, which corresponds to native luciferin impurity generated from solvolysis. A peak at 660 nm is observed in both emission spectra corresponding to the first overtone of the excitation wavelength.

Luciferin adamantanoate (**XII**) was shown to have a Michaelis-Menton constant of 21.3  $\mu\text{M}$  with porcine liver esterase; this was used to design the inhibition assays based on the Michael-Menton constant representing the concentration at which the enzyme is operating at  $\frac{1}{2}V_{\text{max}}$ . In this regime, the response of enzyme activity to changes in the environment should be approximately linear because the enzyme is not saturated with substrate.

Michaelis-menton kinetics (following equation) were used to fit the data in Figure 3.7:

$$v = V_{\max} * \frac{[S]}{K_M + [S]}$$

Where  $v$  represents the observed initial reaction velocity,  $[S]$  represents the substrate concentration, and  $K_M$  represents the Michaelis-Menton constant. The fitting was performed to minimize the sum of squared residuals between the observed reaction velocity,  $v$ , and the predicted reaction velocity. These values were derived from a plot akin to Figure 3.8.

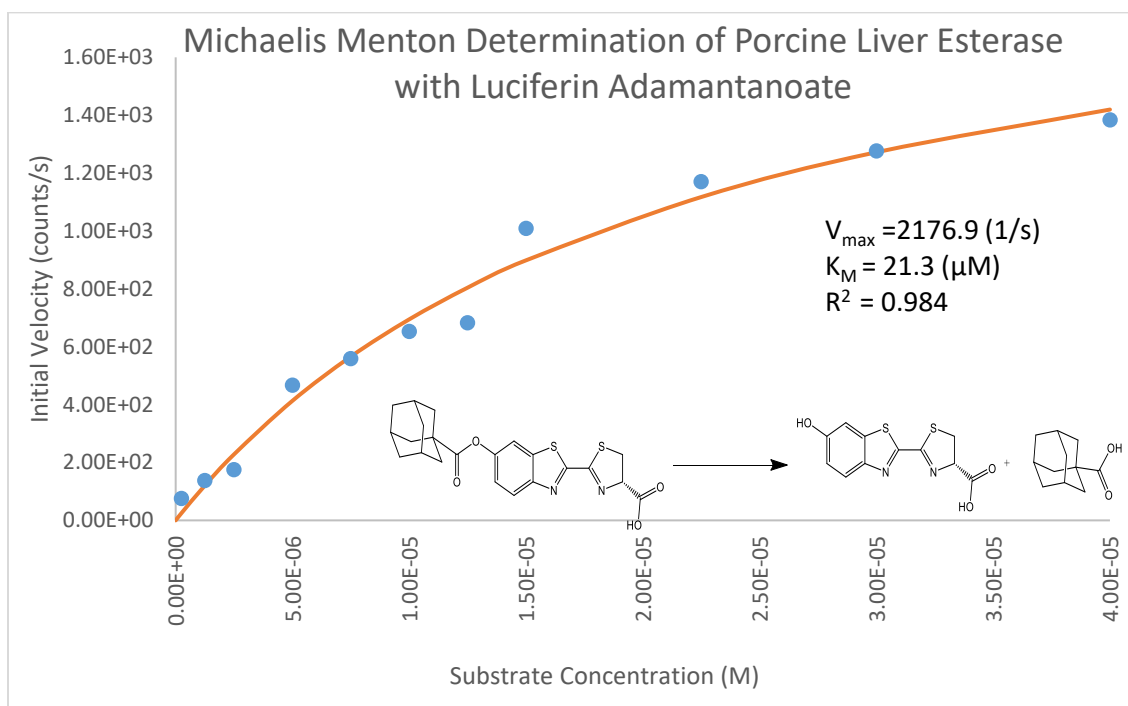


Figure 3.7: A Michaelis-Menton plot was used to determine the  $K_M$  and maximum velocity of the reaction. Fitting was performed in Microsoft Excel by minimizing the summed square difference.

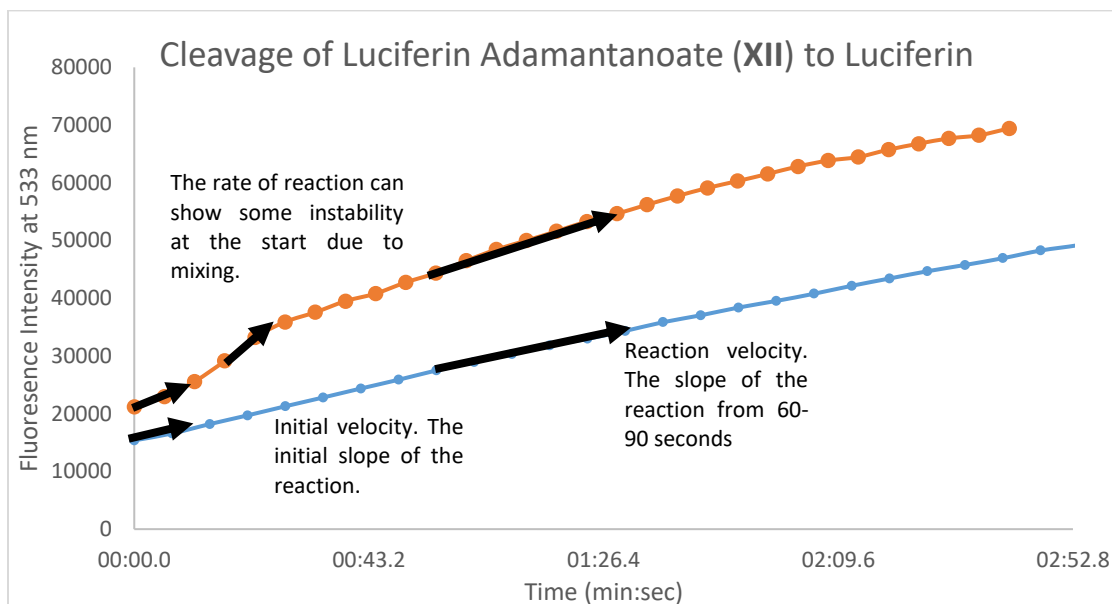
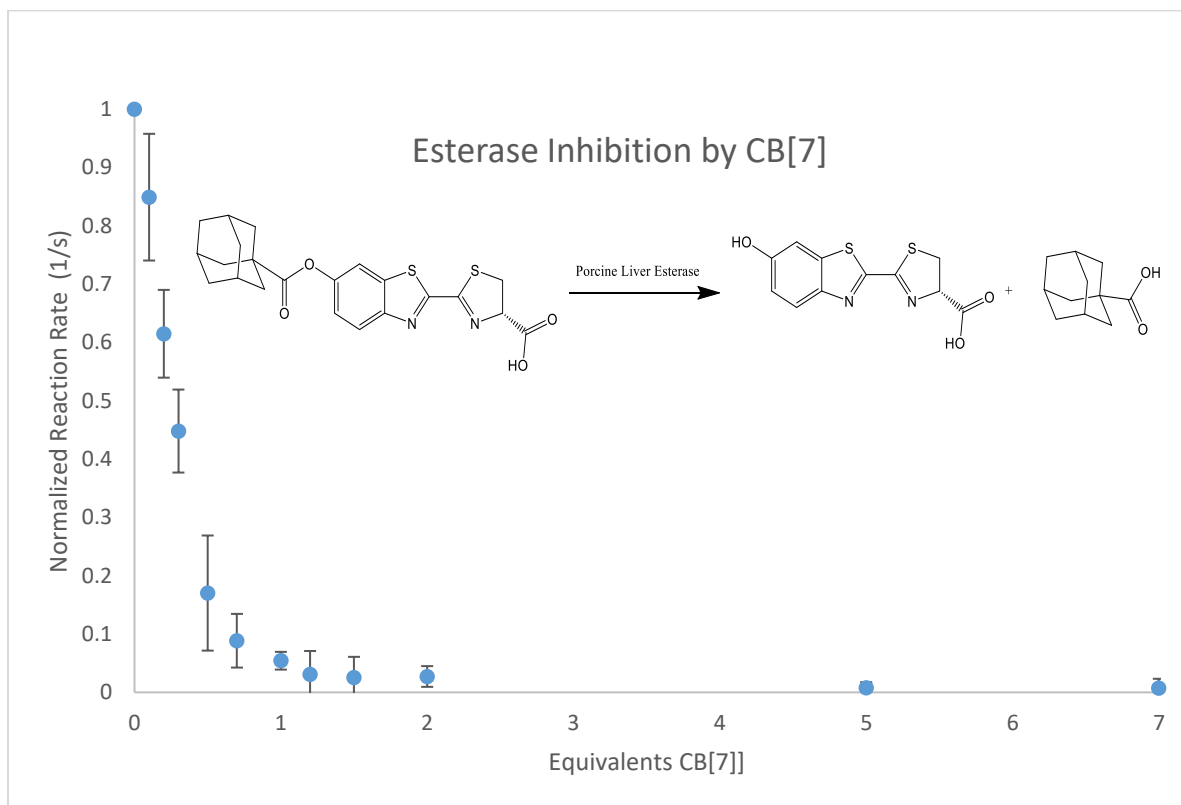
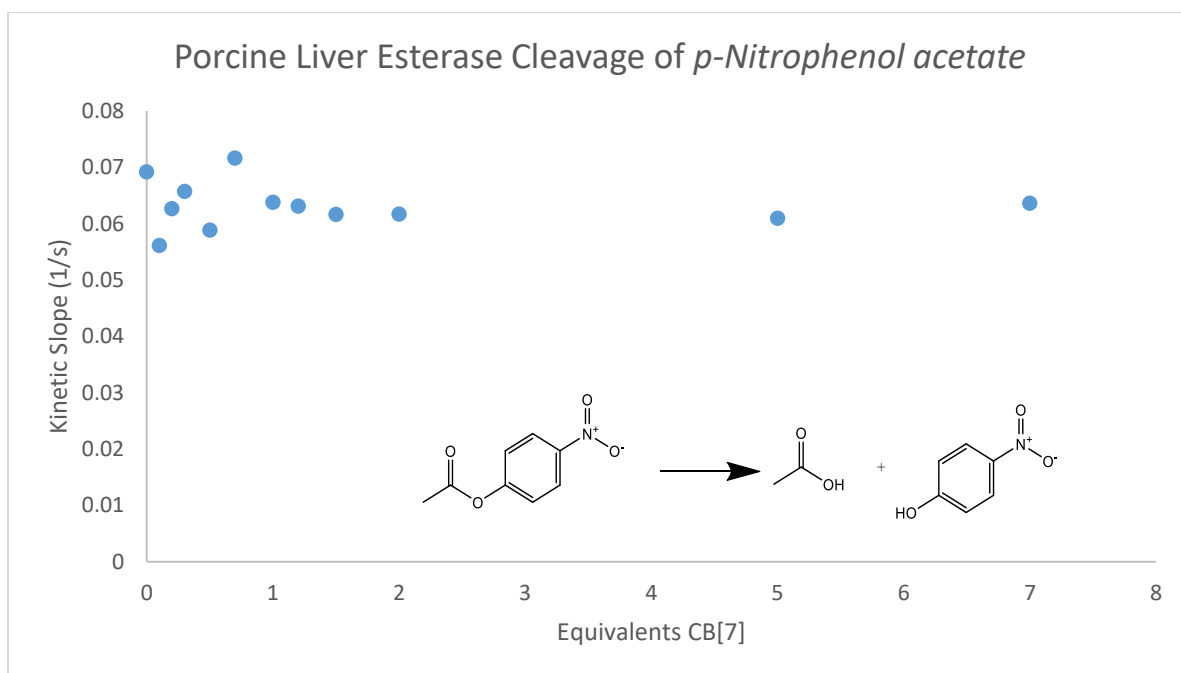


Figure 3.8: The cleavage of luciferin adamantanoate (XII) to native luciferin was monitored by fluorescence intensity at 533 nm after excitation at 330 nm. The initial velocity used to determine the Michael-Menton parameters was derived from the initial slope of the reaction. This is based off the assumption that the concentration of substrate is approximately equal to the concentration of substrate after the first data point is collected. Reaction velocity used to demonstrate inhibition of the esterase by host-guest assembly of luciferin-adamantanoate and CB[7] was determined from the average change in fluorescence between 60 and 90 seconds. This was used to minimize fluctuations in signal following the initial addition of esterase that could occur from diffusion or mixing.

Addition of CB[7] showed a precipitous drop in porcine liver esterase activity as monitored by the emission at 533 nm following excitation at 330 nm. At 1 equivalent of CB[7] the reaction progressed at  $5.4 \pm 1.5\%$  of its original rate. By 5 equivalents of CB[7] the reaction had slowed to  $0.75 \pm 0.1\%$  of its original rate (Figure 3.9). Additionally, using *p*-nitrophenol acetate as a non-CB[7]-binding substrate, it was shown CB[7] has no effect on enzyme activity due to interaction with the enzyme (Figure 3.10). The reaction rate was relatively stable during the first minutes of the reaction after an initial jump and instability following addition of the esterase. This initial jump was more likely a result of reaching equilibrium thus the reaction rate was determined from the second minute of monitoring (Figure 3.8).



**Figure 3.9:** The luciferin adamantanoate:CB[7] complex is effectively shielded from esterase activity. At 1 equivalent the reaction has slowed to  $5.4 \pm 1.5\%$  of its original rate. Error bars represent standard error from six experiments.



**Figure 3.10:** CB[7] concentration has no effect on the kinetics of porcine liver esterase as determined by absorbance at 405 nm.

Aside from the initial fluorescence data, data points were taken 3 and 19 hours after the addition of enzyme. These showed the CB[7] continued to inhibit the enzymatic cleavage long after the enzyme was added. After 3 hours the fluorescent signal of the well with 5 equivalents of CB[7] was about 21% that of the well with no CB[7]. After 19 hours this had increased to about 65% (See SI-46).

In a displacement assay to demonstrate reactivation of the luciferin-adamantanoate (**XII**) after complexation with CB[7], it was shown that 1 equivalent of adamantyl trimethylammonium to CB[7] would increase the rate of reaction by about 4 times. Following this 5 equivalents and 10 equivalents of adamantyl trimethylammonium (ATMA) to CB[7] caused the rate to asymptotically approach about 65% the original rate of hydrolysis by porcine liver esterase (Figure 3.11). This demonstrates the ability to displace CB[7] from the luciferin adamantanoate and thus restoring enzyme activity reversibly.

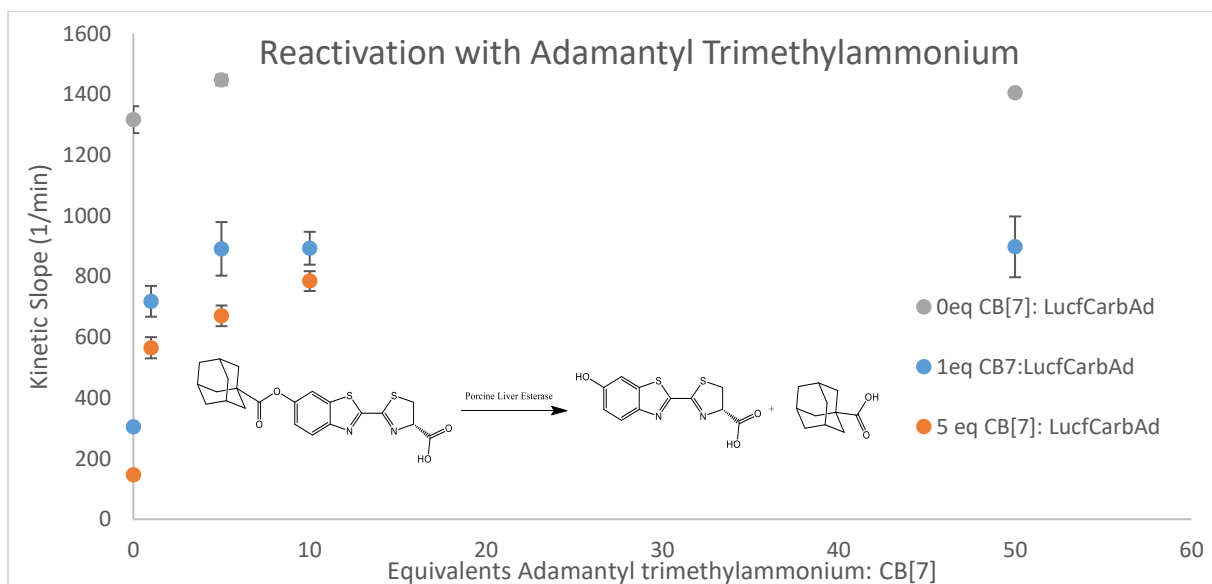


Figure 3.11: As determined by fluorescence, the addition of adamantyl trimethyl ammonium has no significant effect on the rate of enzyme catalyzed hydrolysis of luciferin adamantanoate (**XII**) to luciferin and adamantane carboxylic acid. To an already complexed system, CB[7] can be displaced by adamantyl trimethyl ammonium to restore hydrolytic susceptibility to luciferin adamantanoate.

Additionally, the conversion of luciferin adamantanoate (**XII**) to 1-adamantane carboxylic acid and native luciferin by enzymatic cleavage using porcine liver esterase was observed by bioluminescence in a tandem enzyme assay using luciferase to generate the signal photon (Figure 3.12). Knowing the 500-fold difference between native luciferin and the bioluminescence of luciferin adamantanoate by oxidation with luciferase made monitoring the enzymatic cleavage of luciferin adamantanoate to luciferin possible. Thus, this was an extremely powerful technique compared to the systems in chapter 2 with ether functionalized luciferins (Table 1.1). There is a consistent drop in kinetic slope as the concentration of CB[7] in the well increases. By 1 equivalent of CB[7] to luciferin adamantanoate the reaction rate drops to about 50% of its original velocity, and by 10 equivalents it is at about 7% of its original velocity (SI-47). Bioluminescence shows the same trend as fluorescence monitoring of the reaction thus the formation of the host-guest complex can be detected by either fluorescence or bioluminescence (Figure 3.9, Figure 3.12).

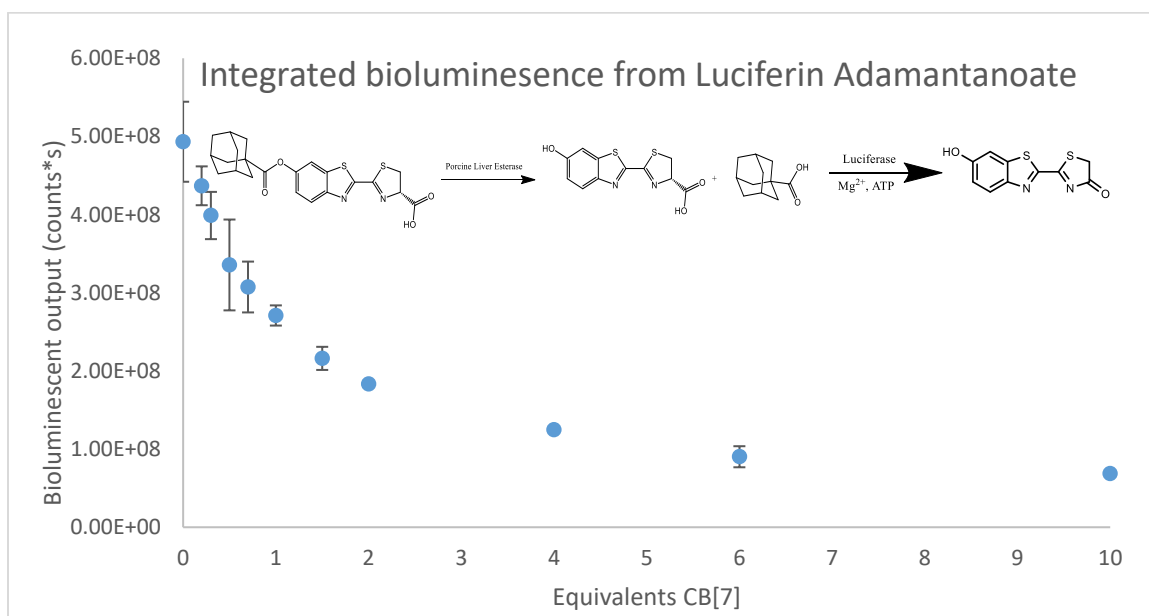


Figure 3.12: As the concentration of CB[7] increases, there is a quick drop in porcine liver esterase activity as determined by the bioluminescent output of the Luciferin-Luciferase reaction.



A displacement assay analogous to that performed using fluorescence was run with bioluminescence as the detection method. In this assay it was shown that incubation with adamantyl trimethylammonium could displace CB[7], making the luciferin adamantanoate (**XII**) a viable substrate for porcine liver esterase. The product of this hydrolysis, luciferin, is detectable in the presence of luciferase, ATP, and  $Mg^{2+}$ . The kinetic slope of the bioluminescence reaction increased to 53% to that of the uninhibited rate after 1 equivalent of ATMA was used to displace the CB[7] from the CB[7]:luciferin-adamantanoate complex. After 5 equivalents of ATMA to CB[7], the rate increased to 60% of its original rate. This same trend was observed using fluorescence to monitor displacement thus the dissociation of a host-guest complex using this system design could be shown using both fluorescence and bioluminescence (SI-48).

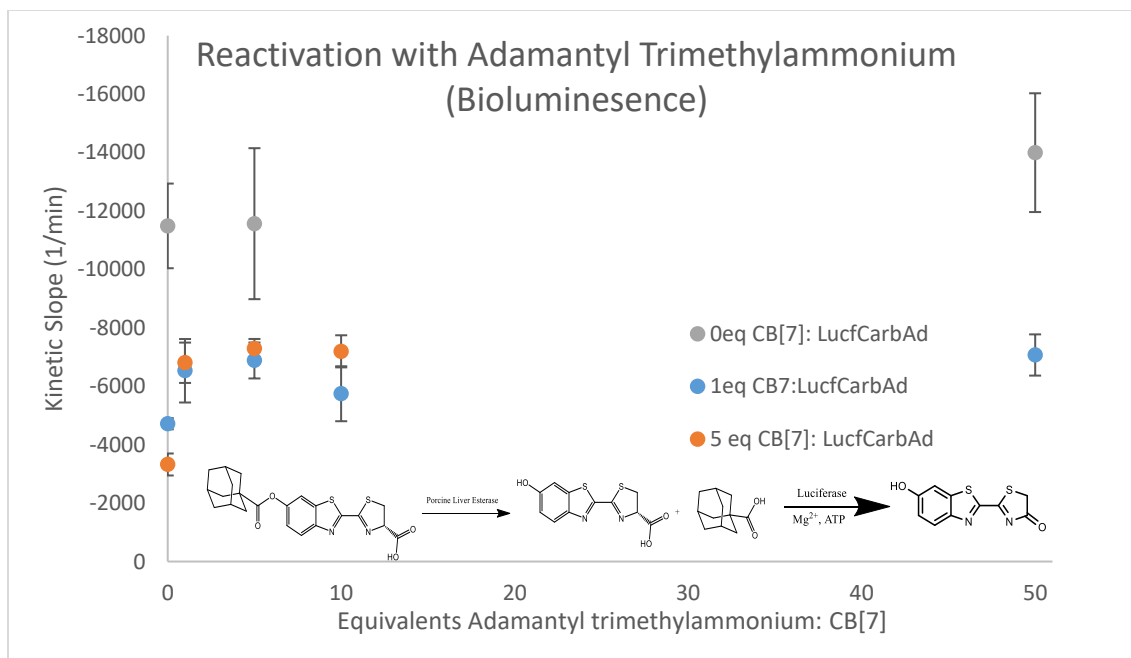


Figure 3.13: As determined by bioluminescence, the addition of adamantyl trimethyl ammonium has no significant effect on the rate of enzyme catalyzed hydrolysis of luciferin adamantanoate (**XII**) to luciferin and adamantane carboxylic acid, though there is an increase. To an already complexed system, CB[7] can be displaced by adamantyl trimethyl ammonium to restore hydrolytic susceptibility to luciferin adamantanoate.

Collectively these assays show successful design of a luciferin analogue is that a viable enzyme substrate for both luciferase and porcine liver esterase. Furthermore, this substrate show changes in reactivity with porcine liver esterase as the concentration of CB[7] increases in the solution, meaning the rate of reaction can be used as a proxy to measure complexation with CB[7] *in situ*.

CB[7] either protects the ester linkage of luciferin adamantanoate (**XII**) from porcine liver esterase or makes the complex too bulky to enter the enzyme pocket. This results in a decrease in reaction rate as measured by both fluorescence and bioluminescence. Controls using *p*-nitrophenol acetate as substrate for porcine liver esterase showed CB[7] had no effect on the reaction rate, thus only the formation of the host-guest complex effected the rate of cleavage of luciferin adamantanoate to luciferin and 1-adamantylcarboxylic acid. Secondly, there is a measurable change in reaction rate when a strong competitive binder, ATMA, is added to displace the guest from the CB[7]. An important note is that luciferin adamantanoate eventually degrades by solvolysis in solution thus optimization of this assay could include the development of a stronger linker such as an amide coupled with an amidase and modified luciferase

With this data, the development of luciferin analogues that can be used to characterize host-guest chemistry *in vivo* for specific applications can begin. In all, this data shows both up regulation and down regulation of a luciferase-luciferin system is possible and detectable by bioluminescence which is novel and provides more tools to probe the complex cellular environment. In the future, work will be carried out to show that this strategy is viable in complex cellular environments.

This thesis continued to explicate the development of modified luciferins for applications in biocompatible detection of supramolecular interactions, most specifically, host-guest chemistry. Fluorescence as a technique has been used in many occasions to observe host-guest chemistry, but the major limitation is the requirement for 2 photons to pass through a cell or tissue.<sup>[23]</sup> Bioluminescence eliminates the excitation photon so only a single photon needs to pass through tissue or a cell to be detected. It can also be used in the near future to detect, *in vivo*, any number of strong CB[7] binders such as pharmaceutically relevant molecules with poor solubility.<sup>[24]</sup>

As a biologically viable set of small molecules there is a huge potential for applications using the ligation techniques developed in the work preceding this thesis to tune the effects that were demonstrated successfully in this thesis. The next logical step in this work will be to perform assays in luciferase transfected cells to show the effects shown *in vitro* will be observable in the complex *in vivo* environment.

### Section 3.4: Experimental

Note: For further reference, solutions used in these assays had the following composition and were adjusted to pH 8.

- General Buffer Solution (30.0 mM HEPES, 5.00 mM MgSO<sub>4</sub>)
- Luciferase Solution (30.0 mM HEPES, 5.00 mM MgSO<sub>4</sub>, 70.0 mM DTT, 9 µg/mL Luciferase)
- Porcine Liver Esterase Solution (30.0 mM HEPES, 5.00 mM MgSO<sub>4</sub>, 30 µg/mL)
- Initiator Solution (30 mM HEPES, 5 mM MgSO<sub>4</sub>, 7.42mM Na<sub>2</sub>ATP)
- Enzyme Substrate Solution (30 mM HEPES, 5 mM MgSO<sub>4</sub>, 50 µM Luciferin analogue)
- CB[7] Solution (30 mM HEPES, 5 mM MgSO<sub>4</sub>, 100 µM CB[7])

#### *Fluorescence Spectra*

In general, a QS High Precision Cell (10mm Pathlength, Hellma Analytics) with 1mL enzyme substrate solution (30 mM HEPES, 5 mM MgSO<sub>4</sub>, 50 µM Luciferin/analogue) was excited at 330 nm and scanned from 350-800 nm in a fluorimeter (Cary Eclipse). The blank was taken as the general buffer solution (30 mM HEPES, 5 mM MgSO<sub>4</sub>). It showed no signal besides the Overtone

#### *Bioluminescence with Luciferase*

In general, assays were performed in triplicate in a white 96-well plate. Each well contained 20 µL enzyme substrate solution, 10 µL luciferase solution, 0-100 µL of 100 µM CB[7] solution, and 100-0 µL of general buffer to give a volume of 130 µL. After shaking for 10 minutes, 70 µL of initiator solution was added manually and the plate was

inserted into the Platerreader. Kinetics were monitored by luminescence at 5 second intervals for 50 repeats.

(Final concentrations: 30 mM HEPES, 5 mM MgSO<sub>4</sub>, 3.5 mM DTT, 2.60 mM Na<sub>2</sub>ATP, 5μM luciferin analogue 0.45 μg/mL Luciferase)

#### *Michaelis Menton Parameter Determination*

Assays were performed in triplicate in a black 96-well plate. Each well contained 0-160 μL luciferin adamantanoate (**XII**) solution (1% DMSO) and 160-0 μL of general buffer solution to give a volume of 160 μL. To this, 40 μL of Porcine Liver Esterase was added manually and the plate was inserted into the Platerreader. Kinetics was monitored by fluorescent emission at 533 nm after excitation at 330nm.

(Final concentrations: 30 mM HEPES, 5 mM MgSO<sub>4</sub>, 0-40 μM luciferin adamantanoate, 0-0.8% DMSO, 6 μg/mL Porcine Liver Esterase)

#### *Hydrolysis of Luciferin Adamantanoate*

Assays were performed in triplicate in a black 96-well plate. Each well contained 40μL luciferin adamantanoate (**XII**) solution (1% DMSO) 0-140 μL of 100 μM CB[7] solution, and 140-0 μL of general buffer solution a volume of 180 μL. After shaking for 10 minutes, 20 μL of Porcine Liver Esterase Solution was added manually and the plate was inserted into the Platerreader. Kinetics was monitored by fluorescent emission at 533 nm after excitation at 330nm. This was done at 5 second intervals for 30 repeats. A subsequent scan of the plate was performed 3 hours and 19 hours later.

(Final concentrations: 30 mM HEPES, 5 mM MgSO<sub>4</sub>, 10 μM luciferin adamantanoate, 0.2% DMSO, 3 μg/mL Porcine Liver Esterase, 0-70 μM CB[7])

Displacement assays were performed in triplicate in a black 96-well plate. Each well contained 20 μL luciferin adamantanoate (**XII**) solution (1% DMSO), 0, 10, or 50 μL of 100 μM CB[7] solution, 0-50 μL of 1mM adamantyl trimethylammonium in general buffer and 60-160 μL of general buffer solution to a total volume of 180 μL. After shaking for 30 minutes, 20 μL of Porcine Liver Esterase Solution was added manually and the plate was inserted into the Platereader. Kinetics was monitored by fluorescent emission at 533nm after excitation at 330nm. This was done at 40 second intervals for 100 repeats (Final concentrations: 30 mM HEPES, 5 mM MgSO<sub>4</sub>, 5 μM luciferin adamantanoate, 0.1% DMSO, 3 μg/mL Porcine Liver Esterase, 0-50 μM CB[7], 0-250 μM adamantyl trimethylammonium)

#### *Hydrolysis of p-nitrophenol acetate*

**CB[7]:** Assays were performed in a clear 96-well plate. Each well contained 5 μL *p*-nitrophenol acetate (1mM), 0-70 μL 100 μM CB[7] solution, and 85-15 μL of general buffer to give a solution volume of 90 μL. To this 10 μL of Porcine Liver Esterase solution was added manually to start the reaction. The reaction was monitored by absorbance at 405nm and repeats were taken every 12 seconds

(Final concentrations: 30 mM HEPES, 5 mM MgSO<sub>4</sub>, 50 μM *p*-nitrophenol acetate, 3 μg/mL Porcine Liver Esterase, 0-70 μM CB[7])

*Hydrolysis of Luciferin Adamantanoate as determined by Bioluminescence*

Assays were performed in triplicate in a white 96-well plate. Each well contained 20  $\mu\text{L}$  luciferin adamantanoate (**XII**) solution, 10  $\mu\text{L}$  luciferase solution, 0-100  $\mu\text{L}$  of CB[7] solution, and 100-0  $\mu\text{L}$  of general buffer to give a volume of 130  $\mu\text{L}$ . After shaking for 10 minutes, 50  $\mu\text{L}$  of initiator solution and 20  $\mu\text{L}$  Porcine Liver Esterase Solution of was added manually (simultaneously). and the plate was inserted into the Platereader.

Kinetics were monitored by luminescence.

(Final concentrations: 30 mM HEPES, 5 mM  $\text{MgSO}_4$ , 3.5 mM DTT, 1.86 mM  $\text{Na}_2\text{ATP}$ , 5  $\mu\text{M}$  luciferin adamantanoate, 0-50  $\mu\text{M}$  CB[7], 0.45  $\mu\text{g}/\text{mL}$  Luciferase, 3  $\mu\text{g}/\text{mL}$  Porcine Liver Esterase.

Displacement assays were performed in triplicate in a white 96-well plate. Each well contained 20  $\mu\text{L}$  luciferin adamantanoate (**XII**) solution (1% DMSO), 0, 10, or 50  $\mu\text{L}$  of 100  $\mu\text{M}$  CB[7] solution, 0-50  $\mu\text{L}$  of 1mM adamantyl trimethylammonium in general buffer, and 0-160  $\mu\text{L}$  of general buffer solution a total volume of 130  $\mu\text{L}$ . After shaking for 30 minutes, 50  $\mu\text{L}$  of initiator solution and 20  $\mu\text{L}$  Porcine Liver Esterase Solution of was added manually (simultaneously) and the plate was inserted into the Platereader.

Kinetics were monitored by luminescence.

(Final concentrations: 30 mM HEPES, 5 mM  $\text{MgSO}_4$ , 3.5 mM DTT, 1.86 mM,  $\text{Na}_2\text{ATP}$ , 5  $\mu\text{M}$  luciferin adamantanoate, 0.1% DMSO, 0-50  $\mu\text{M}$  CB[7], 0-250  $\mu\text{M}$  adamantyl trimethylammonium, 0.45  $\mu\text{g}/\text{mL}$  Luciferase, 3  $\mu\text{g}/\text{mL}$  Porcine Liver Esterase)

## References

1. Steed, J. W.; Atwood, J. L. *Supramolecular Chemistry*; Wiley-blackwell: Chicester, 2013.
2. Rekharsky, M. V.; Mori, T.; Yang, C.; Ko, Y. H.; Selvapalam, N.; Kim, H.; Sobransingh, D.; Kaifer, A. E.; Liu, S.; Isaacs, L.; Chen, W.; Moghaddam, S.; Gilson, M. K.; Kim, K.; Inoue, Y. *Proceedings of the National Academy of Sciences* 2007, 104 (52), 20737–20742.
3. Wyman, I. W. *Host-guest chemistry between cucurbit[7]uril and neutral and cationic guests*, 2010.
4. Assaf, K. I.; Nau, W. M. *Chem. Soc. Rev.* 2015, 44 (2), 394–418.
5. Wang, Q.; Chen, Y.; Liu, Y. *Polymer Chemistry* 2013, 4 (15), 4192.
6. Gould, S. J.; Subramani, S. *Analytical Biochemistry* 1988, 175 (1), 5–13.
7. Meighen, E.A. *Microbiological Reviews* 1991, 55 (1), 123-142
8. Fan, F.; Binkowski, B. F.; Butler, B. L.; Stecha, P. F.; Lewis, M. K.; Wood, K. V. *ACS Chemical Biology* 2008, 3 (6), 346–351.
9. Feng, P.; Zhang, H.; Deng, Q.; Liu, W.; Yang, L.; Li, G.; Chen, G.; Du, L.; Ke, B.; Li, M. *Analytical Chemistry* 2016, 88 (11), 5610–5614. Branchini, B. R.; Behney, C. E.;
10. Southworth, T. L.; Fontaine, D. M.; Gulick, A. M.; Vinyard, D. J.; Brudvig, G. W. *Journal of the American Chemical Society* 2015, 137 (24), 7592–7595.
11. Li, J.; Chen, L.; Du, L.; Li, M. *Chem. Soc. Rev.* 2013, 42 (2), 662–676.
12. Mofford, D. M.; Adams, S. T.; Reddy, G. S. K. K.; Reddy, G. R.; Miller, S. C. *Journal of the American Chemical Society* 2015, 137 (27), 8684–8687.
13. Kojima, R.; Takakura, H.; Kamiya, M.; Kobayashi, E.; Komatsu, T.; Ueno, T.; Terai, T.; Hanaoka, K.; Nagano, T.; Urano, Y. *Angewandte Chemie* 2015, 127 (49), 14981–14984.
14. Steinhardt, R. C.; O'Neill, J. M.; Rathbun, C. M.; Mccutcheon, D. C.; Paley, M. A.; Prescher, J. A. *Chemistry - A European Journal* 2016, 22 (11), 3671–3675.
15. Jones, K. A.; Porterfield, W. B.; Rathbun, C. M.; Mccutcheon, D. C.; Paley, M. A.; Prescher, J. A. *Journal of the American Chemical Society* 2017, 139 (6), 2351–2358.
16. Kaskova, Z. M.; Tsarkova, A. S.; Yampolsky, I. V. *Chem. Soc. Rev.* 2016, 45 (21), 6048–6077.
17. Reddy, G. R.; Thompson, W. C.; Miller, S. C. *Journal of the American Chemical Society* 2010, 132 (39), 13586–13587.
18. St-Jacques, A. D.; Wyman, I. W.; Macartney, D. H. *Chemical Communications* 2008, No. 40, 4936.
19. Saleh, N. E. I.; Suwaid, A. R. B.; Alhalabi, A.; Abuibaid, A. Z. A.; Maltsev, O. V.; Hintermann, L.; Naumov, P. *The Journal of Physical Chemistry B* 2016, 120 (31), 7671–7680.
20. Thordarson, P. *Chem. Soc. Rev.* 2011, 40 (3), 1305–1323.
21. Conti, E.; Franks, N. P.; Brick, P. *Structure* 1996, 4 (3), 287–298.
22. Nakatsu, T.; Ichiyama, S.; Hiratake, J.; Saldanha, A.; Kobashi, N.; Sakata, K.; Kato, H. *Nature* 2006, 440 (7082), 372–376.
23. Guo, D.-S.; Uzunova, V. D.; Su, X.; Liu, Y.; Nau, W. M. *Chemical Science* 2011, 2 (9), 1722.



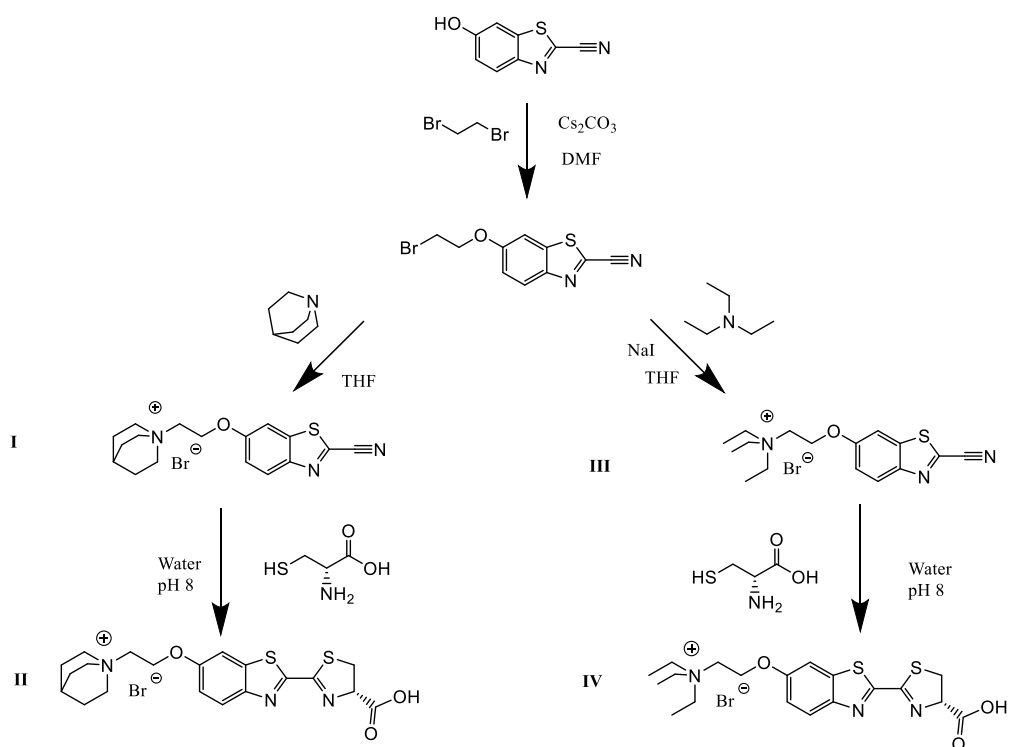
24. Ma, D.; Hettiarachchi, G.; Nguyen, D.; Zhang, B.; Wittenberg, J. B.; Zavalij, P. Y.; Briken, V.; Isaacs, L. *Nature Chemistry* 2012, 4 (6), 503–510.
25. Rahn, H. P. Unpublished manuscript 2016, Tulane University, New Orleans, LA
26. Toya, Y.; Takagi, M.; Kondo, T.; Nakata, H.; Isobe, M.; Goto, T. *Bulletin of the Chemical Society of Japan* 1992, 65 (10), 2604–2610.
27. BindFit v0.5 | Supramolecular. (n.d.). Retrieved April 16, 2017, from <http://app.supramolecular.org/bindfit/>
28. Yi, S.; Kaifer, A. E. *The Journal of Organic Chemistry* 2011, 76 (24), 10275–10278.

## Supporting Information:

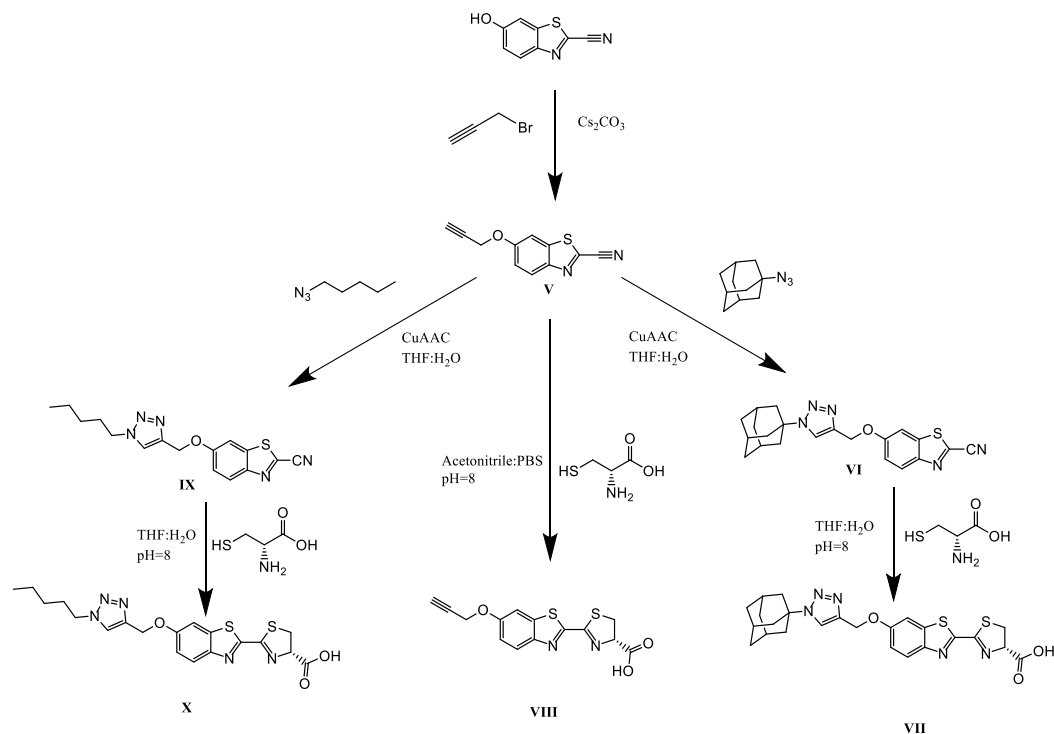
### SI.1 Synthesis of Functionalized Luciferins

\*High resolution mass spectrometry was performed at the Georgia Institute of Technology Bioanalytical Mass Spectrometry Facility.

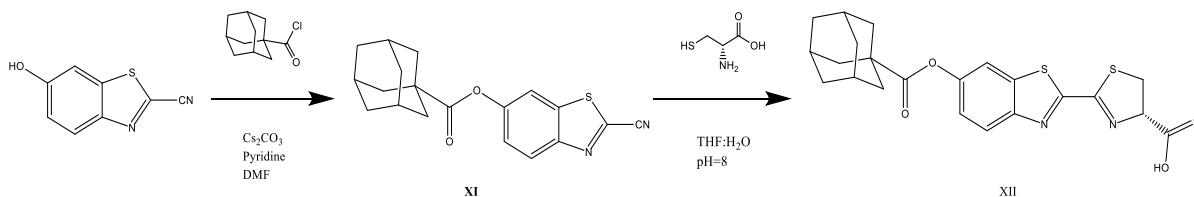
\*Much of the synthesis work was completed to satisfy the Honor's Thesis requirement. Work specifically created for this thesis includes mass spectrometry of all samples, synthesis of luciferin-adamantanoate (**XII**), and finalized characterization of all samples<sup>[25]\*</sup>



Scheme SI.1: Synthetic scheme of cationic 6'-hydroxyl functionalized luciferins, luciferin-oxyethyl-quinuclidinium bromide (**II**), luciferin-oxyethyl-triethylammonium bromide (**IV**).



Scheme SI.2: Synthetic scheme of “Click” ligated 6'- Hydroxyl Functionalized Luciferins: *luciferin-triazole-pentane (X)*, *luciferin-triazole-adamantane (VII)*, *luciferin-alkyne (VIII)*.



Scheme SI.3: Synthetic scheme of Adamantyl Ester Luciferin (**XII**).

### Synthesis of Luciferin Adamantanoate (**XII**)

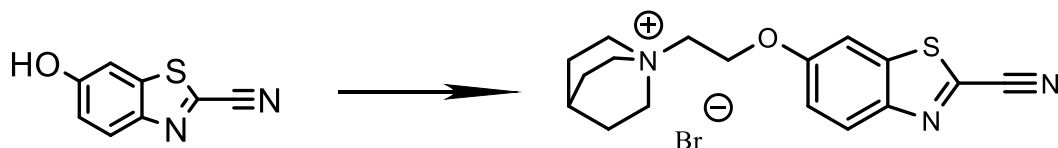
The last molecule synthesized for this study is a phenolic ester with an adamantyl alkoxy group. This species is neutrally charged at its 6' end and should have similar properties to the luciferin made from the click reaction with 1-azidoadamantane. However, this molecule has two key differences. Firstly, it is labile to solvolysis in basic aqueous conditions; secondly it is labile to esterases which are found throughout living cells. The product of the esterase reaction is 1-adamantylcarboxylic acid and native luciferin which is evolutionarily optimized for binding and bioluminescence with the luciferase enzyme, thus overcoming the reduced luminescence of common luciferin analogues. Secondly binding of CB[7] to the ester can protect the ester from esterase activity, rendering the molecule inert to both esterases and luciferase until the host is unbound. This product will need to overcome severe penalties in solubility due to its very hydrophobic nature.

The synthesis of the 2-cyanobenzothiazole adamantanoate (**XI**) was originally modeled after a synthesis of several similar molecules by Toya *et. al* (1992)<sup>[26]</sup>, but this

synthesis was unsuccessful because of a lack of organic soluble base and low temperatures. However, a successful route was created using DMF as solvent with two equivalents of pyridine as catalyst. The poorly soluble product which was easily purified by column chromatograph after extraction into organic solvent and acidification.

The resulting white powder was transformed into the corresponding luciferin analogue by identical reaction conditions as the triazole compounds. Purification was unique because of the products high solubility in methanol and poor solubility in water. After all THF was removed and the mixture was extracted into ethyl acetate the crude was obtained by removal of ethyl acetate under reduced pressure. The crude was dissolved in minimal warm methanol. After the addition of water a white precipitate formed which was collected by centrifugation. The precipitate formed a yellow amber like substance with a distinct blue glow when put under UV light. The supernatant was green under UV-light corresponding to native luciferin formed by solvolysis in the previous reaction. Further purification to remove the 1-adamantyl carboxylic acid impurity was performed by sonicating the amber with hexanes and filtering or decanting. Characterization of the compound was achieved with both ESI and NMR.

Characterization data suggested the synthesis of the luciferin adamantanoate (**XII**) was successful. This compound should be suitable for binding of cucurbiturils, interaction with esterases and luciferase, and intentional degradation to native luciferin as a probe for host-guest interactions *in vivo*.



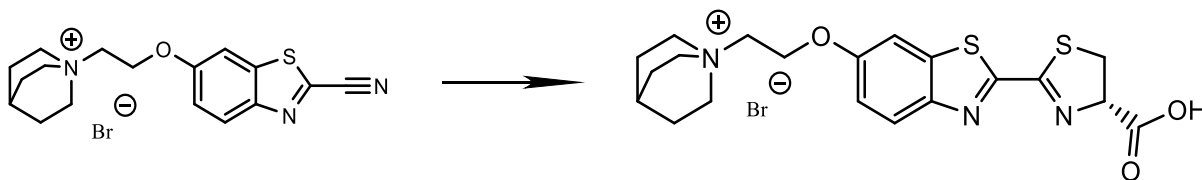
I

**(I) 1-(2-((2-cyanobenzo[d]thiazol-6-yl)oxy)ethyl)quinuclidin-1-ium bromide.** 6-hydroxybenzo[d]thiazole-2-carbonitrile (176 mg, 1 mmol) was dissolved in 25 mL DMF with Cs<sub>2</sub>CO<sub>3</sub> (650 mg, 2 mmol) and 860  $\mu$ L 1,2 dibromoethane (10 mmol). The reaction was held at 80<sup>o</sup>C for 72 hours. Solution was diluted with ethyl acetate and washed with 1M HCl solution and brine. The organic layer was isolated and the solvent was removed under vacuum to yield a yellow solid. 10mL of chloroform was then added to remove product from residual cesium salts. Solvent was removed under reduced pressure to yield 580 mg of crude mixture which was then placed under High Vacuum to remove all residual 1,2 dibromoethane. The crude was dissolved in 25 mL THF with quinuclidine (220 mg, 2 mmol). The solution was allowed to react at 40<sup>o</sup>C for 12 hours. A white precipitate was formed and collected by vacuum filtration and washed with THF to yield 154 mg (40%) of **I**, a white solid.

<sup>1</sup>H NMR (400 MHz D<sub>2</sub>O):  $\delta$  7.86 (d,  $J$  = 7 Hz, 1H), 7.42 (d,  $J$  = 4 Hz, 1H), 7.148 (dd,  $J$  = 9 Hz, 2Hz, 1H), 4.38 (t,  $J$  = 9 Hz, 2H), 3.50 (t,  $J$  = 9 Hz, 2H), 3.39 (t,  $J$  = 8 Hz, 6H), 2.00 (m,  $J$  = 3 Hz, 1H), 1.81 (t,  $J$  = 6Hz, 6H)

<sup>13</sup>C NMR (100 MHz D<sub>3</sub>CO):  $\delta$  158.4, 147.5, 137.7, 134.7, 125.5, 118.74, 112.9, 104.9, 63.2, 62.0, 55.6, 23.7, 19.6

ESI (m/z 314.125, [M-Br])<sup>+</sup>: Calculated for C<sub>17</sub>H<sub>20</sub>N<sub>3</sub>OS (314.132)



I

II

**(II) Luciferin-Oxyethyl-Quinuclidinium bromide.** **I** (50 mg, 0.127 mmol) was dissolved in 10 mL of a 1:4 acetonitrile: PBS mixture. D-cysteine (20 mg, 0.165 mmol) was added to the reaction mixture which was then allowed to stir at room temperature for 24 hours. The solvent was removed under reduced pressure to yield a brown crude mixture. A portion of this mixture was run through high performance liquid chromatography with a water acetonitrile gradient (0-100% over 30 minutes) to yield 22 mg of **II** as a white solid.

<sup>1</sup>H NMR (400 MHz D<sub>2</sub>O):  $\delta$  7.65 (d,  $J$  = 9 Hz, 1H), 7.32 (d,  $J$  = 2 Hz, 1H), 7.00 (dd,  $J$  = 9 Hz, 2 Hz, 1H), 5.00 (td,  $J$  = 8 Hz, 2 Hz, 1H), 4.32 (t,  $J$  = 4 Hz, 2H), 3.62 (t,  $J$  = 10 Hz, 1H), 3.46 (t,  $J$  = 4 Hz, 2H), 3.42 (d,  $J$  = 2 Hz, 1H), 3.38 (t,  $J$  = 8 Hz, 6H), 2.00 (m, 1H) 1.80 (t,  $J$  = 6 Hz, 6H)

HR-MS (ESI) (m/z 418.1240, [M-Br])<sup>+</sup>: Calculated for C<sub>20</sub>H<sub>24</sub>N<sub>3</sub>O<sub>3</sub>S<sub>2</sub> (418.1254)

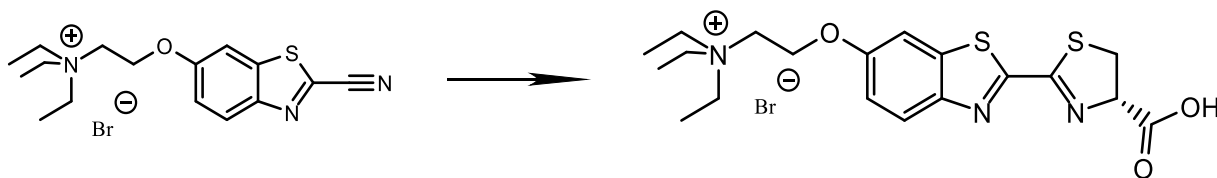
**III****(III) 2-((2-cyanobenzo[d]thiazol-6-yl)oxy)-N,N,N-triethylethan-1-aminium bromide.**

6-hydroxybenzo[d]thiazole-2-carbonitrile (176 mg, 1 mmol) was dissolved in 25 mL DMF with Cs<sub>2</sub>CO<sub>3</sub> (650 mg, 2 mmol) and 860  $\mu$ L 1,2 dibromoethane (10 mmol). The reaction was held at 80 °C for 24 hours. Solution was diluted with ethyl acetate and washed with 1 M HCl solution and brine. The organic layer was isolated and the solvent was removed under vacuum to yield a yellow solid. 10 ml of chloroform was then added to remove product from residual Cesium salts. Solvent was removed under reduced pressure to yield a crude oil then placed under High Vacuum to remove all residual 1,2 dibromoethane. The crude was dissolved in 25 mL THF with excess triethylamine (2 mL, 7.16 mmol) and a catalytic amount of NaI. The solution was allowed to reflux for 24 hours. A white precipitate was formed and collected by vacuum filtration and washed with THF to yield 85 mg (22%) of **III**, a white solid.

<sup>1</sup>H NMR (400 MHz D<sub>2</sub>O):  $\delta$  8.00 (d,  $J$  = 9 Hz, 1H), 7.56 (s, 1H), 7.28 (d,  $J$  = 7 Hz, 1H), 4.49 (t,  $J$  = 4 Hz, 2H), 3.73 (t,  $J$  = 4 Hz, 2H), 3.39 (q,  $J$  = 4 Hz, 6H), 1.27 (t,  $J$  = 7 Hz, 9H)

<sup>13</sup>C NMR (100 MHz D<sub>3</sub>CO):  $\delta$  162.0, 157.0, 156.5, 148.0, 138.0, 124.8, 117.2, 105.4, 62.1, 55.8, 53.8, 6.68

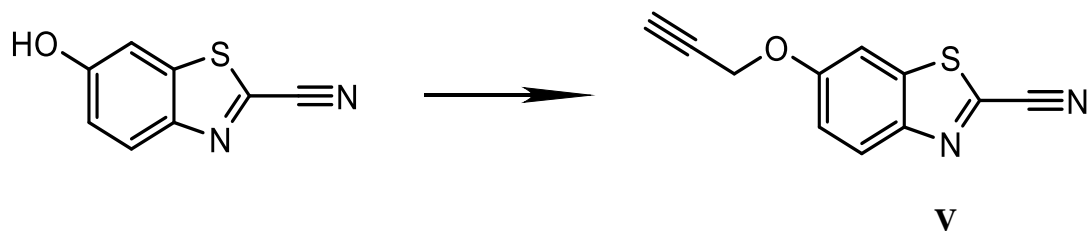
ESI (m/z 304.154 [M-Br]<sup>+</sup>): Calculated for C<sub>16</sub>H<sub>22</sub>N<sub>3</sub>OS (304.148)

**III****IV**

**(IV) Luciferin-Oxyethyl-Triethylammonium bromide.** **III** (50 mg, 0.13 mmol) was dissolved in 10 mL of water. D-cysteine HCl hydrate (30 mg, 0.17 mmol) was added to the reaction mixture. The pH was adjusted to 8.0 by addition of 2M NaOH and then allowed to stir at room temperature for 24 hours. The solution was dried under reduced pressure resulting in 80 mg of a crude brown solid. This was run through high performance liquid chromatography with a water-acetonitrile gradient (0-100% over 30 minutes) to yield a white solid, **IV**.

<sup>1</sup>H NMR (400 MHz D<sub>2</sub>O):  $\delta$  7.62 (d,  $J$  = 5 Hz, 1H), 7.27 (d,  $J$  = 1 Hz, 1H), 6.95 (dd,  $J$  = 5 Hz, 2 Hz, 1H), 4.99 (t,  $J$  = 9 Hz, 1H), 4.26 (t,  $J$  = 4.2 Hz, 2H), 3.62 (t,  $J$  = 10 Hz, 1H), 3.54 (t,  $J$  = 4.2 Hz, 2H), 3.43 (dd,  $J$  = 10 Hz 8 Hz, 1H), 3.24 (q,  $J$  = 7 Hz, 6H), 1.13 (t,  $J$  = 7 Hz, 9H)

HR-MS (ESI) (m/z 408.1398, [M-Br]<sup>+</sup>): Calculated for C<sub>19</sub>H<sub>26</sub>N<sub>3</sub>O<sub>3</sub>S<sub>2</sub> (408.1410)

**Method 1:**

**(V) 6-(prop-2-yn-1-yloxy)benzo[d]thiazole-2-carbonitrile:** 6-hydroxybenzo[d]thiazole-2-carbonitrile (176 mg, 1.00 mmol) was dissolved in 10 mL DMF with  $\text{Cs}_2\text{CO}_3$  (650 mg, 2.00 mmol) and stirred for 30 minutes. 870  $\mu\text{L}$  propargyl bromide solution (10 mmol, 80% in toluene) was added to the reaction mixture. The reaction was stirred for 24 hours at 80  $^\circ\text{C}$ . The reaction mixture was washed once with 50 ml 1M HCl after dilution into 30ml ethyl acetate. The mixture was then washed twice with brine. The crude mixture was then purified via column chromatography in a 1:3 EA: hexanes system and the product was then collected (RF= 0.5) and solvent was removed under reduced pressure to yield 60 mg (28 % yield) of **V** as an off yellow solid.

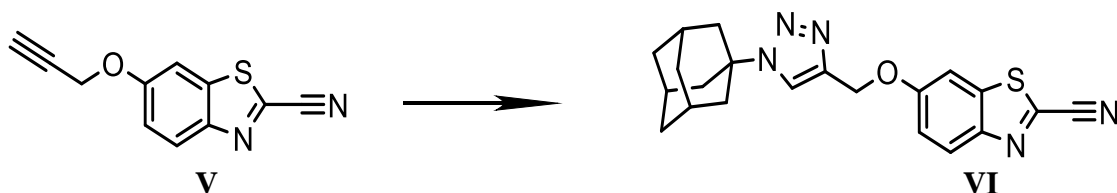
**Method 2:**

6-hydroxybenzo[d]thiazole-2-carbonitrile (176 mg, 1.00 mmol) was mixed with  $\text{Cs}_2\text{CO}_3$  (650 mg, 2.00 mmol). 870  $\mu\text{L}$  propargyl bromide solution (10 mmol, 80% in toluene) was added to the reaction mixture, with a catalytic amount of NaI. The reaction was allowed to stir at room temperature for 24 hours. The reaction mixture was then extracted into ethyl acetate, washed with water, and prepared for column chromatography with a 1:3 EA: Hexanes. The product migrated with an RF= 0.5. Solvent was removed under reduced pressure to yield 194 mg (91% yield) of **V**, an off yellow solid.

$^1\text{H}$  NMR (400 MHz  $\text{CDCl}_3$ ):  $\delta$  8.10 (d,  $J$ = 9.1 Hz, 1H), 7.47 (d,  $J$ = 4 Hz, 1H), 7.29 (dd,  $J$ = 9.1 Hz, 2.2 Hz, 1H), 4.80 (d,  $J$ = 1.9 Hz, 2H), 2.57 (s, 1H)

$^{13}\text{C}$  NMR (100 MHz  $\text{CD}_2\text{Cl}_2$ ):  $\delta$  158.4, 147.6, 137.5, 134.3, 126.0, 118.9, 113.4, 104.9, 77.7, 76.5, 56.7

ESI (m/z 215.046  $[\text{M}+\text{H}]^+$ : Calculated for  $\text{C}_{11}\text{H}_7\text{N}_2\text{OS}$  (215.027)

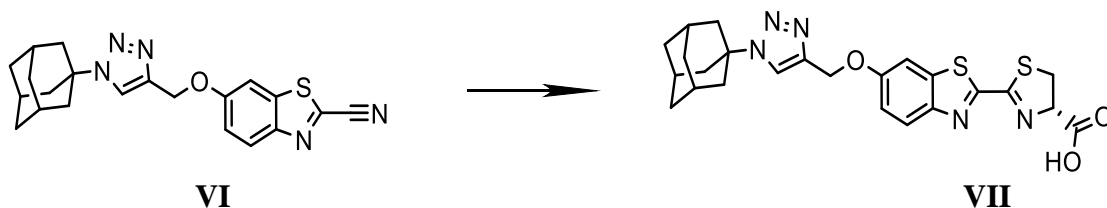


**(VI) 6-((1-((1S,3S)-adamantan-1-yl)-1H-1,2,3-triazol-4-yl)methoxy)benzo[d]thiazole-2-carbonitrile.** **V** (100 mg, 0.46 mmol) and 1-Azidoadamantane (83 mg, 0.46 mmol) were dissolved in 20 mL of 9:1 THF:  $\text{H}_2\text{O}$  and degassed with argon. Sodium ascorbate (240 mg, 5eq) and copper (II) sulphate pentahydrate (60 mg, 0.5eqs) were then added. The resulting mixture was refluxed at 50 $^\circ\text{C}$  for 24 hours, and the solvents were removed by rotary evaporation, extracted into EA, and washed with water and brine. The organic layer was removed. and solvent reduced to prepare for column chromatography in a 2:1 EA: Hexanes (RF=0.65) system to yield 74 mg of **VI** (40%) as a yellow-white solid.

$^1\text{H}$  NMR (400 MHz  $\text{CD}_2\text{Cl}_2$ ):  $\delta$  8.10 (d,  $J$ = 9Hz, 1H), 7.75 (s, 1H), 7.60 (d,  $J$ = 2 Hz, 1H), 7.30 (dd,  $J$ = 9 Hz, 2Hz, 1H), 5.27 (s, 2H), 2.25 (m, 9H), 1.79 (t,  $J$ = 15 Hz, 6 H)

$^{13}\text{C}$  NMR (100 MHz  $\text{CDCl}_3$ ):  $\delta$  159.3, 147.3, 137.7, 133.9, 126.1, 119.2, 113.4, 104.5, 62.9, 60.3, 43.2, 36.0, 29.9, 29.6

ESI ( $m/z$  414.134,  $[\text{M}+\text{Na}]^+$ ): Calculated for  $\text{C}_{21}\text{H}_{21}\text{N}_5\text{OSNa}$  (414.136)



VI

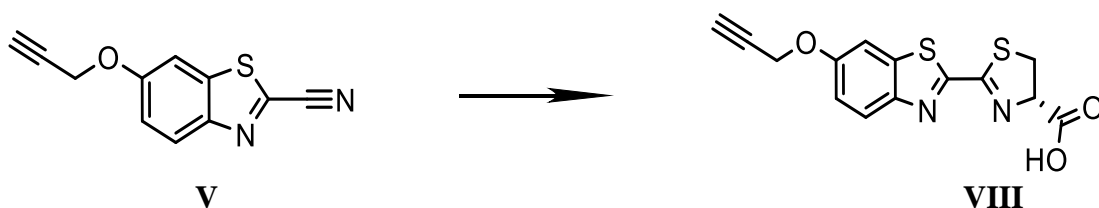
VII

**(VII) Luciferin-triazole-adamantane.** **VI** (30 mg, 0.07 mmol) and D-cysteine HCl hydrate (25 mg, 0.14 mmol) was dissolved in 20 mL of degassed 7:3 THF:PBS buffer mixture. Then 2M NaOH solution was added to the reaction mixture until the pH reached 7.9, which was then allowed to stir at RT for 6 hours. The solution was acidified and solvent reduced. The mixture was extracted into ethyl acetate three times. The extract was washed with 10 mL deionized water. The solvent was removed under reduced pressure to yield 41 mg of Crude **VII**, a yellow solid.

$^1\text{H}$  NMR (400 MHz  $\text{CD}_2\text{Cl}_2$ ):  $\delta$  8.00 (d,  $J$  = 4 Hz, 1H) 7.78 (s, 1H), 7.56 (s, 1H), 7.20 (d,  $J$  = 4 Hz, 1H) 5.41 (t,  $J$  = 8 Hz, 1H) 5.28 (s, 2H), 3.76 (d,  $J$  = 4.5 Hz, 2H), 2.2 (m, 9H), 1.79 (t,  $J$  = 15 Hz, 6 H)

$^{13}\text{C}$  NMR (100 MHz  $\text{CD}_2\text{Cl}_2$ ):  $\delta$  172.7, 166.5, 158.3, 148.2, 142.3, 137.9, 136.0, 125.4, 120.1, 117.6, 105.1, 78.6, 68.0, 62.5, 60.4, 43.1, 36.0, 35.2, 34.3, 30.3, 29.8, 21.0

HR-MS (ESI) ( $m/z$  496.1453,  $[\text{M}+\text{H}]^+$ ): Calculated for  $\text{C}_{24}\text{H}_{26}\text{N}_5\text{O}_3\text{S}_2$  (496.1472)



V

VIII

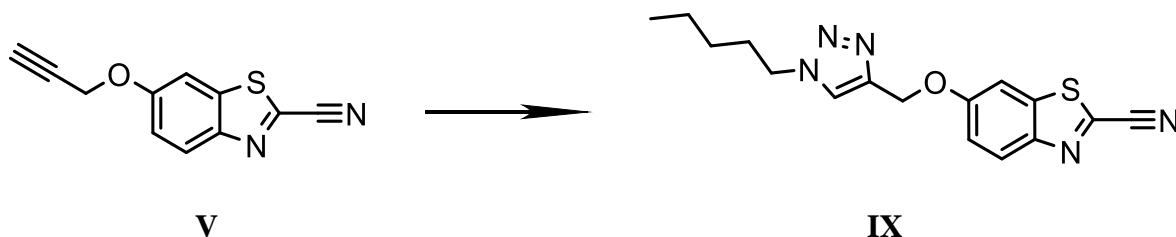
**(VIII) Luciferin-Alkyne.** **V** (30 mg, 1.4 mmol) was dissolved in 5 mL of a 1:4 Acetonitrile:PBS buffer mixture. D-cysteine (24 mg, 0.25 mmol) was then added to the reaction mixture. The mixture was allowed to stir at RT for 24 hours. The solvent was removed under reduced pressure, and the mixture was extracted into acidified ethyl acetate three times. The extract was washed with 10 mL deionized water followed by 10 mL brine. The solvent was removed under reduced pressure to yield 35 mg (79 %) of **VIII**, a pale green solid.

$^1\text{H}$  NMR (400 MHz  $\text{CD}_3\text{OD}$ ):  $\delta$  7.98 (d,  $J$  = 4 Hz, 1H), 7.64 (d,  $J$  = 3 Hz, 1H), 7.22 (dd,  $J$  = 4 Hz,  $J$  = 3 Hz), 5.40 (t,  $J$  = 9 Hz, 1H), 4.86 (d,  $J$  = 3 Hz, 2H), 3.77 (m, [2-dd], 2H), 3.02 (t,  $J$  = 2 Hz, 1H)

$^{13}\text{C}$  NMR (100 MHz  $\text{CD}_3\text{OD}$ ):  $\delta$  172.1, 166.4, 158.8, 157.6, 148.0, 137.6, 124.6, 117.5, 105.4, 78.3, 78.02, 76.2, 56.0, 34.7, 29.7

HR-MS (ESI) ( $m/z$  319.0199,  $[\text{M}+\text{H}]^+$ ): Calculated for  $\text{C}_{14}\text{H}_{11}\text{N}_2\text{O}_3\text{S}_2$  (319.0206)



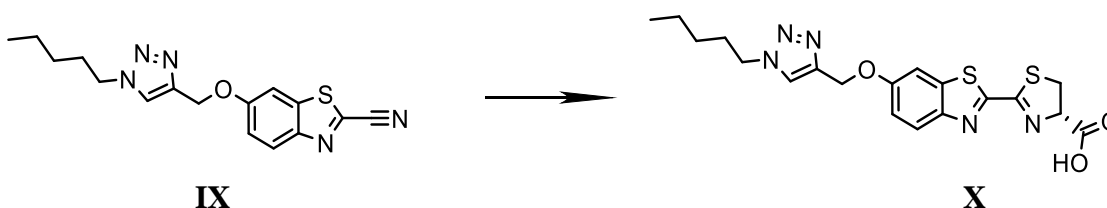


**(IX) 6-((1-pentyl-1H-1,2,3-triazol-4-yl)methoxy)benzo[d]thiazole-2-carbonitrile.** **V** (60 mg, 0.28 mmol) and 0.200 mL crude 1-azidopentane were dissolved in 20 mL of 9:1 THF: H<sub>2</sub>O and degassed with argon. Sodium ascorbate (240 mg, 5eq) and copper (II) sulphate pentahydrate (60 mg, 0.5eqs) were added. The resulting mixture was refluxed at 50°C for 24 hours, then solvents were removed by rotary evaporation, extracted into EA, washed with water and brine. The organic layer was removed and solvent reduced to prepare for column chromatography in a 2:1 EA: hexanes system (RF=0.45) to yield 28 mg of **IX** (30%) an off white solid.

<sup>1</sup>H NMR (400 MHz D<sub>2</sub>O): δ 8.00 (d, *J* = 9.1 Hz, 1H), 7.59 (s, 1H), 7.51 (d, *J* = 2.0 Hz, 1H), 7.23 (dd, *J* = 9 Hz, 2 Hz), 5.21 (s, 2H), 4.27 (t, *J* = 7 Hz, 2H), 1.82 (p, *J* = 7.2 Hz), 1.28-1.18 (m [p,h], ~4H), 0.81 (t, *J* = 7.2 Hz, 3H)

<sup>13</sup>C NMR (100 MHz CD<sub>2</sub>Cl<sub>2</sub>): δ 159.2, 147.4, 142.9, 137.7, 134.0, 126.0, 123.2, 119.1, 113.5, 104.7, 62.9, 50.7, 30.1, 28.7, 22.3, 13.8

ESI (m/z 350.106, [M+Na])<sup>+</sup>: Calculated for C<sub>16</sub>H<sub>17</sub>N<sub>5</sub>OSNa (335.105)

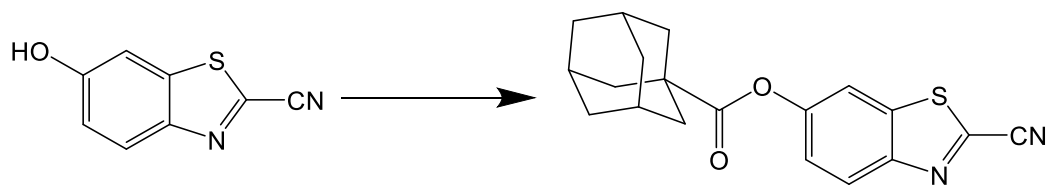


**(X) Luciferin-triazole-pentane.** **IX** (17.5 mg, 0.05 mmol) and D-cysteine HCl hydrate (12 mg, 0.07 mmol) were dissolved in 14 mL of degassed 1:1 THF: H<sub>2</sub>O. Then 2M NaOH solution was added to the reaction mixture until the pH reached 7.9 which was then allowed to stir at RT for 6 hours. The solution was acidified and solvent was reduced. The mixture was extracted into ethyl acetate three times. The extract was washed with 10 mL deionized water. The solvent was removed under reduced pressure to yield 22 mg of Crude **X**, an off yellow solid.

<sup>1</sup>H NMR (400 MHz D<sub>2</sub>O): δ 7.91 (d, *J* = 4.5 Hz, 1H), 7.62 (s, 1H), 7.47 (s, 1H), 7.12 (d, *J* = 7 Hz, 1H), 5.34 (t, *J* = 9 Hz, 1H), 5.21 (s, 2H), 4.281 (t, *J* = 7 Hz, 2H), 3.69 (dd, *J* = 9 Hz, 3 Hz, 2H), 1.83 (p, *J* = 7 Hz, 2H), 1.28-1.18 (m, 4H), 0.81 (t, *J* = 7.2 Hz, 3H)

<sup>13</sup>C NMR (400 MHz CD<sub>2</sub>Cl<sub>2</sub>): δ 171.1, 158.2, 148.3, 143.2, 138.0, 125.4, 123.2, 117.7, 105.3, 78.3, 62.6, 50.78, 34.9, 30.1, 28.7, 22.3, 13.8

HR-MS (ESI) (m/z 432.1148, [M+H])<sup>+</sup>: Calculated for C<sub>19</sub>H<sub>22</sub>N<sub>5</sub>O<sub>3</sub>S<sub>2</sub> (432.1159)

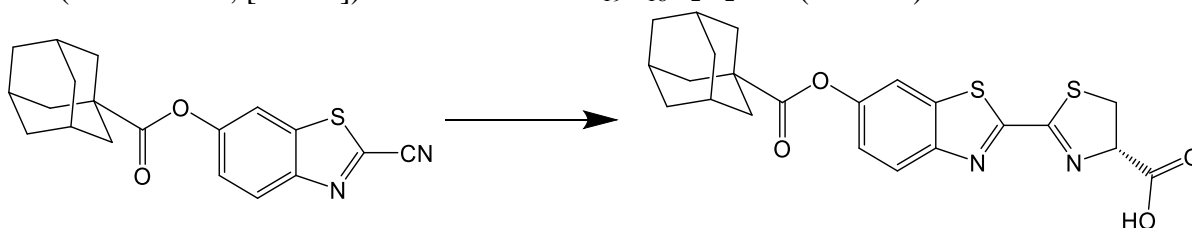
**XI****(XI) 2-cyanobenzo[d]thiazol-6-yl (3r,5r,7r)-adamantane-1-carboxylate:**

6-hydroxybenzothiazole-2-carbonitrile (176 mg, 1.00 mmol) was dissolved in 10 mL anhydrous, degassed DMF with Cs<sub>2</sub>CO<sub>3</sub> (325 mg, 1.00 mmol). 1.32 mL anhydrous pyridine (excess) was added to the reaction mixture along with 1-adamantanecarbonyl chloride (198mg, 1.00 mmol). The reaction was stirred for 24 hours at 80 °C. The reaction mixture was diluted into 30ml ethyl acetate and acidified with 1M aqueous HCl. The crude mixture was washed with water three times to yield a crude organic extract. This was evaporated under reduced pressure to yield a thick brown oil. The crude mixture was then purified via column chromatography in a 2:5 EA: hexanes system and the product was then collected (RF= 0.8) and solvent was removed under reduced pressure to yield 276 mg (81% yield) of **XI** a white solid.

<sup>1</sup>H NMR (400 MHz CDCl<sub>3</sub>): δ 8.20 (d, *J*=9 Hz, 1H), 7.74 (d, *J*=2 Hz, 1H), 7.35 (dd, *J*=9 Hz, *J*=2 Hz, 1H), 2.07 (broad s, 9H), 1.79 (m, 6H)

<sup>13</sup>C NMR (100 MHz CDCl<sub>3</sub>): δ 176.0, 151.6, 150.1, 136.8, 136.4, 125.8, 123.2, 114.8, 113.1, 41.4, 38.8, 36.5, 28.2

ESI (m/z 361.096, [M+Na]<sup>+</sup>): Calculated for C<sub>19</sub>H<sub>18</sub>N<sub>2</sub>O<sub>2</sub>SNa (361.098)

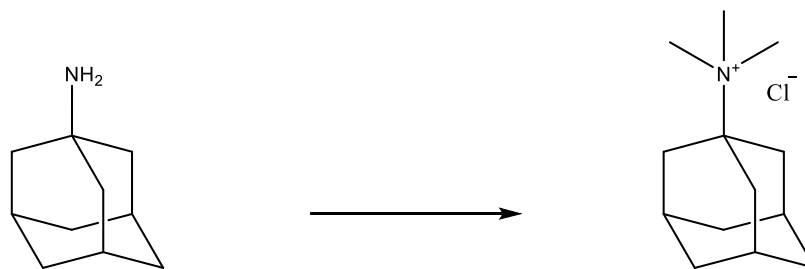
**XI****XII**

**(XII) Luciferin-Adamantanoate.** **XI** (120 mg, 0.36mmol) and D-cysteine HCl hydrate (71 mg, 0.40 mmol) was dissolved in 50mL of degassed 7:3 THF: H<sub>2</sub>O mixture. Then 2M NaOH solution was added to the reaction mixture until the pH reached 7.9, and it was allowed to stir at RT for 18 hours. The solution was acidified with 1M aqueous HCl and organic solvent removed under reduced pressure. The mixture of solvent and precipitate was extracted into ethyl acetate three times. The extract was washed with 10 mL deionized water. The solvent was removed under reduced pressure to yield 141mg of Crude **XII**. The crude solid was dissolved in minimal methanol. Ultrapure water was added resulting in a white precipitate that was collected by centrifugation to yield a yellow solid that yielded yellow-white crystals upon scratching totaling 98 mg (67% yield) of pure **XII**

<sup>1</sup>H NMR (400 MHz CD<sub>2</sub>Cl<sub>2</sub>): δ 8.10 (d, *J*=9 Hz, 1H), 7.68 (d, *J*=2 Hz, 1H), 7.24 (dd, *J*=9 Hz, *J*=2 Hz), 5.45 (t, *J*= 10 Hz, 1H), 3.80 (m, 2H), 2.07 (broad s, 9H), 1.79 (m, 6H)

<sup>13</sup>C NMR (100 MHz CD<sub>2</sub>Cl<sub>2</sub>): δ 176.2, 172.5, 167.5, 160.5, 151.0, 150.5, 136.9, 125.1, 122.0, 115.0, 78.2, 41.3, 38.9, 36.5, 35.1, 28.2

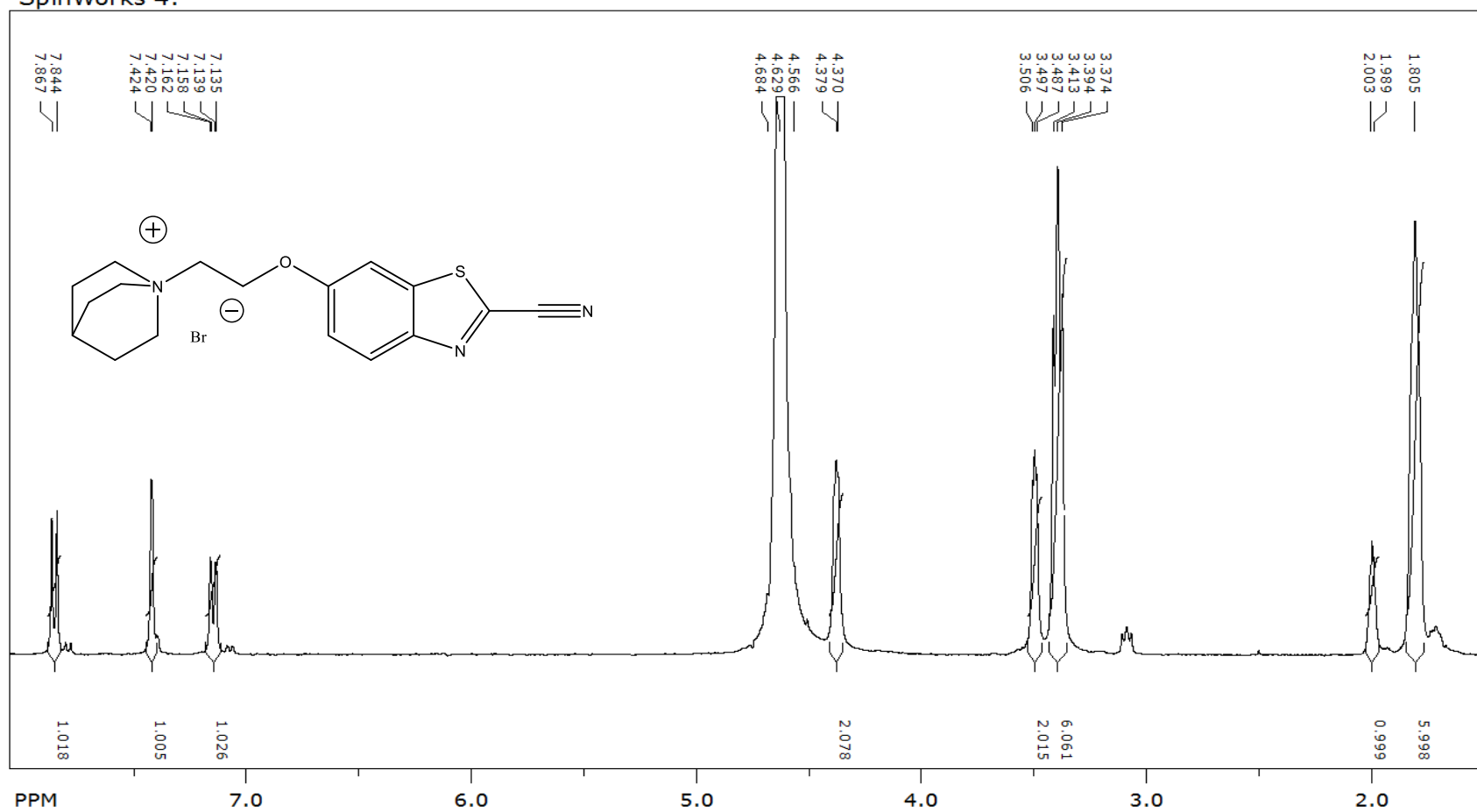
HR-MS (ESI) (m/z 443.1079, [M+H]<sup>+</sup>): Calculated for C<sub>22</sub>H<sub>23</sub>N<sub>2</sub>O<sub>4</sub>S<sub>2</sub> (443.1094)



**1-(trimethylammonium) adamantyl chloride** (Courtesy of Jacobs H. Jordan): To a stirred solution of 5 mL DCM-MeOH (9:1) was added 203 mg (1.34 mmol) of 1-adamantylamine and potassium carbonate (667 mg, 4.83 mmol) and stirred 5 minutes. To the stirred solution was added methyl iodide (0.28 mL, 4.50 mmol) and the solution stirred at room temperature overnight. The solution was filtered and the solids washed with DCM (5mL), and MeOH (5 mL), and the organic filtrates were combined and the solvent removed under reduced pressure and dried at 77 °C to give 397.2 mg (92 %) of the iodide salt as an off-white, crystalline solid. The salt was dissolved in a minimum volume (~1 mL) of 18.2 MΩ H<sub>2</sub>O and passed through a Dowex® anion exchange resin (chloride form) and collected over sixteen mL of eluant. The eluant was flash frozen in liquid nitrogen and lyophilized to give the desired product (266.3 mg, 86 %).  
<sup>1</sup>H NMR (400 MHz D<sub>2</sub>O) δ 2.81 (s, 9H), 2.18 – 2.07 (m, 3H), 1.88 (d, J = 3.1 Hz, 6H), 1.59 – 1.43 (m, 6H).  
 ESI (m/z 194.185, [M]<sup>+</sup>: Calculated for C<sub>13</sub>H<sub>24</sub>N (194.191)

## SI.2 NMR Spectra of Novel

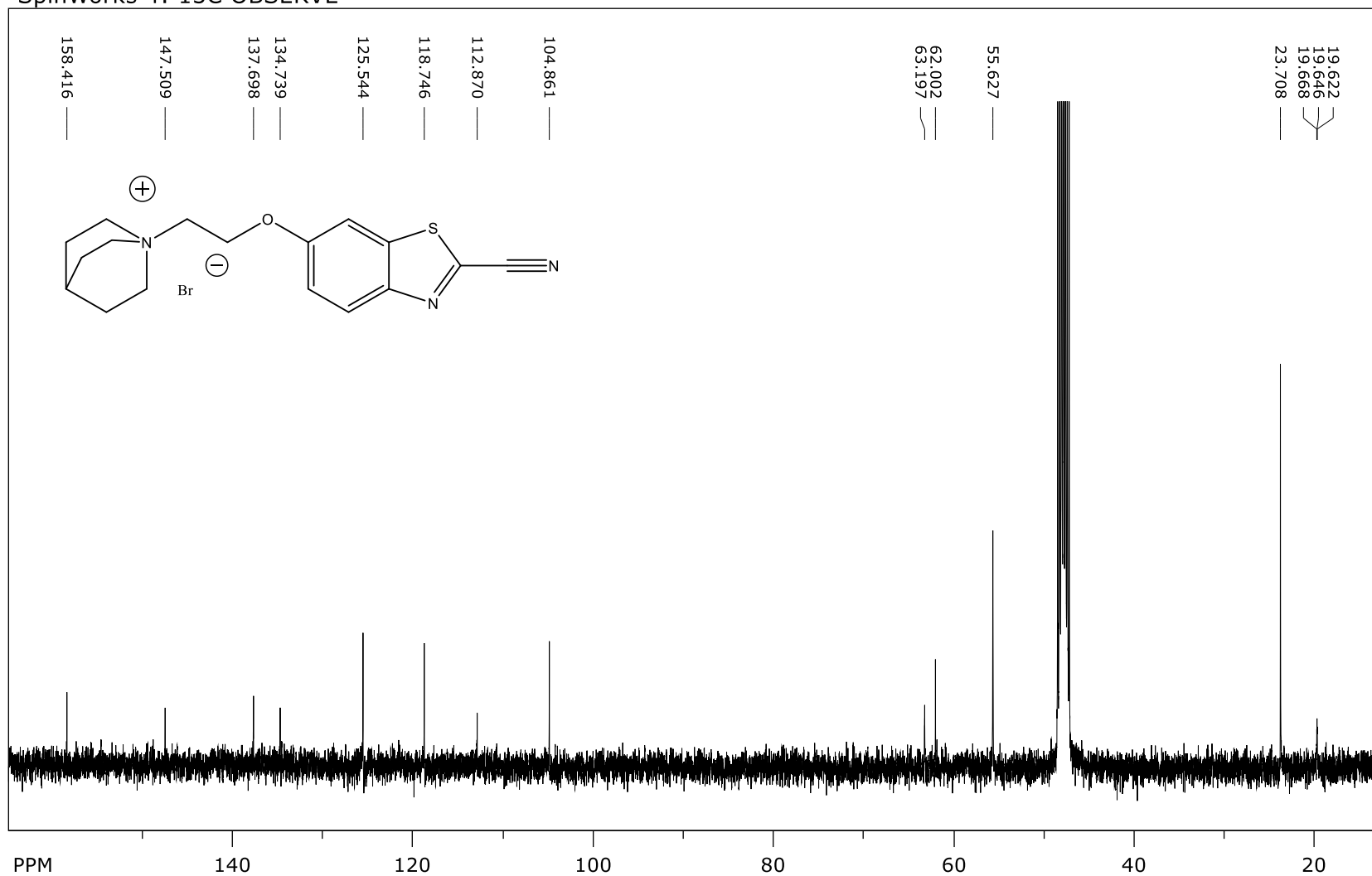
SpinWorks 4:



file: ...24May2016\_24May2016\PROTON.fid\fid block# 1 expt: "s2pul"  
 transmitter freq.: 399.749176 MHz  
 time domain size: 35920 points  
 width: 4797.03 Hz = 12.0001 ppm = 0.133547 Hz/pt  
 number of scans: 32

freq. of 0 ppm: 399.747177 MHz  
 processed size: 65536 complex points  
 LB: 1.500 GF: 0.0000

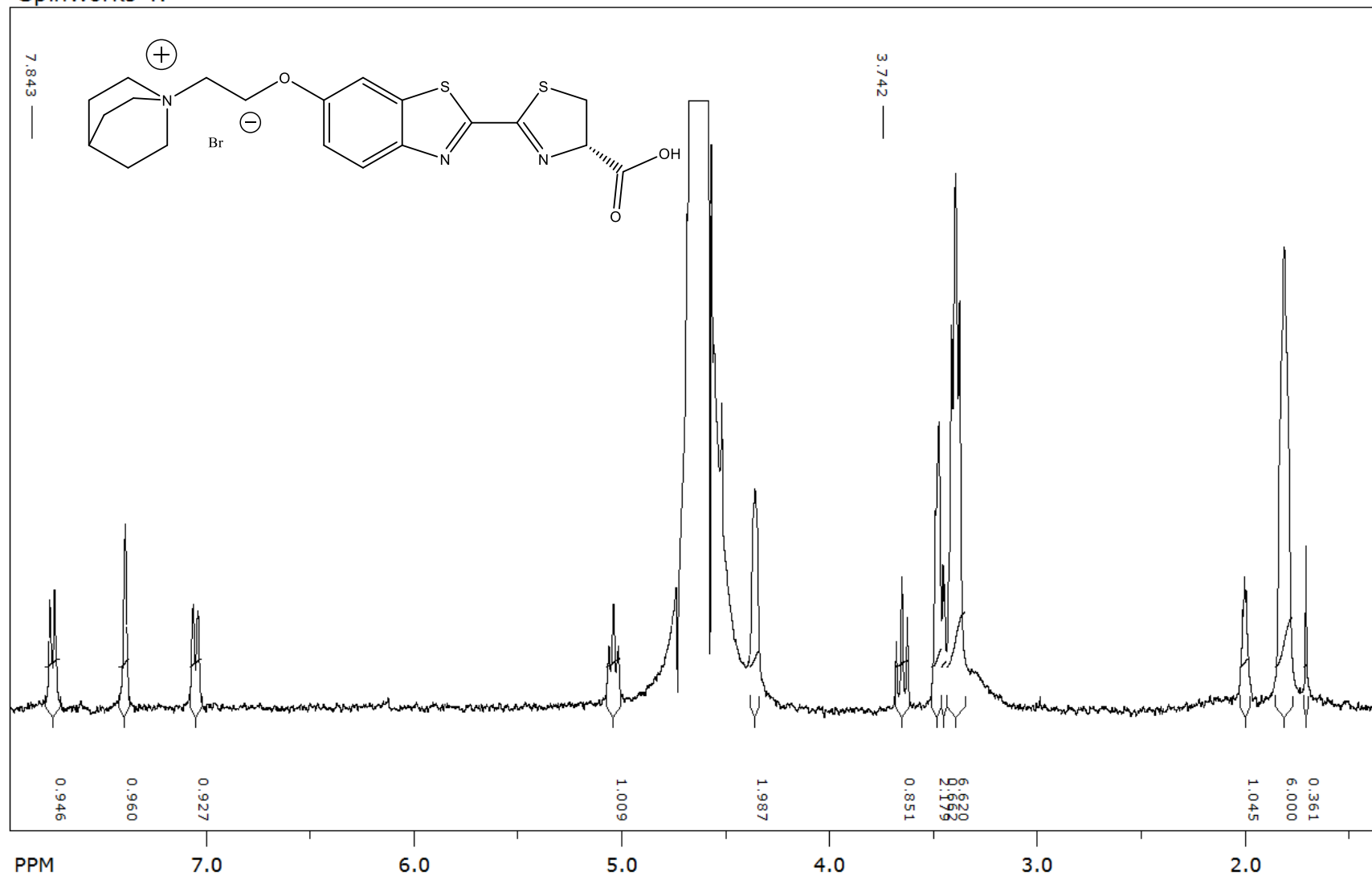
## SpinWorks 4: 13C OBSERVE



file: ...\\hrah27oct2016CBTZOETQ13C.fid\\fid block# 1 expt: "s2pul"  
transmitter freq.: 100.526133 MHz  
time domain size: 59968 points  
width: 25000.00 Hz = 248.6916 ppm = 0.416889 Hz/pt  
number of scans: 20176

freq. of 0 ppm: 100.516621 MHz  
processed size: 65536 complex points  
LB: 1.000 GF: 0.0000

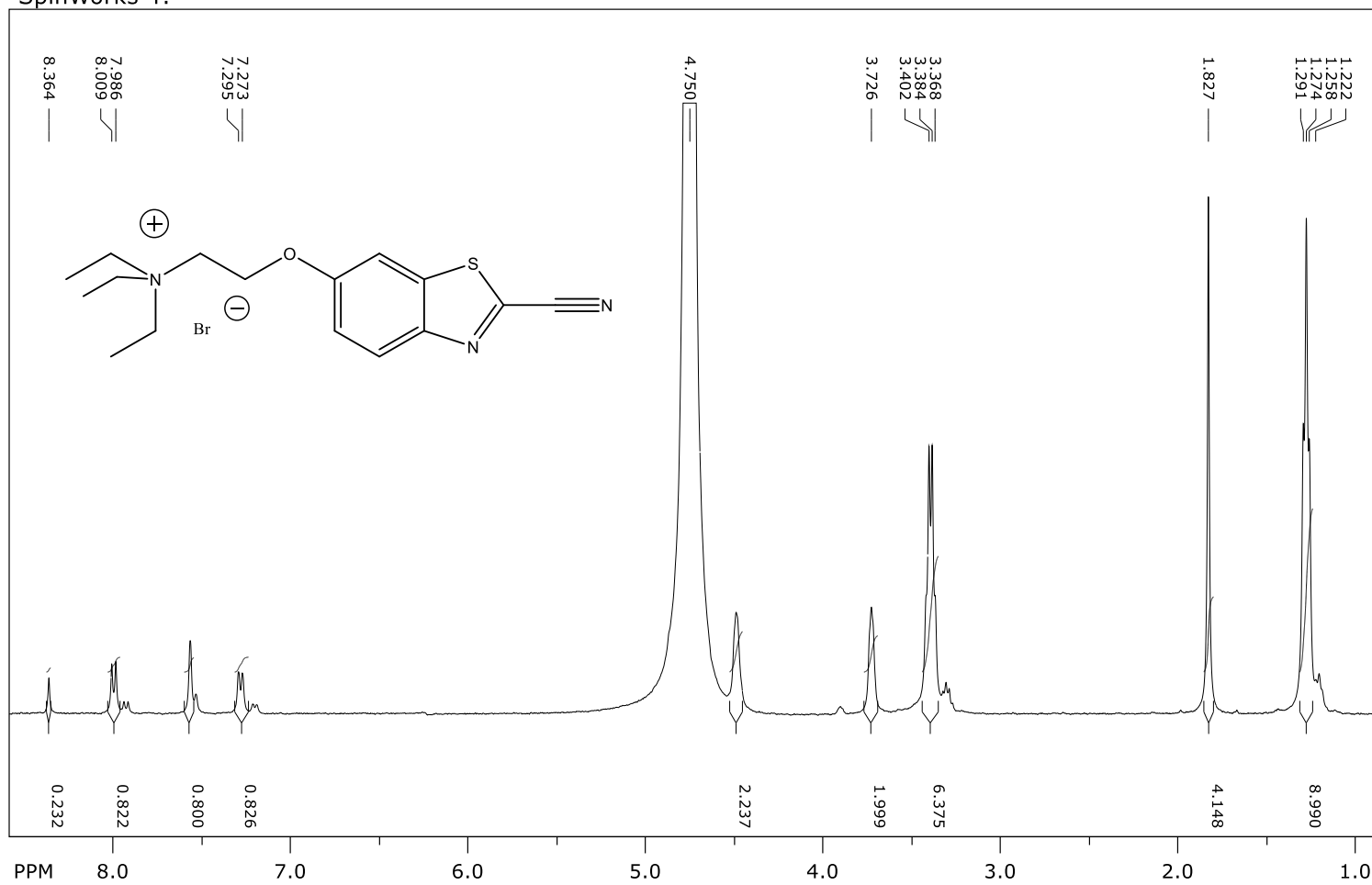
SpinWorks 4:



file: ...\_14Aug2016-12-50-32\PROTON.fid\fid block# 1 expt: "s2pul"  
 transmitter freq.: 399.749176 MHz  
 time domain size: 35920 points  
 width: 4797.03 Hz = 12.0001 ppm = 0.133547 Hz/pt  
 number of scans: 32

freq. of 0 ppm: 399.747177 MHz  
 processed size: 65536 complex points  
 LB: 1.500 GF: 0.0000

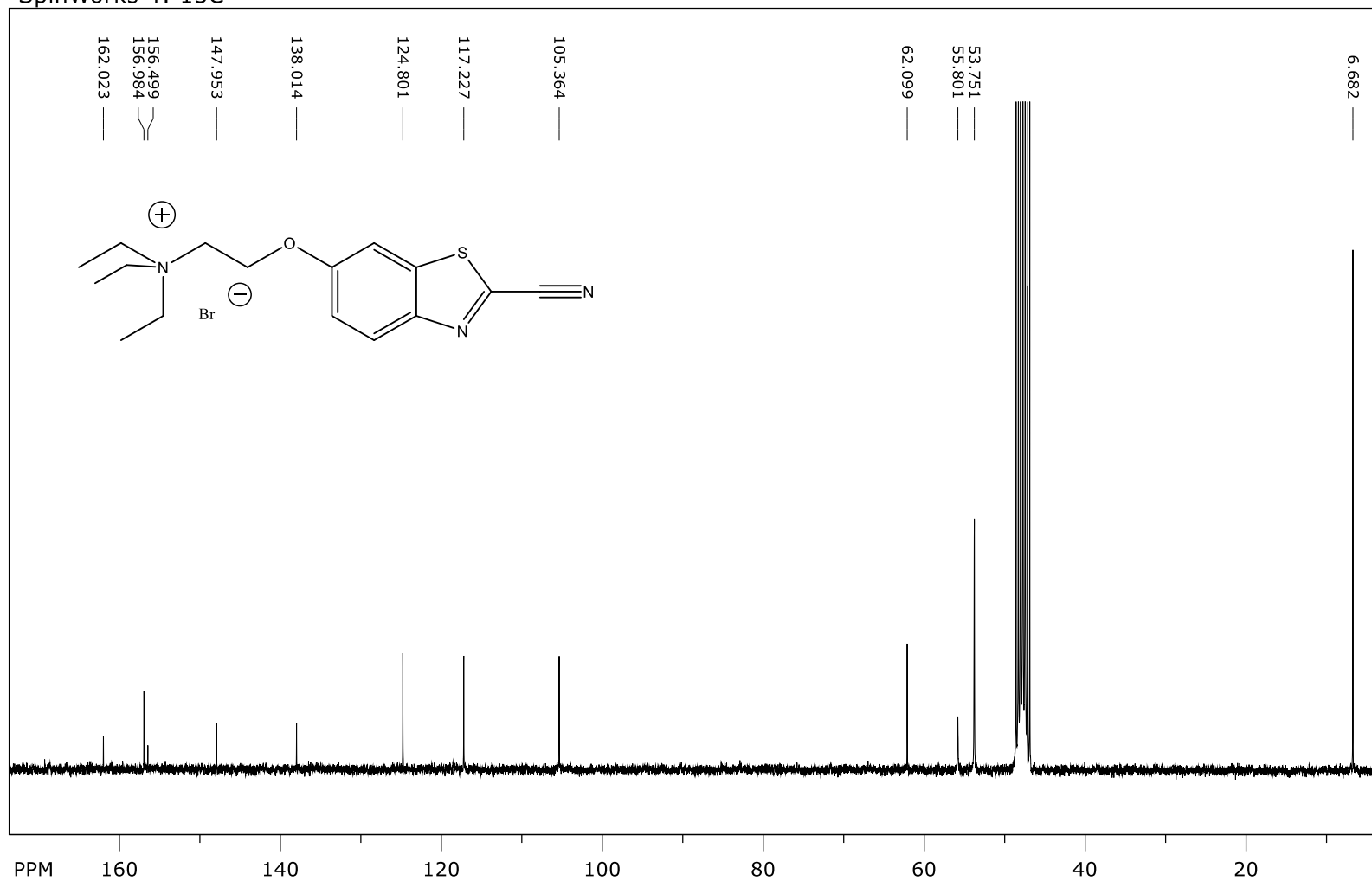
## SpinWorks 4:



file: ...13Oct2016\_13Oct2016\PROTON.fid\fid block# 1 expt: "s2pul"  
transmitter freq.: 399.749176 MHz  
time domain size: 35920 points  
width: 4797.03 Hz = 12.0001 ppm = 0.133547 Hz/pt  
number of scans: 32

freq. of 0 ppm: 399.747129 MHz  
processed size: 65536 complex points  
LB: 1.500 GF: 0.0000

## SpinWorks 4: 13C



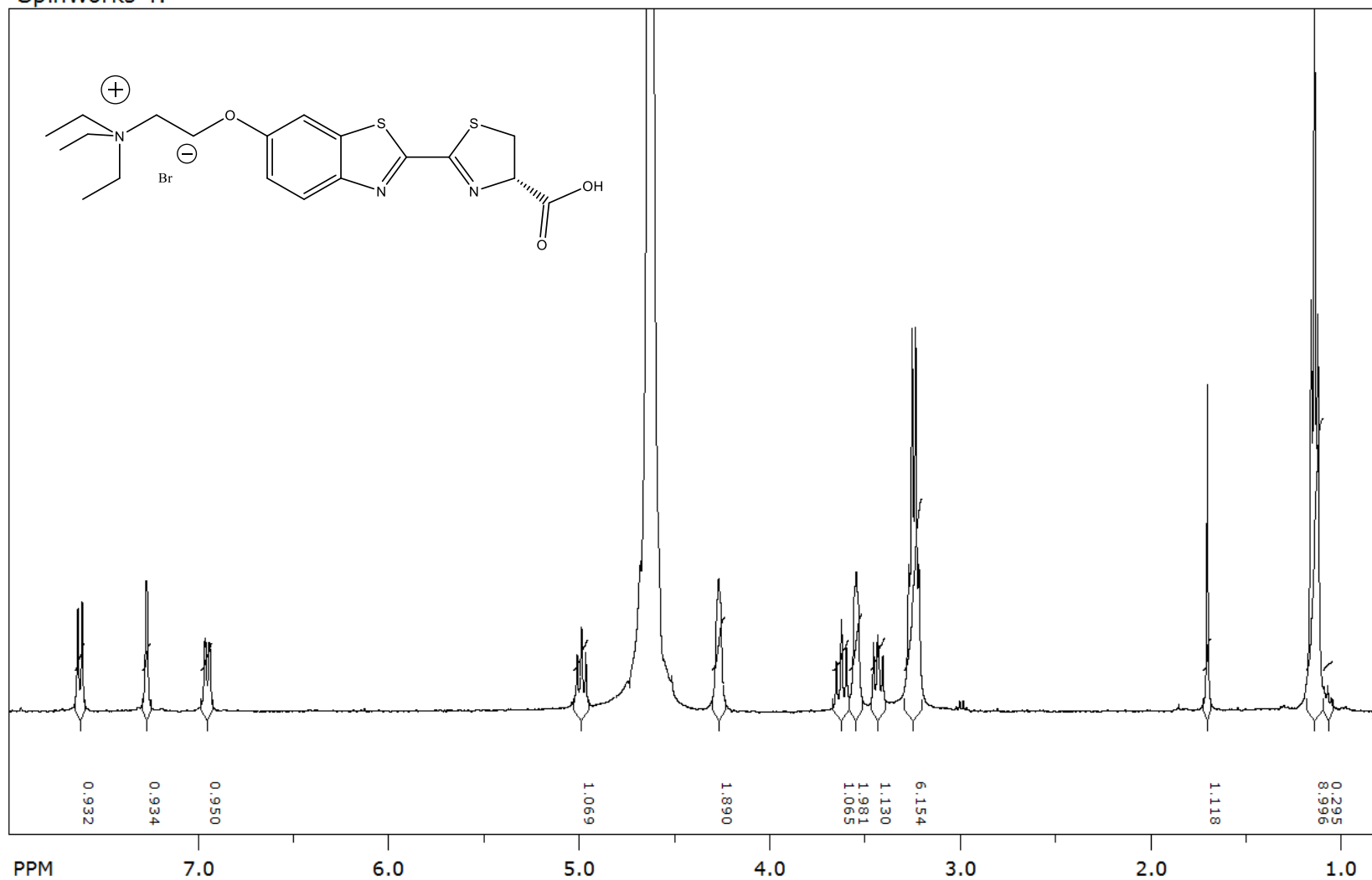
file: ...BTZ-OET-TEA 13C 12 April2017\2\fid expt: <zggp30>  
transmitter freq.: 75.475295 MHz  
time domain size: 65536 points  
width: 17985.61 Hz = 238.2980 ppm = 0.274439 Hz/pt  
number of scans: 13361

freq. of 0 ppm: 75.467741 MHz  
processed size: 32768 complex points  
LB: 1.000 GF: 0.0000



**Luciferin-Oxyethyl-Triethylammonium bromide. IV**

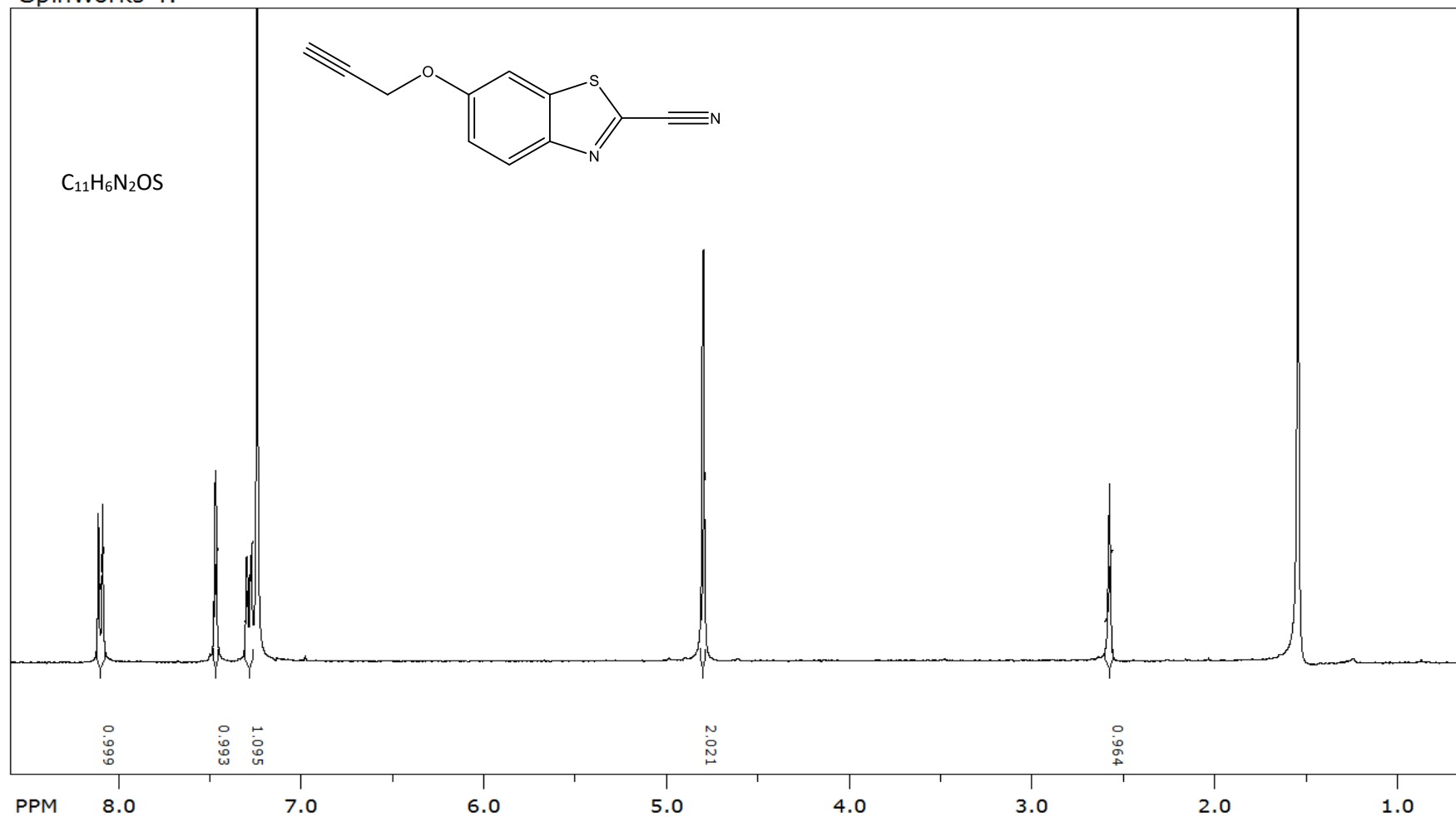
SpinWorks 4:



file: ...14Aug2016\_14Aug2016\PROTON.fid\fid block# 1 expt: "s2pul"  
transmitter freq.: 399.749176 MHz  
time domain size: 35920 points  
width: 4797.03 Hz = 12.0001 ppm = 0.133547 Hz/pt  
number of scans: 32

freq. of 0 ppm: 399.747177 MHz  
processed size: 65536 complex points  
LB: 1.500 GF: 0.0000

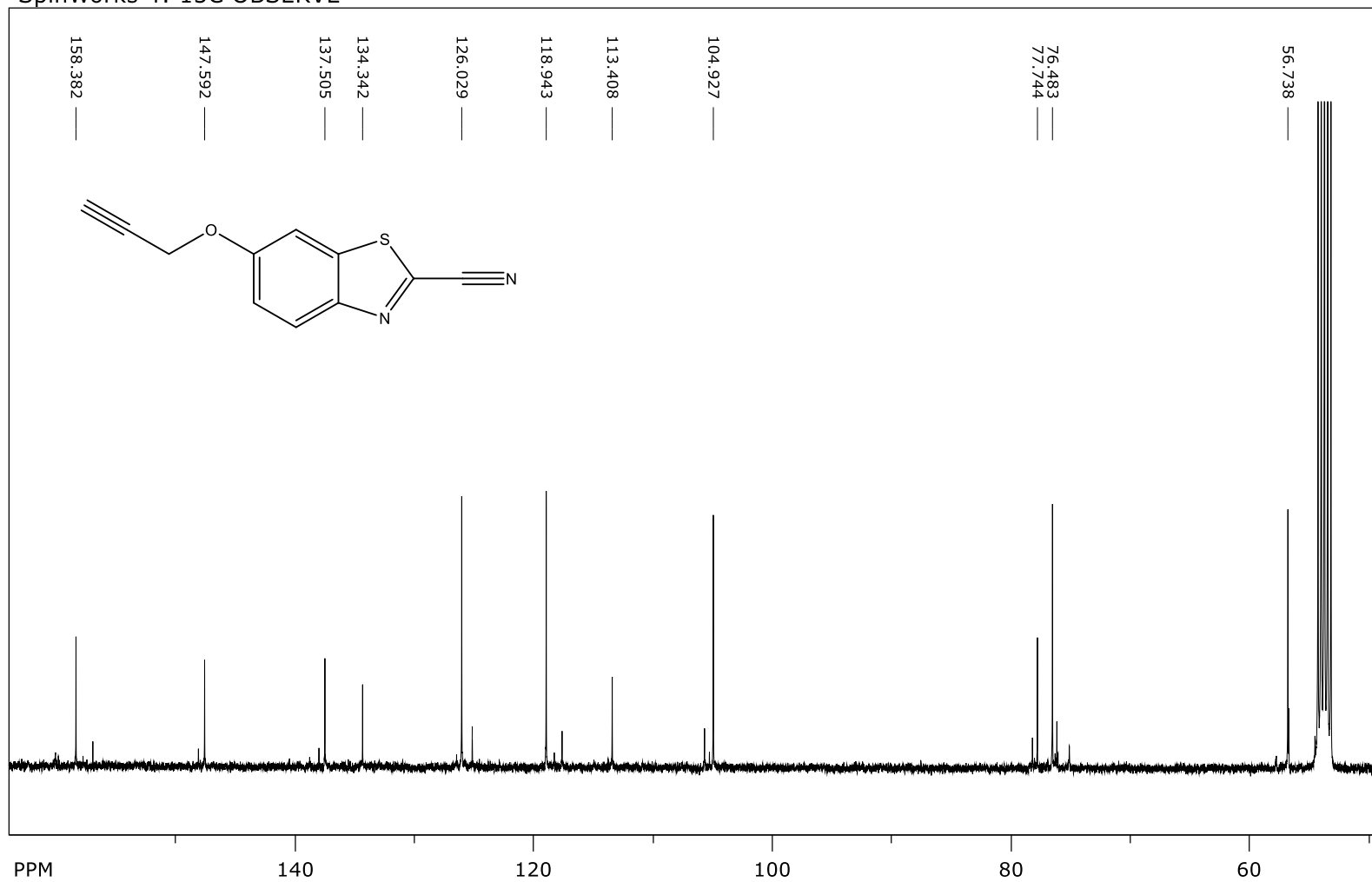
SpinWorks 4:



file: ...28Jul2015\_28Jul2015\PROTON.fid\fid\_block# 1 expt: "s2pul"  
transmitter freq.: 399.748548 MHz  
time domain size: 47892 points  
width: 6395.91 Hz = 15.9998 ppm = 0.133549 Hz/pt  
number of scans: 16

freq. of 0 ppm: 399.746149 MHz  
processed size: 65536 complex points  
LB: 1.500 GF: 0.0000

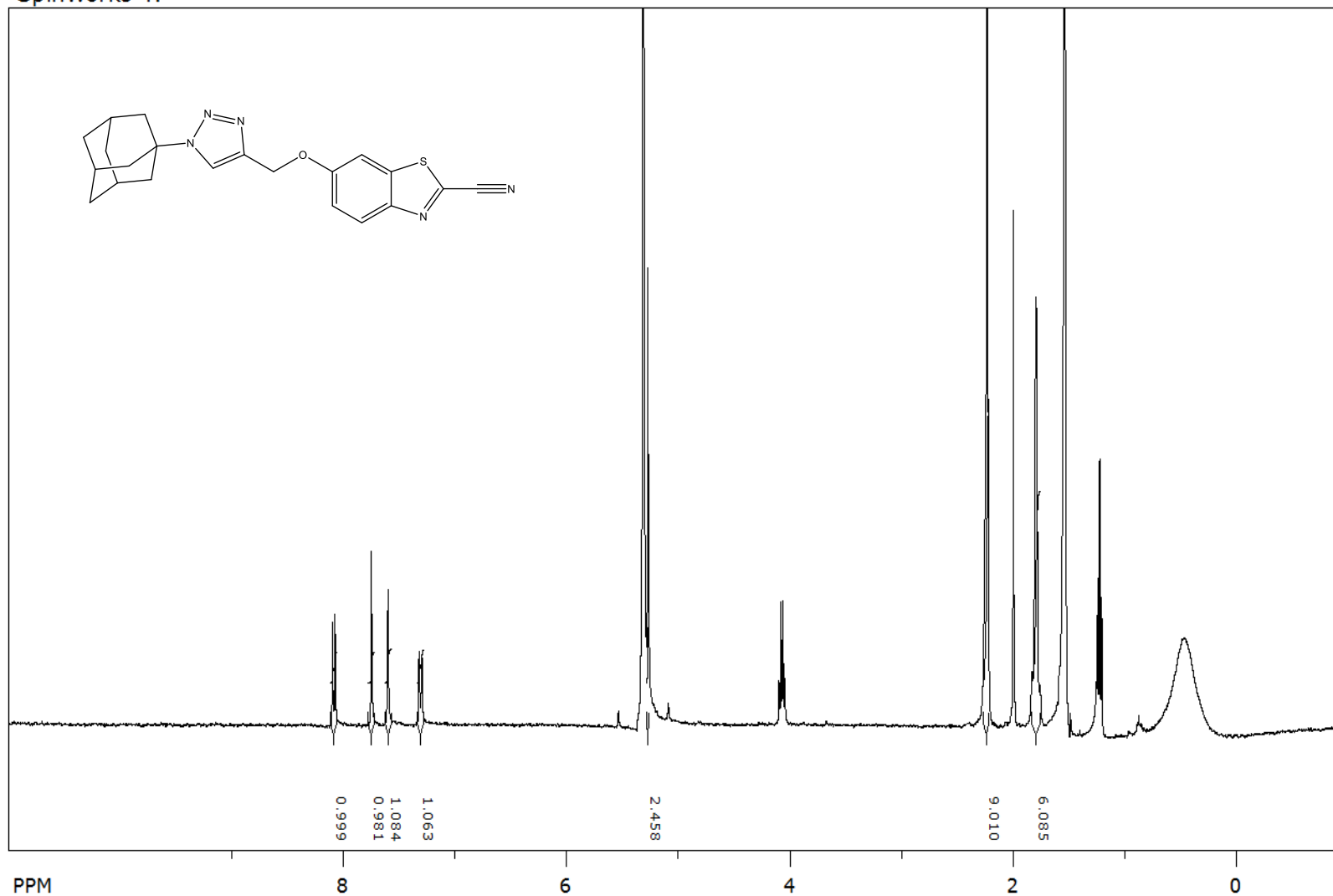
## SpinWorks 4: 13C OBSERVE



file: ...k\NMR's\hrahncBTZAlkyne13C.fid\fid block# 1 expt: "s2pul"  
transmitter freq.: 100.525930 MHz  
time domain size: 59968 points  
width: 25000.00 Hz = 248.6921 ppm = 0.416889 Hz/pt  
number of scans: 13404

freq. of 0 ppm: 100.516418 MHz  
processed size: 65536 complex points  
LB: 1.000 GF: 0.0000

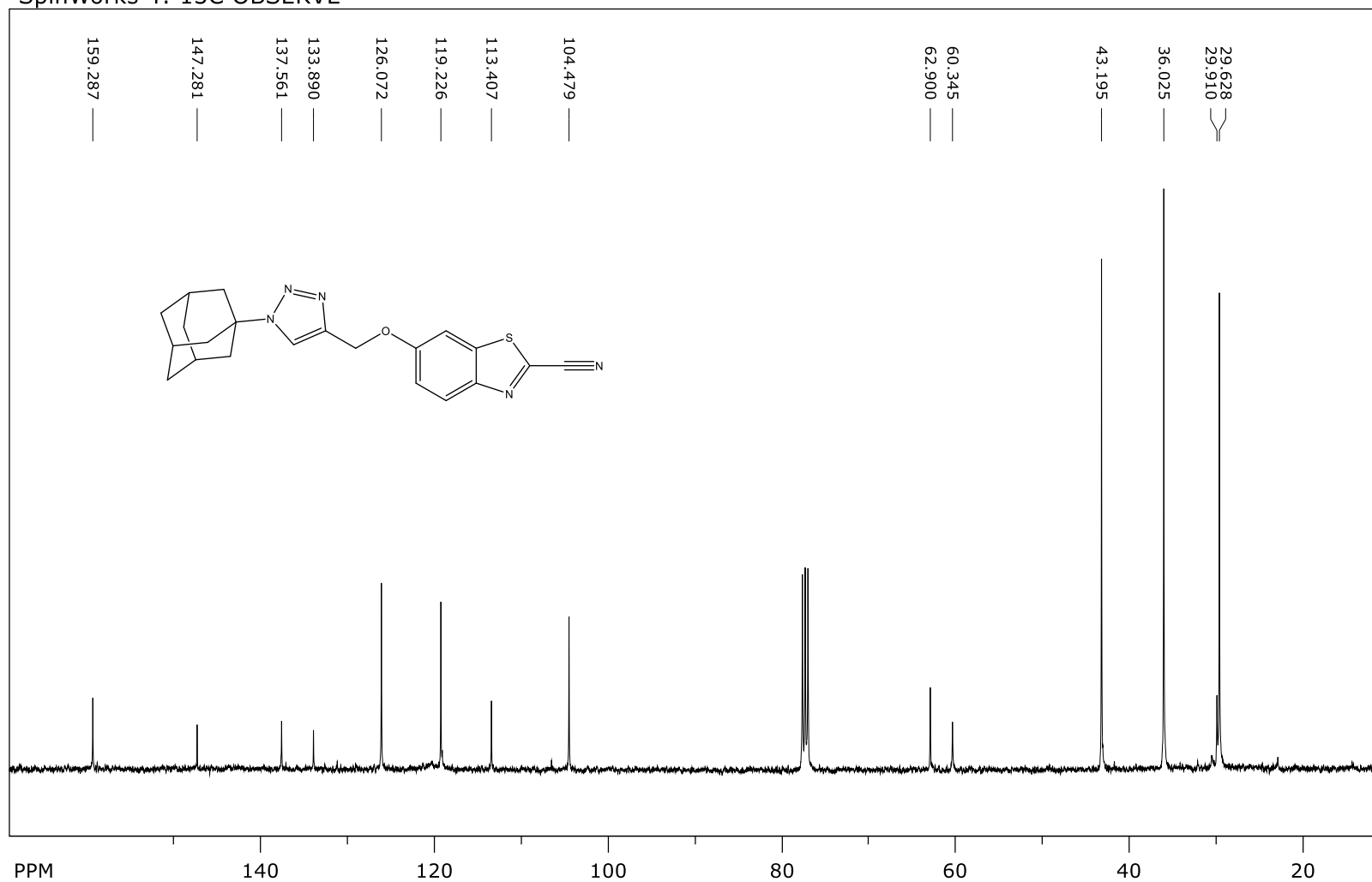
SpinWorks 4:



file: ...12Jul2016\_12Jul2016\PROTON.fid\fid\_block# 1 expt: "s2pul"  
transmitter freq.: 399.748916 MHz  
time domain size: 35920 points  
width: 4797.03 Hz = 12.0001 ppm = 0.133547 Hz/pt  
number of scans: 32

freq. of 0 ppm: 399.746917 MHz  
processed size: 65536 complex points  
LB: 1.500 GF: 0.0000

## SpinWorks 4: 13C OBSERVE

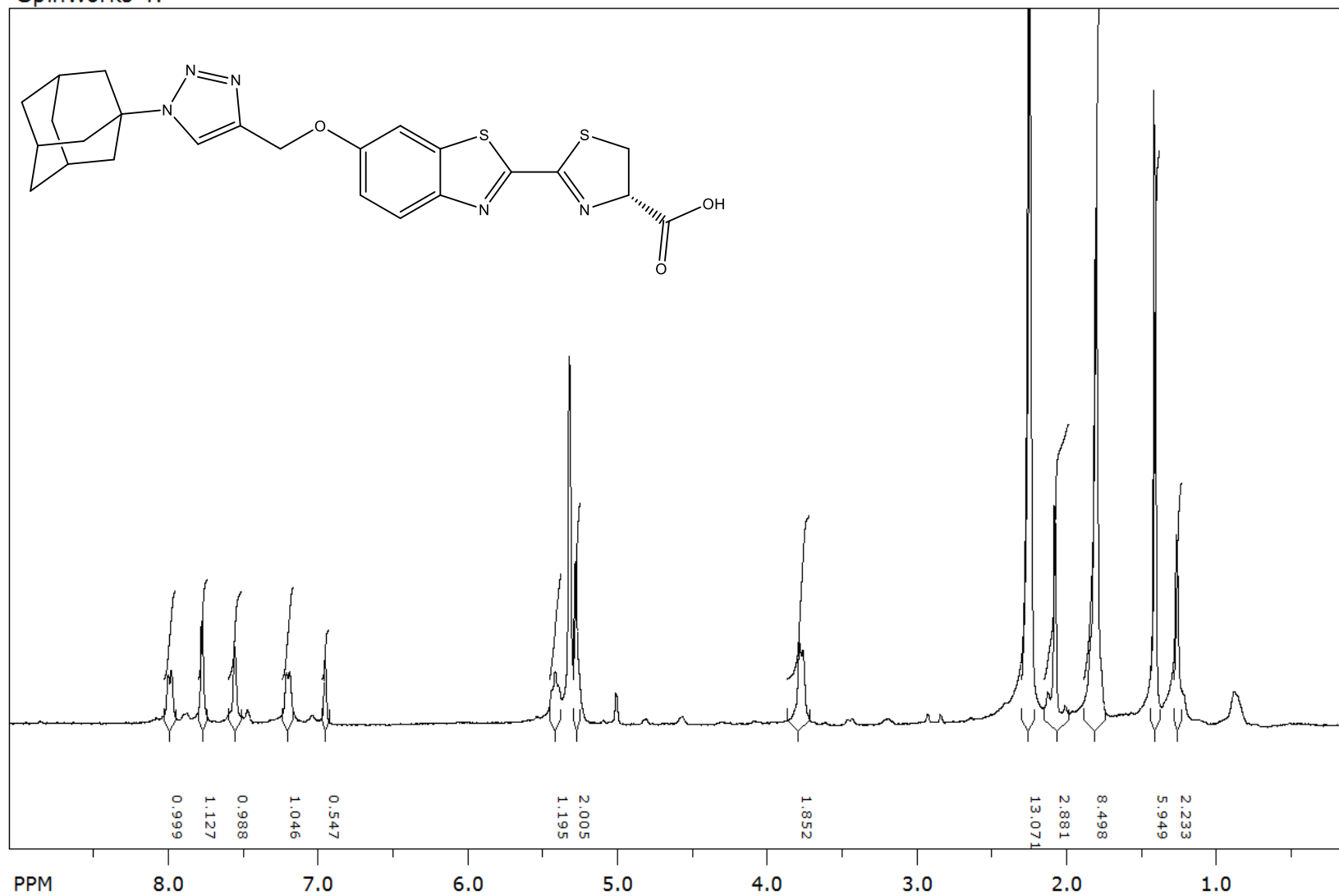


file: ...2April2017\_CBTZ-Trz-Ad\_13C.fid\fid\_block# 1 expt: "s2pul"  
transmitter freq.: 100.525737 MHz  
time domain size: 59968 points  
width: 25000.00 Hz = 248.6925 ppm = 0.416889 Hz/pt  
number of scans: 1204

freq. of 0 ppm: 100.516225 MHz  
processed size: 65536 complex points  
LB: 3.000 GF: 0.0000

**Luciferin-triazole-adamantane**

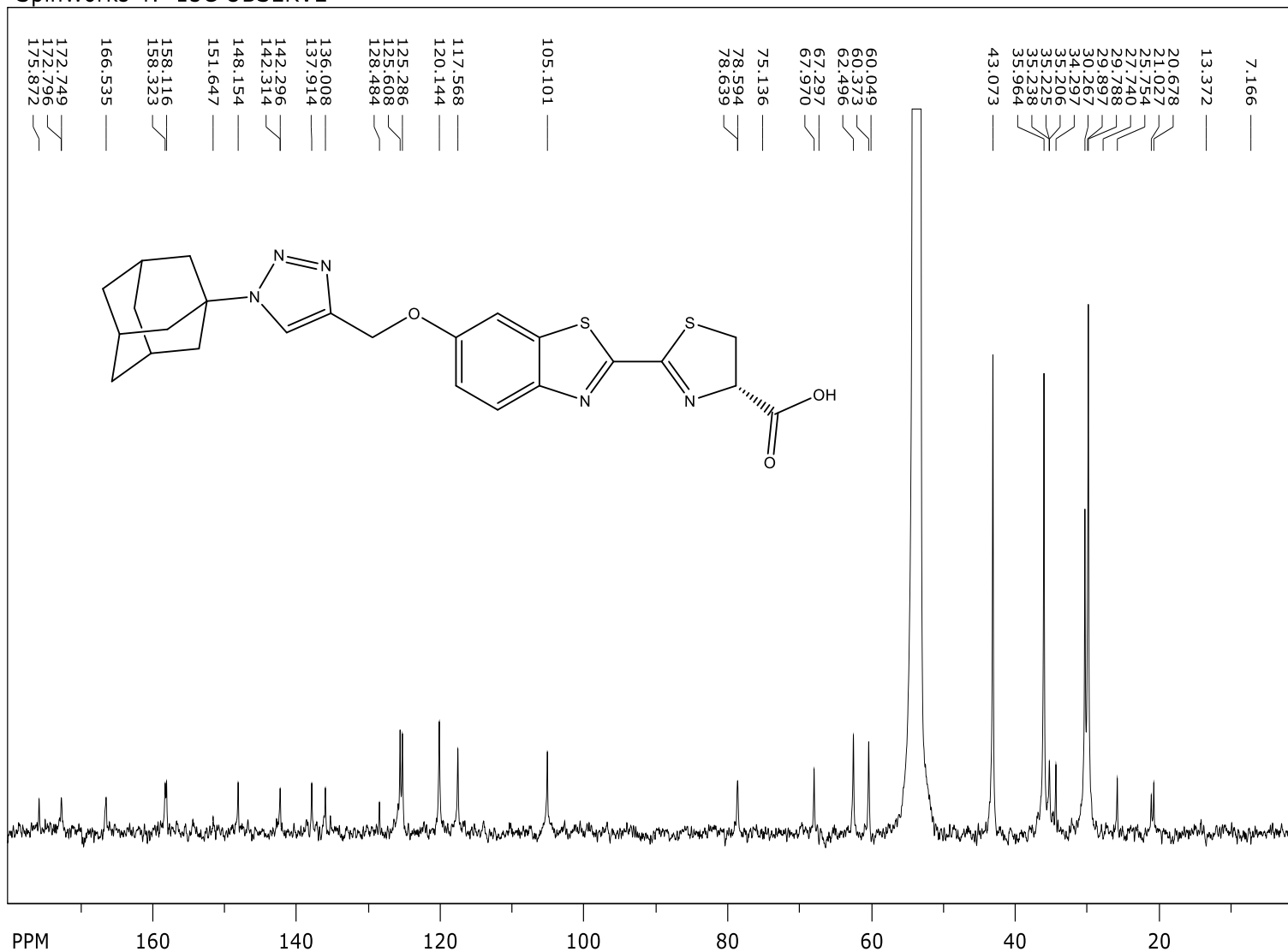
SpinWorks 4:



file: ...25Jul2016\_25Jul2016\PROTON.fid\fid\_block# 1 expt: "s2pul"  
transmitter freq.: 399.748916 MHz  
time domain size: 35920 points  
width: 4797.03 Hz = 12.0001 ppm = 0.133547 Hz/pt  
number of scans: 32

freq. of 0 ppm: 399.746917 MHz  
processed size: 65536 complex points  
LB: 1.500 GF: 0.0000

## SpinWorks 4: 13C OBSERVE

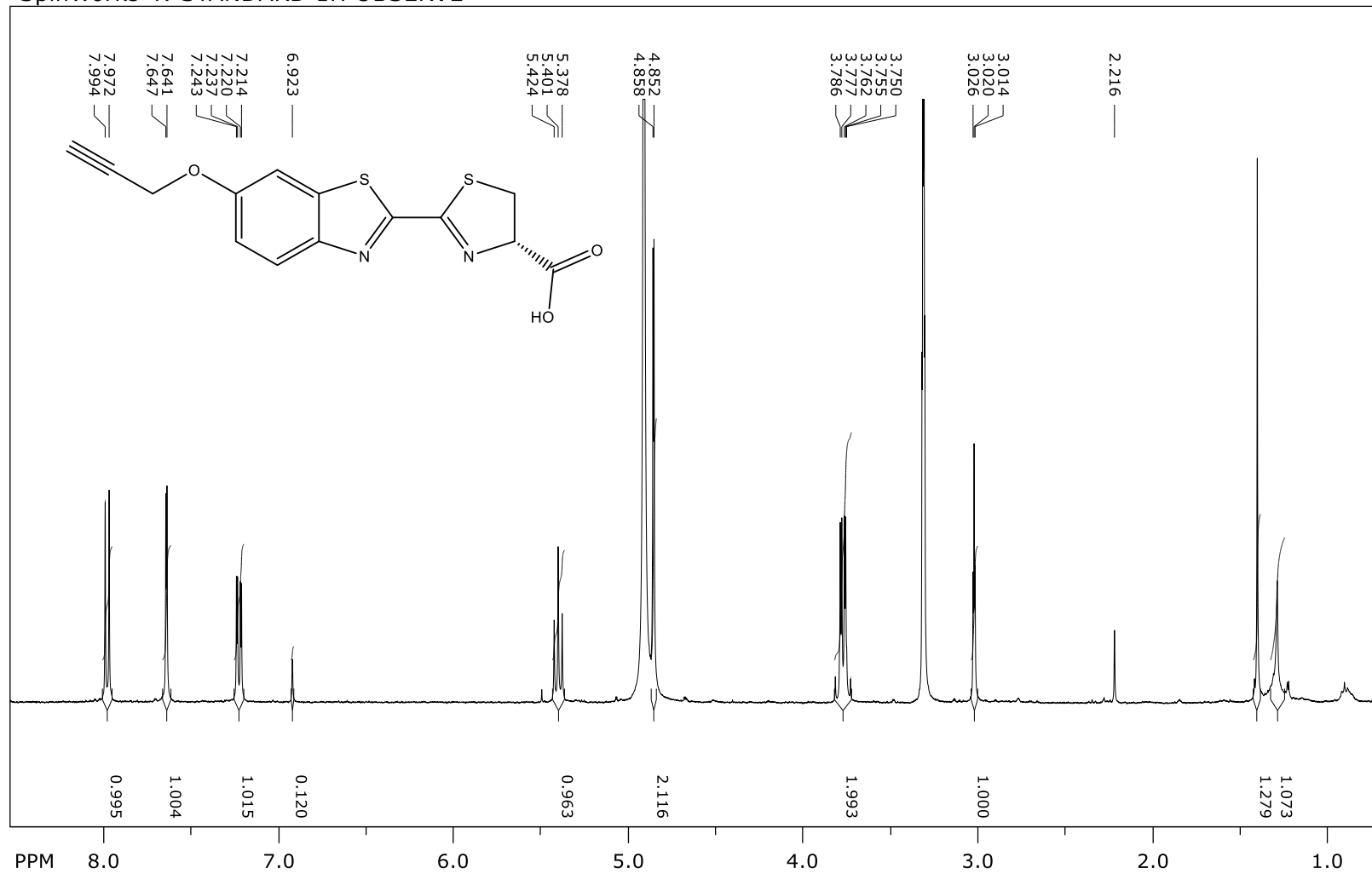


file: ...ucfTrzAd13C\_CD2Cl2.fid\spectrum.dx expt: "s2pul"  
 transmitter freq.: 100.525930 MHz  
 time domain size: 65536 points  
 width: 25000.00 Hz = 248.6921 ppm = 0.381470 Hz/pt  
 number of scans: 0

freq. of 0 ppm: 100.516418 MHz  
 processed size: 65536 complex points  
 LB: 0.000 GF: 0.0000

## Luciferin-Alkyne

SpinWorks 4: STANDARD 1H OBSERVE

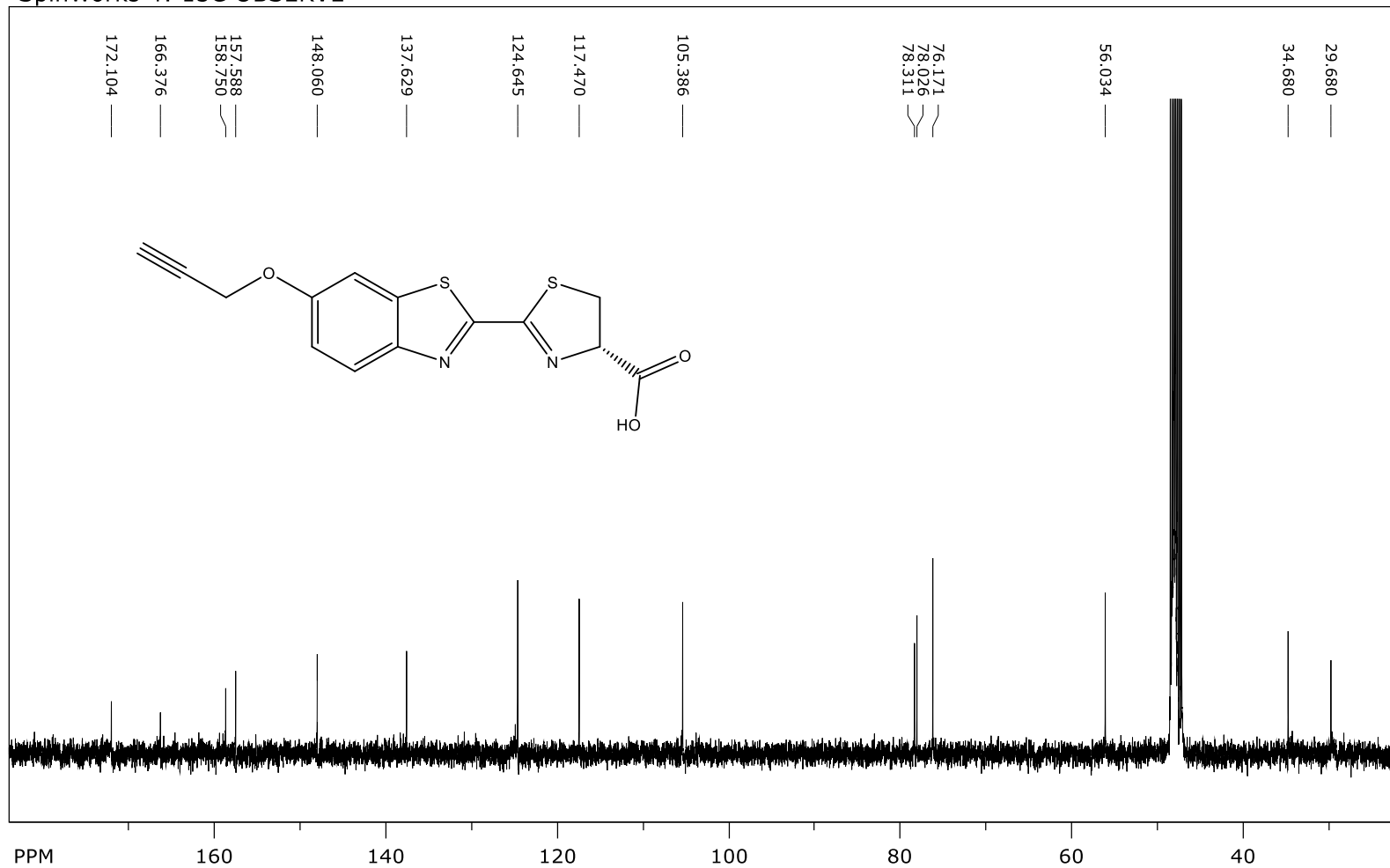


file: ...rk\NMR's\HrahnLucfAlkyne1H.fid\fid\_block# 1 expt: "s2pul"  
 transmitter freq.: 399.749723 MHz  
 time domain size: 44932 points  
 width: 6000.60 Hz = 15.0109 ppm = 0.133548 Hz/pt  
 number of scans: 64

freq. of 0 ppm: 399.747714 MHz  
 processed size: 65536 complex points  
 LB: 0.500 GF: 0.0000



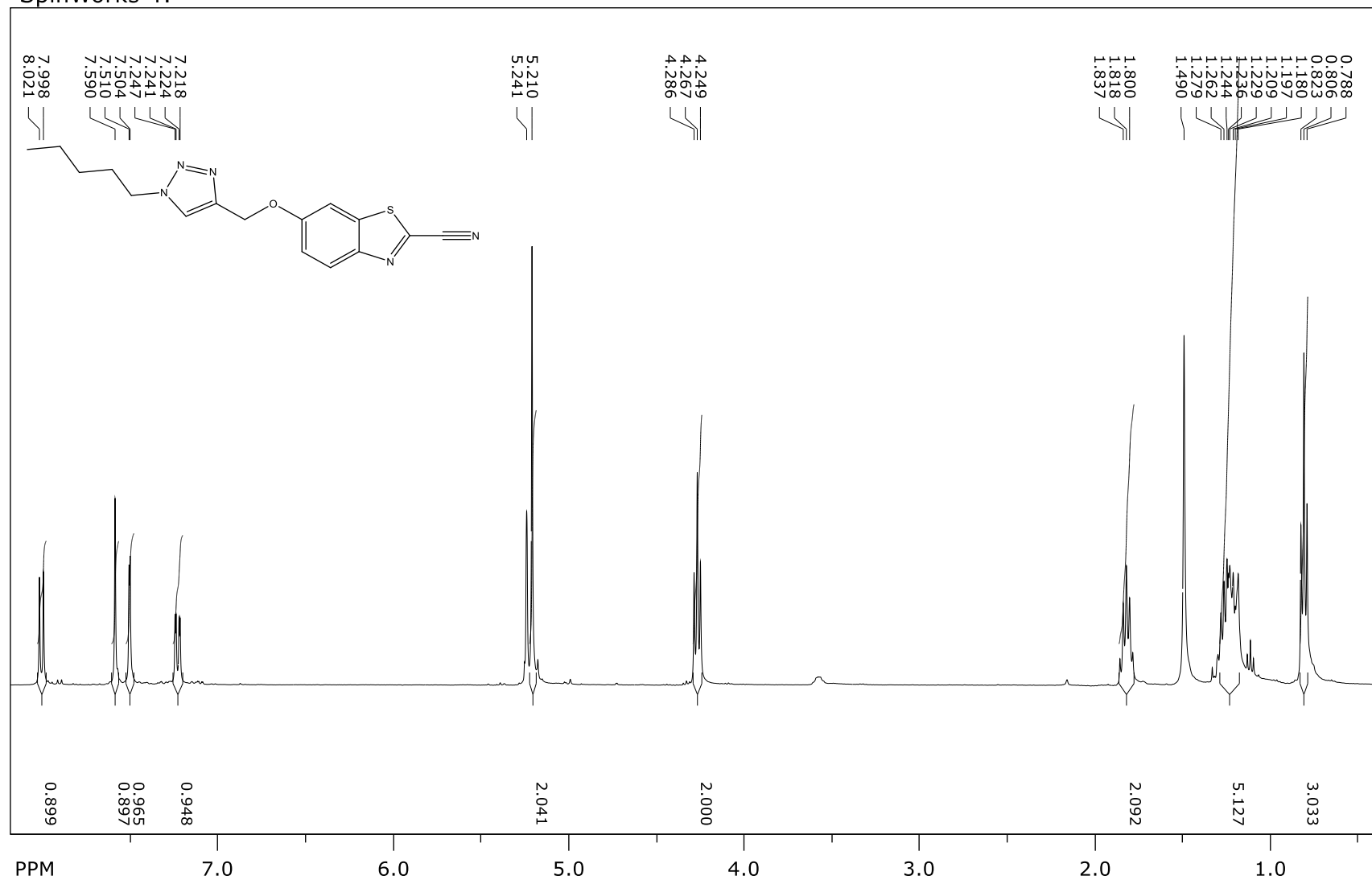
## SpinWorks 4: 13C OBSERVE



file: ...k\NMR's\HrahnLucfalkyne13C.fid\fid block# 1 expt: "s2pul"  
transmitter freq.: 100.526133 MHz  
time domain size: 59968 points  
width: 25000.00 Hz = 248.6916 ppm = 0.416889 Hz/pt  
number of scans: 14108

freq. of 0 ppm: 100.516621 MHz  
processed size: 65536 complex points  
LB: 1.000 GF: 0.0000

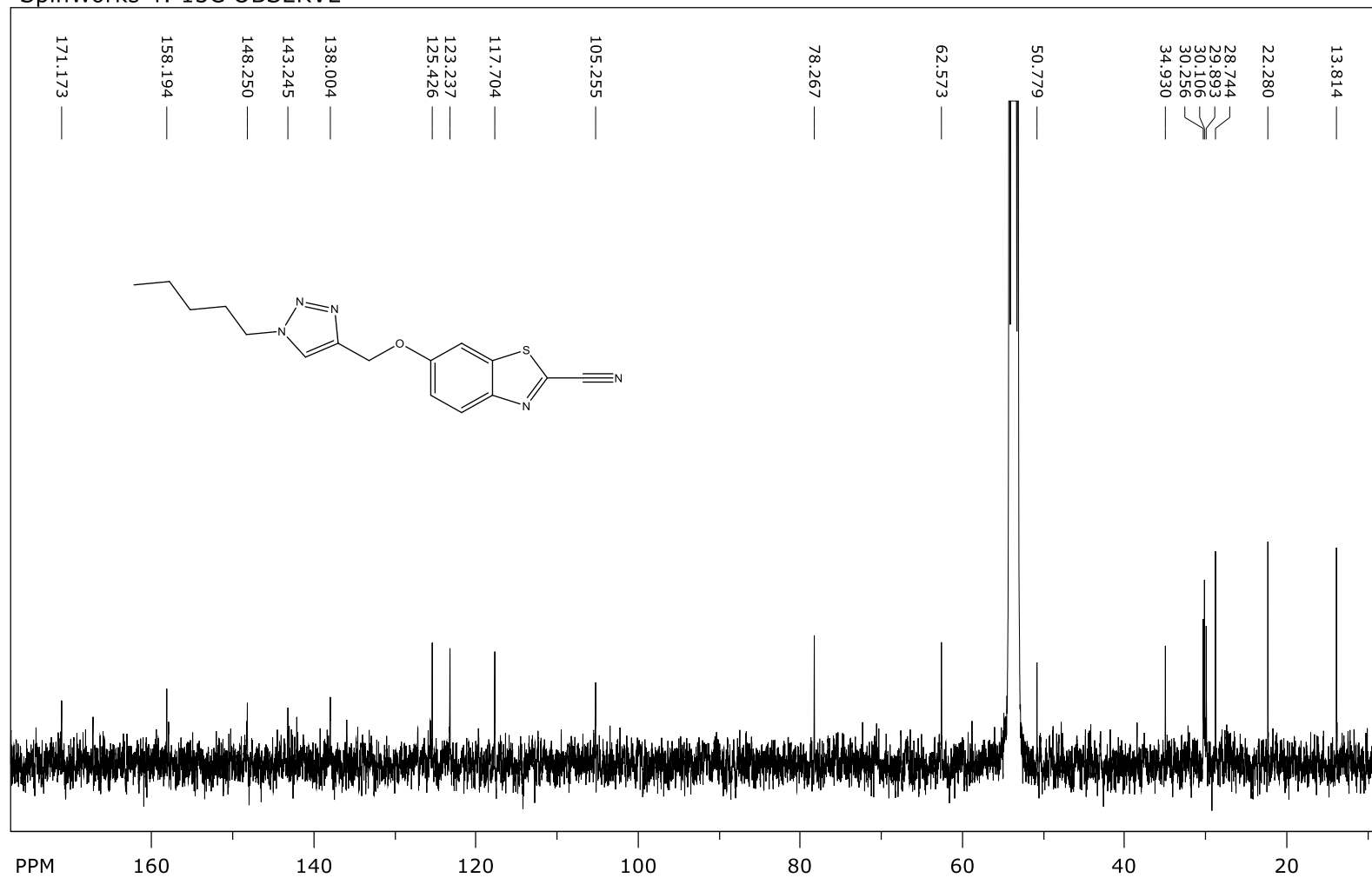
## SpinWorks 4:



file: ...-Trz-Pent\_12Sep2016\PROTON.fid\fid block# 1 expt: "s2pul"  
 transmitter freq.: 399.748916 MHz  
 time domain size: 35920 points  
 width: 4797.03 Hz = 12.0001 ppm = 0.133547 Hz/pt  
 number of scans: 32

freq. of 0 ppm: 399.746947 MHz  
 processed size: 65536 complex points  
 LB: 1.500 GF: 0.0000

## SpinWorks 4: 13C OBSERVE

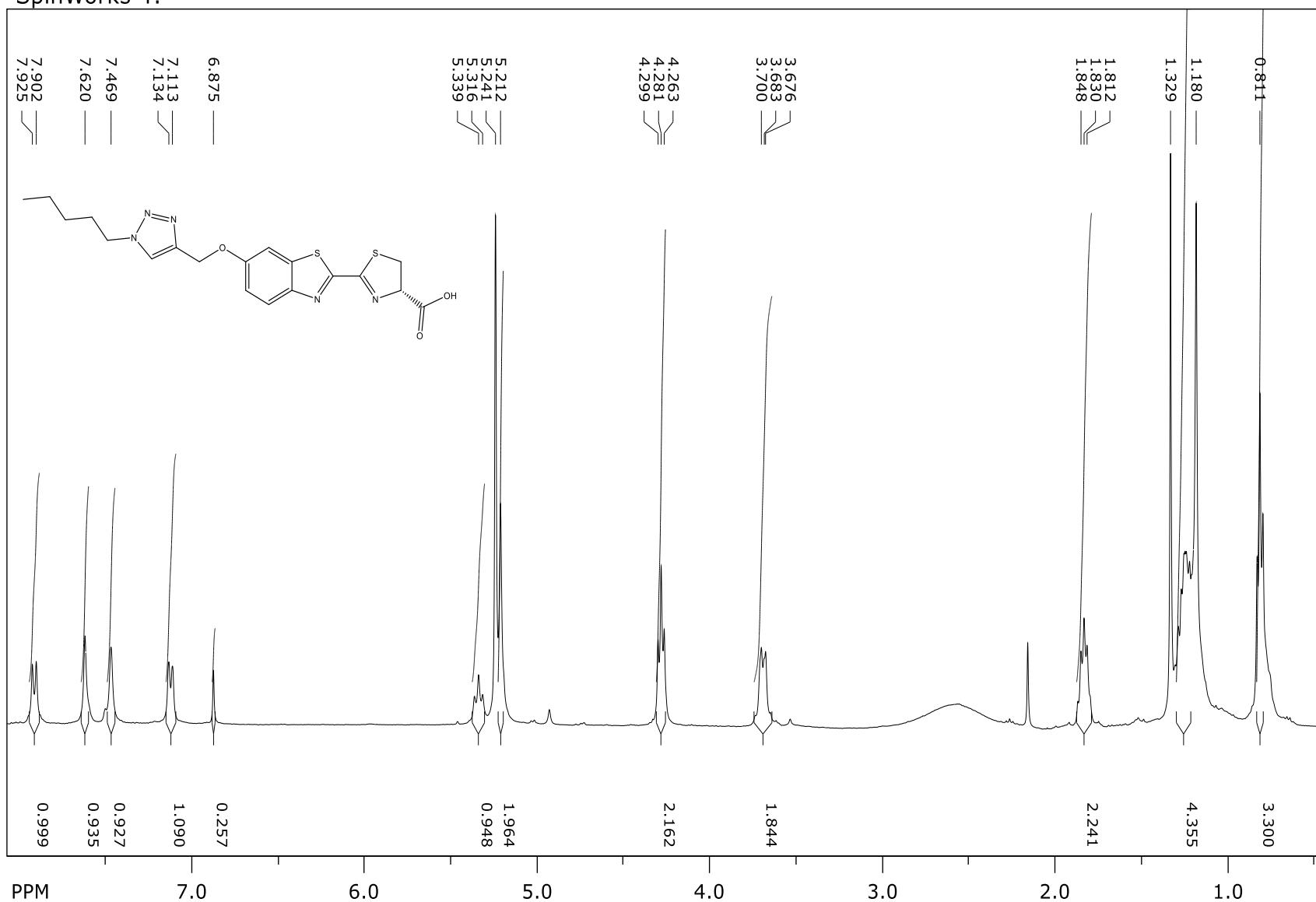


file: ...R's\HrahnLucftrzpentant13C.fid\fid\_block# 1 expt: "s2pul"  
transmitter freq.: 100.525930 MHz  
time domain size: 59968 points  
width: 25000.00 Hz = 248.6921 ppm = 0.416889 Hz/pt  
number of scans: 19040

freq. of 0 ppm: 100.516418 MHz  
processed size: 65536 complex points  
LB: 2.000 GF: 0.0000

## Luciferin-triazole-pentane

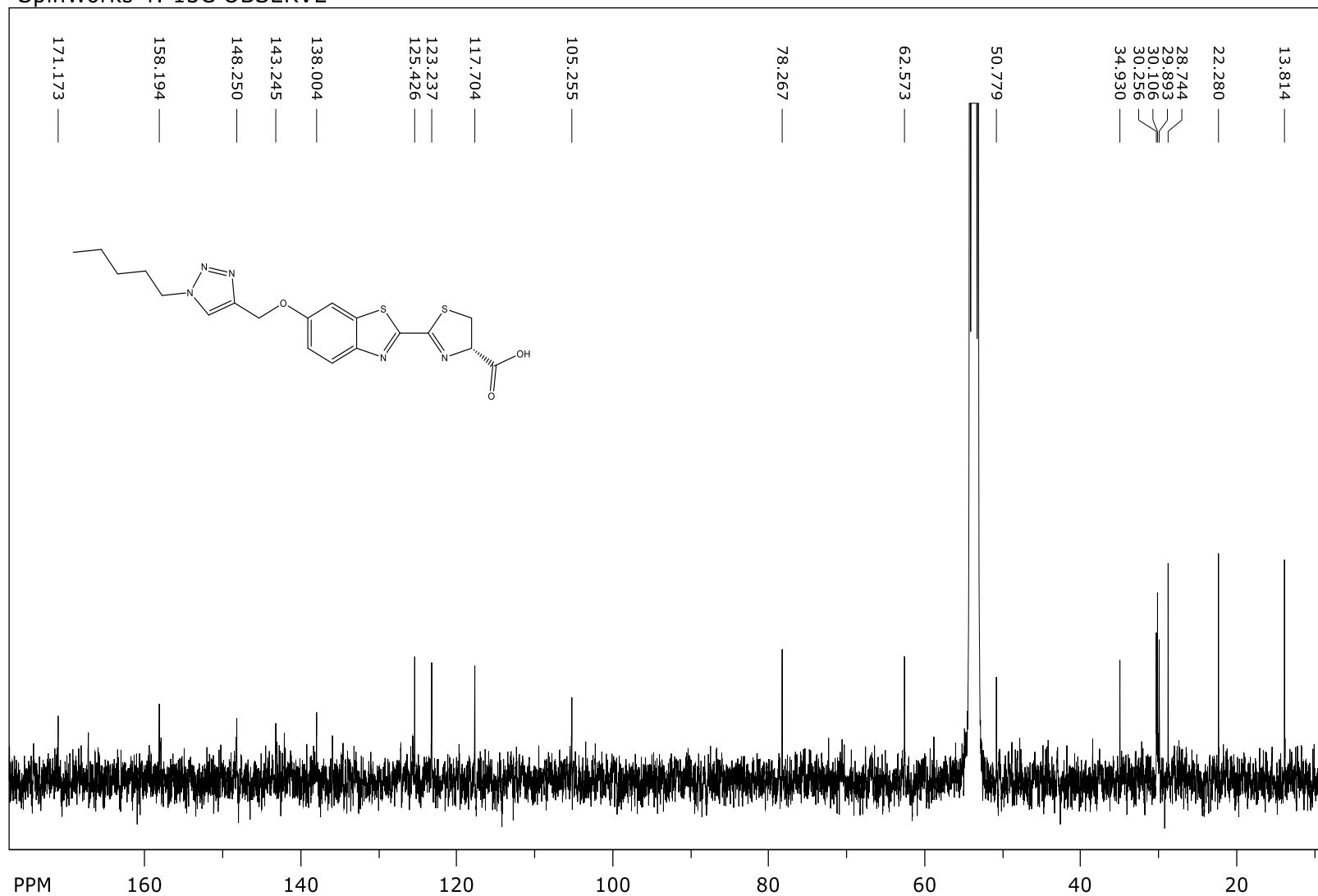
SpinWorks 4:



file: ...23Sep2016\_23Sep2016\PROTON.fid\fid\_block# 1 expt: "s2pul"  
 transmitter freq.: 399.748916 MHz  
 time domain size: 35920 points  
 width: 4797.03 Hz = 12.0001 ppm = 0.133547 Hz/pt  
 number of scans: 32

freq. of 0 ppm: 399.746948 MHz  
 processed size: 65536 complex points  
 LB: 1.500 GF: 0.0000

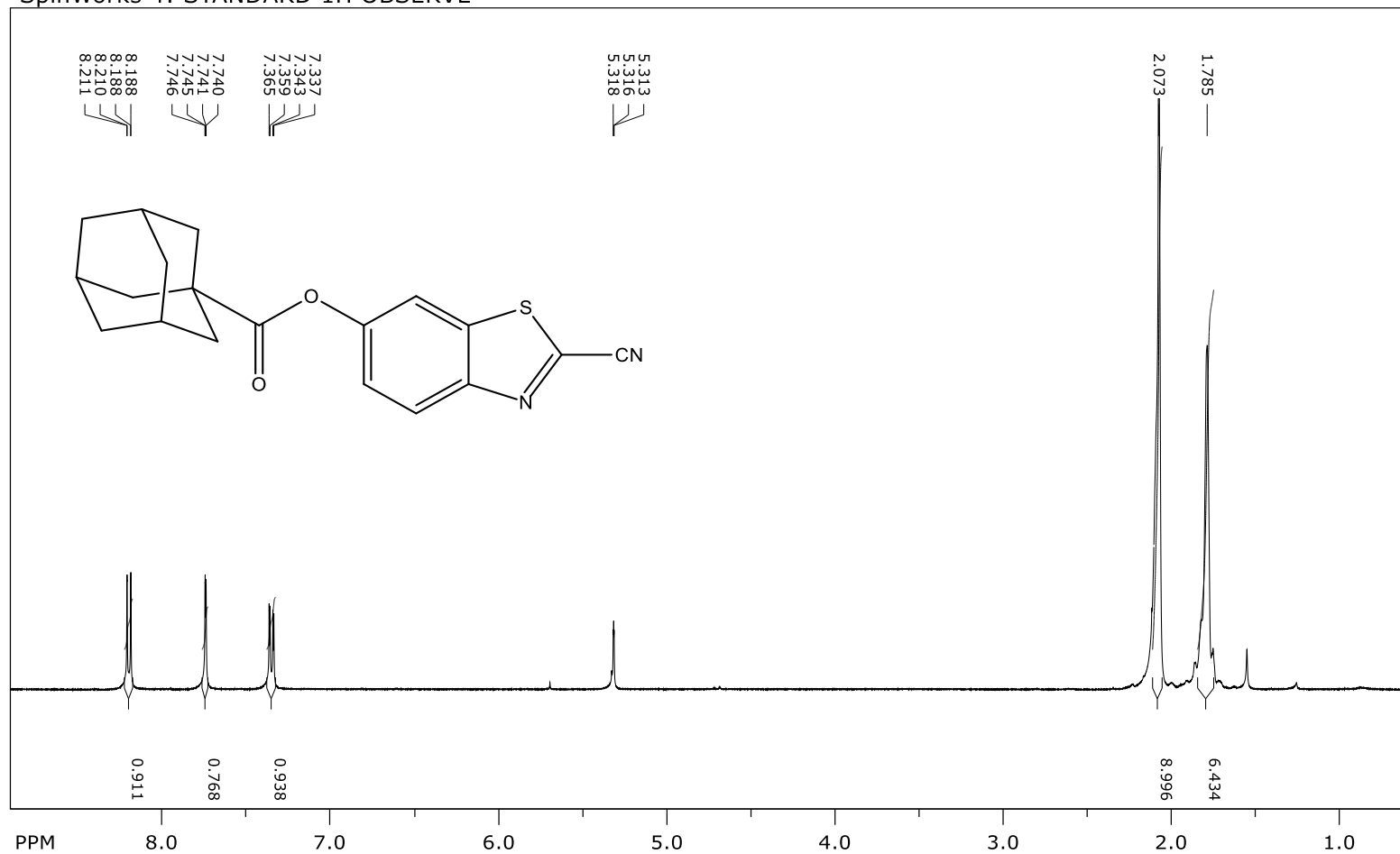
## SpinWorks 4: 13C OBSERVE



file: ...R's\HrahnLucftrzpentant13C.fid\fid block# 1 expt: "s2pul"  
transmitter freq.: 100.525930 MHz  
time domain size: 59968 points  
width: 25000.00 Hz = 248.6921 ppm = 0.416889 Hz/pt  
number of scans: 19040

freq. of 0 ppm: 100.516418 MHz  
processed size: 65536 complex points  
LB: 2.000 GF: 0.0000

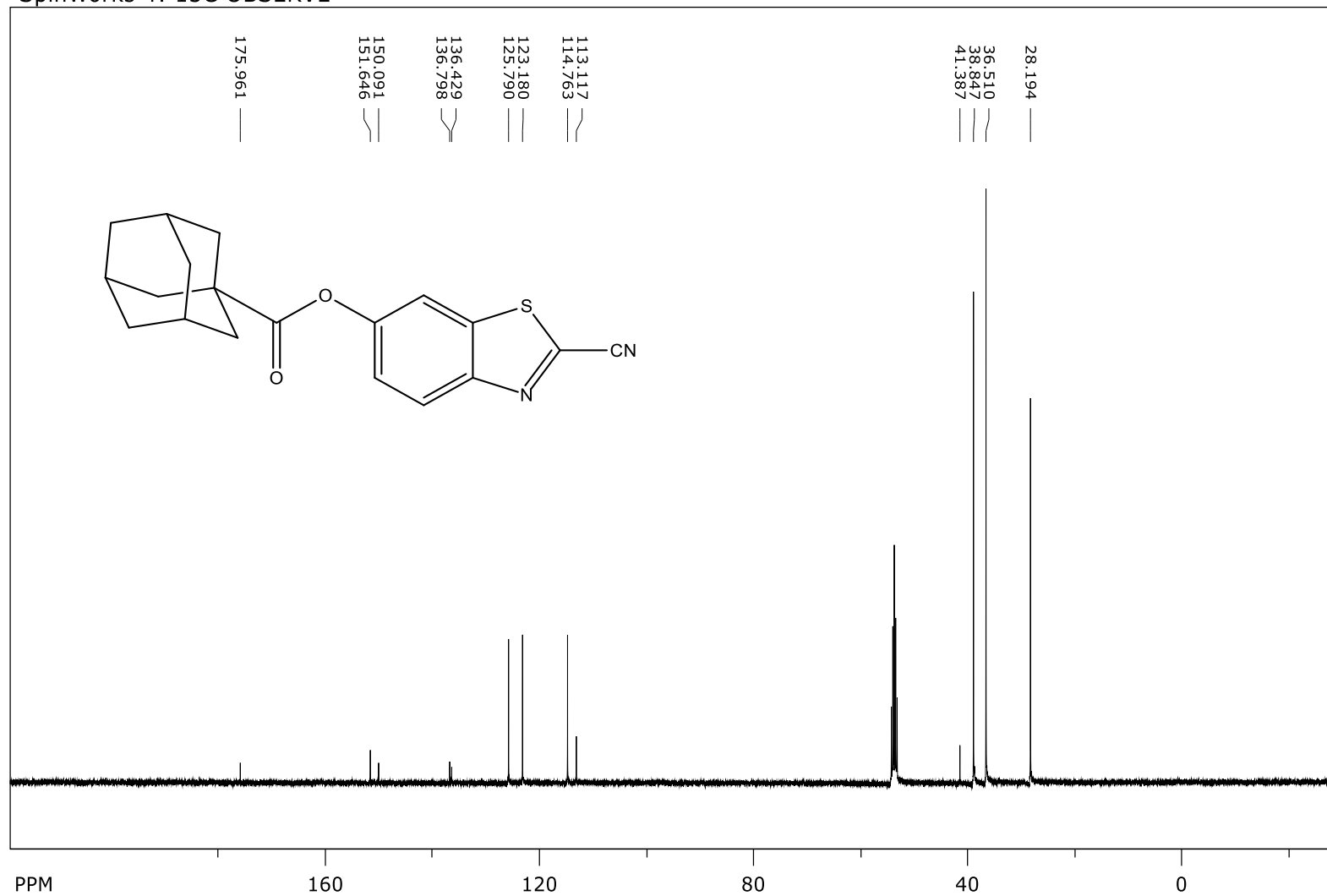
## SpinWorks 4: STANDARD 1H OBSERVE



file: ...nCBTZCarbAd\_1H\_11April2017.fid\fid\_block# 1 expt: "s2pul"  
transmitter freq.: 399.748916 MHz  
time domain size: 44932 points  
width: 6000.60 Hz = 15.0109 ppm = 0.133548 Hz/pt  
number of scans: 64

freq. of 0 ppm: 399.746917 MHz  
processed size: 65536 complex points  
LB: 0.000 GF: 0.0000

## SpinWorks 4: 13C OBSERVE

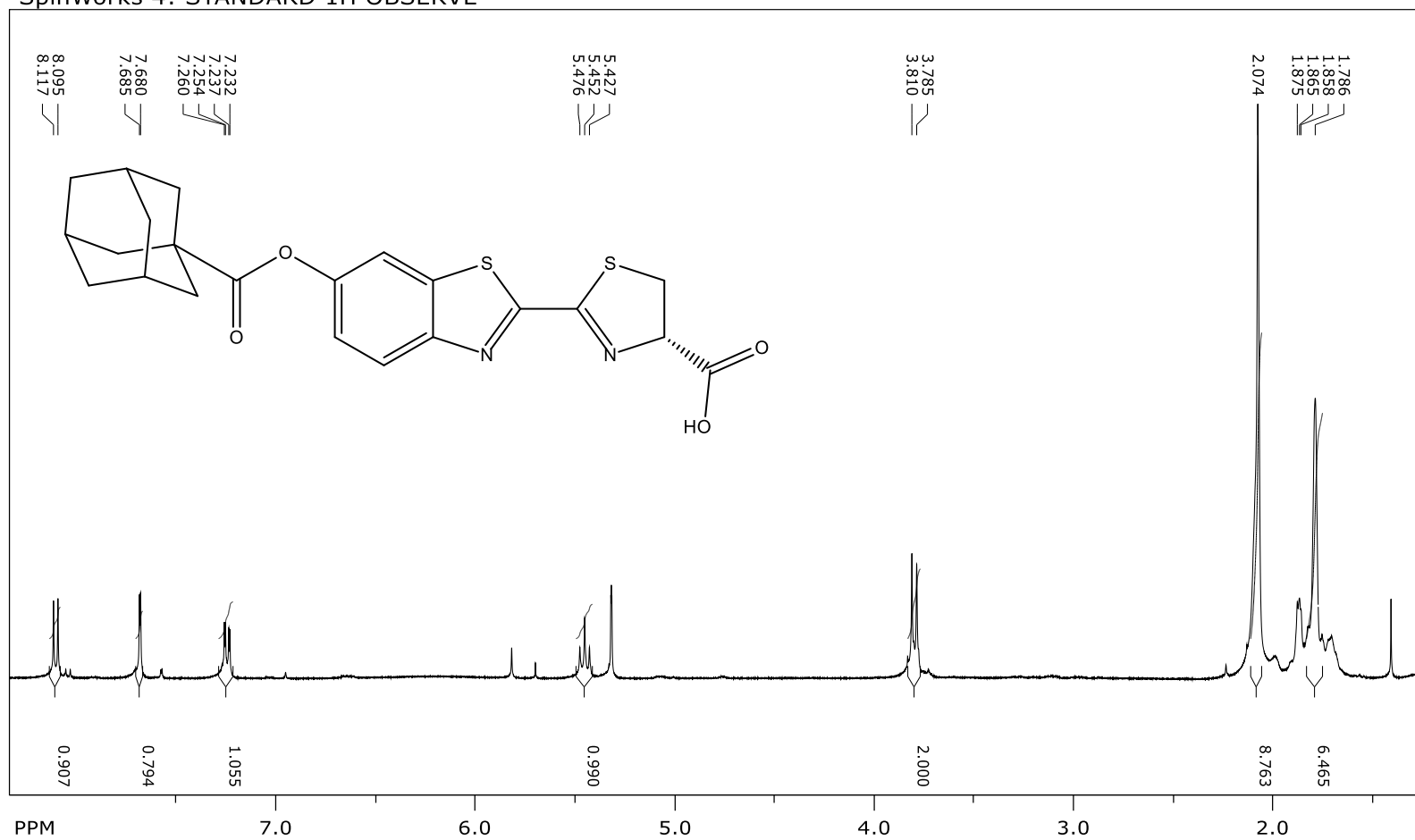


file: ...CBTZCarbAd\_13C\_11April2017.fid\fid\_block# 1 expt: "s2pul"  
transmitter freq.: 100.525930 MHz  
time domain size: 59968 points  
width: 25000.00 Hz = 248.6921 ppm = 0.416889 Hz/pt  
number of scans: 4432

freq. of 0 ppm: 100.516418 MHz  
processed size: 65536 complex points  
LB: 1.000 GF: 0.0000

## Luciferin Adamantanoate

SpinWorks 4: STANDARD 1H OBSERVE

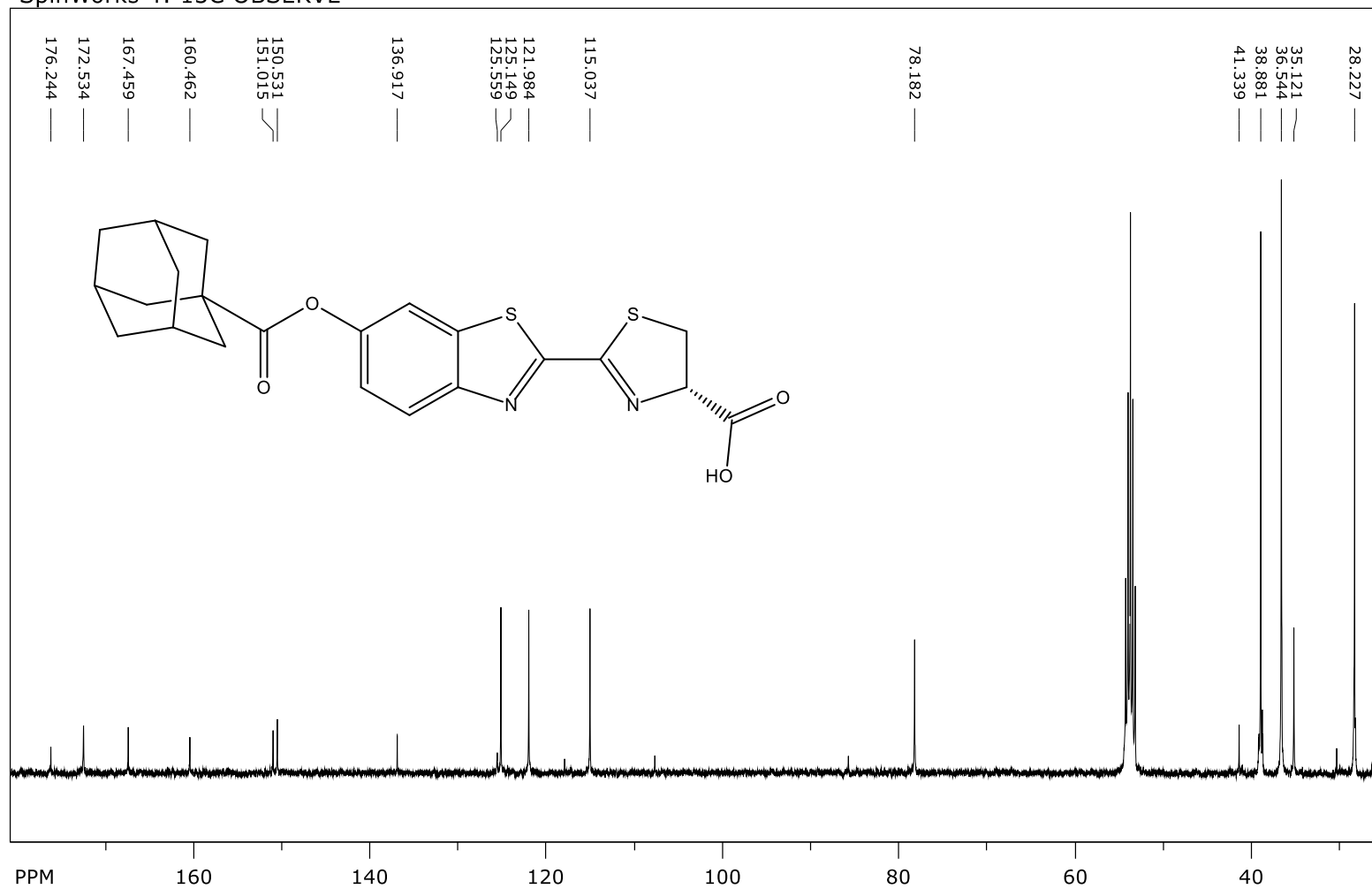


file: ...\_LucfCarbAd\_1H\_11April2017.fid\fid\_block# 1 expt: "s2pul"  
transmitter freq.: 399.748916 MHz  
time domain size: 44932 points  
width: 6000.60 Hz = 15.0109 ppm = 0.133548 Hz/pt  
number of scans: 64

freq. of 0 ppm: 399.746917 MHz  
processed size: 65536 complex points  
LB: 0.000 GF: 0.0000



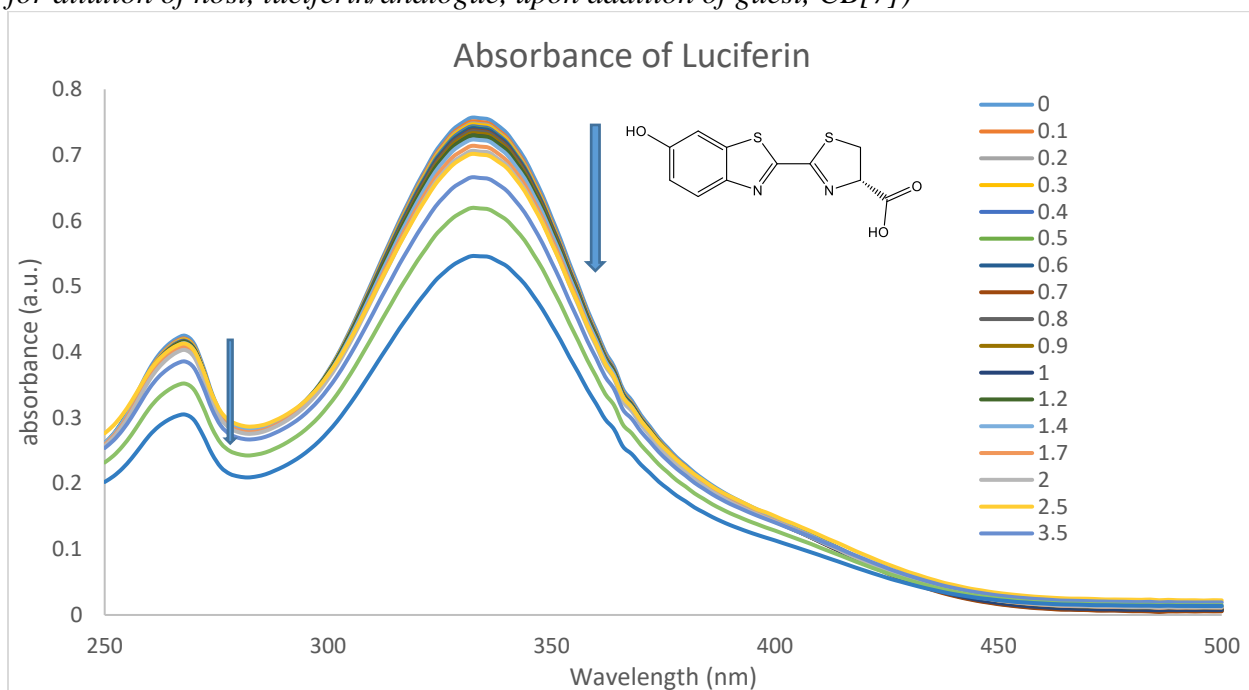
## SpinWorks 4: 13C OBSERVE



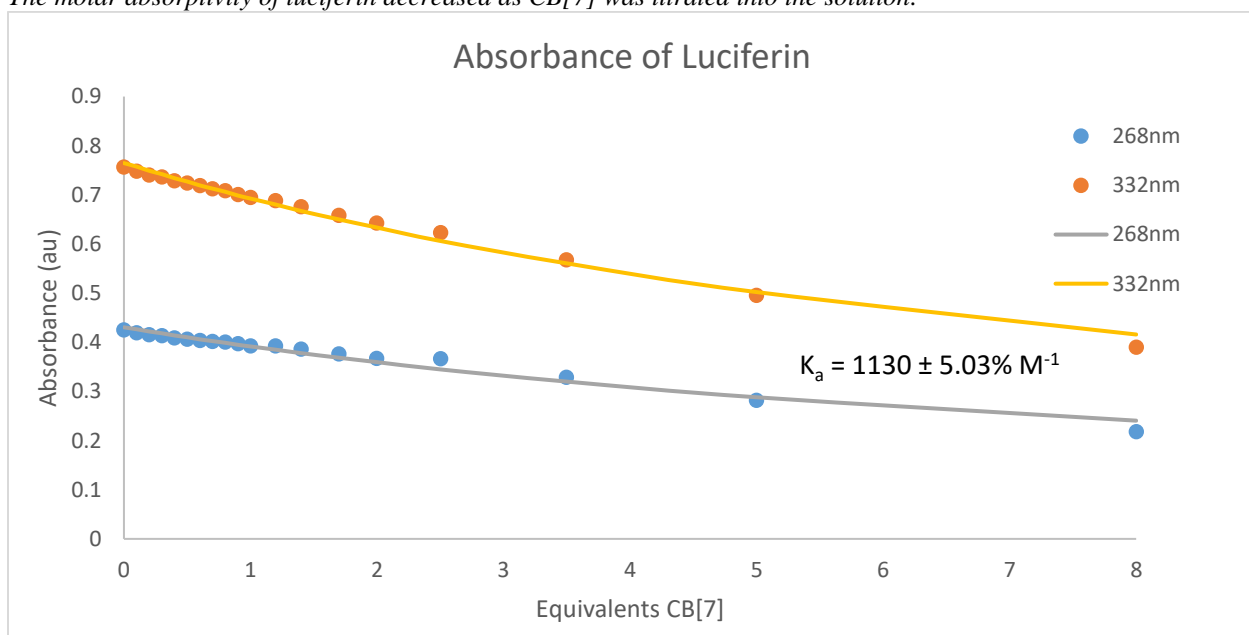
file: ...\\NMR's\HA\_4\_12\_17\_13kscans.fid\fid block# 1 expt: "s2pul"  
transmitter freq.: 100.525930 MHz  
time domain size: 59968 points  
width: 25000.00 Hz = 248.6921 ppm = 0.416889 Hz/pt  
number of scans: 13264

freq. of 0 ppm: 100.516418 MHz  
processed size: 65536 complex points  
LB: 2.000 GF: 0.0000

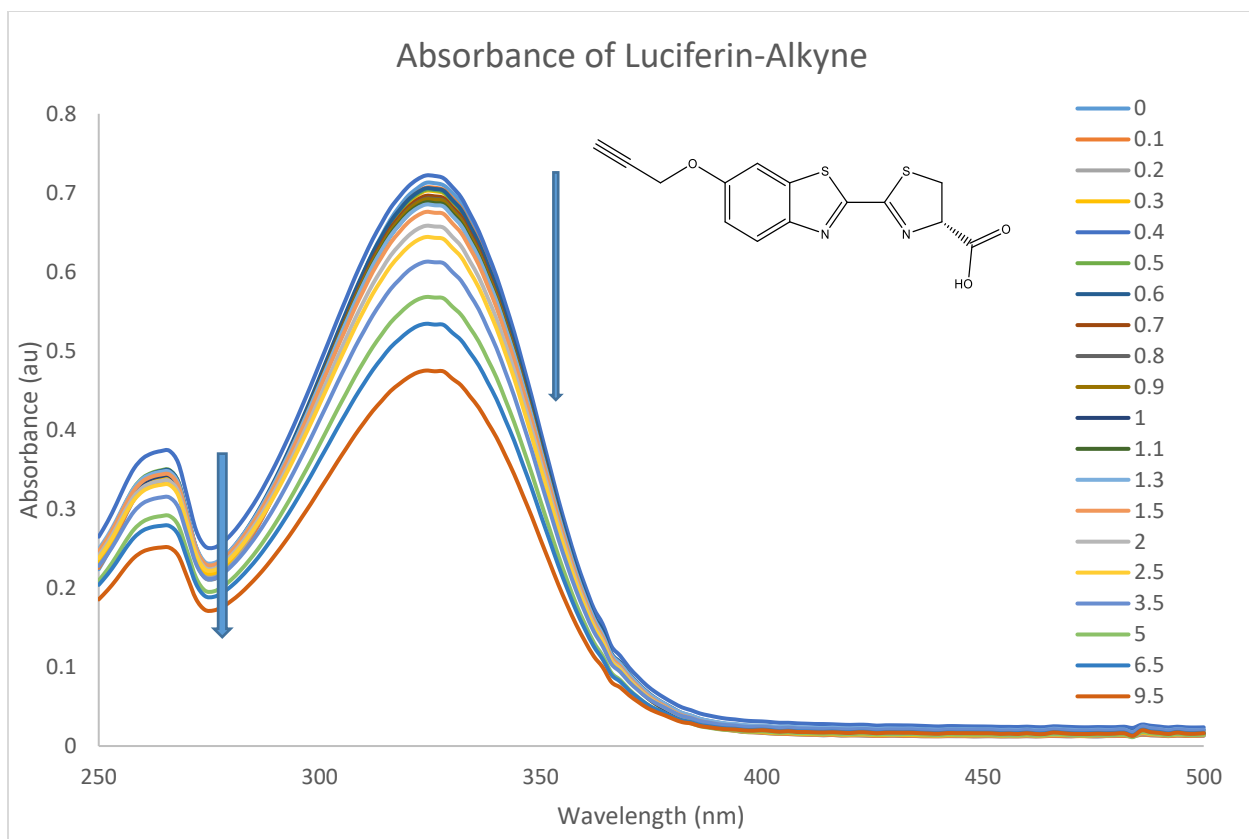
*SI.3 Absorbance Spectra for Binding determination  
(Procedure and conditions for all luciferins is described in Chapter 2.3. Fitting accounts for dilution of host, luciferin/analogue, upon addition of guest, CB[7])<sup>[27]</sup>*



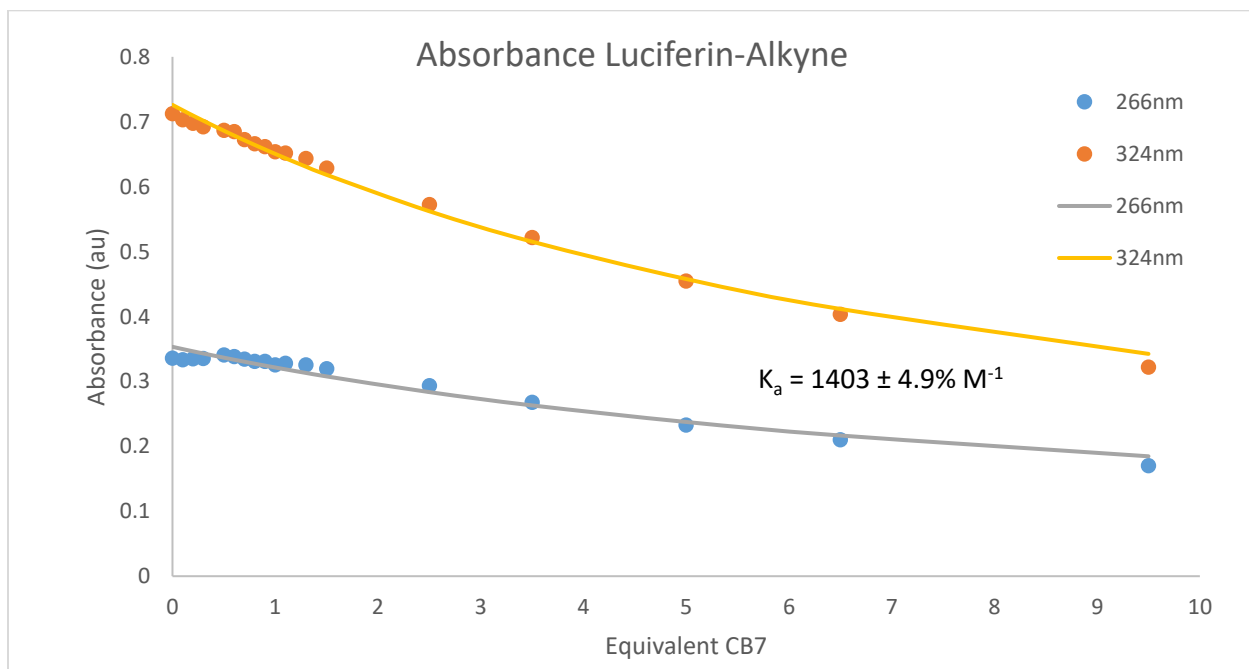
*The molar absorptivity of luciferin decreased as CB[7] was titrated into the solution.*



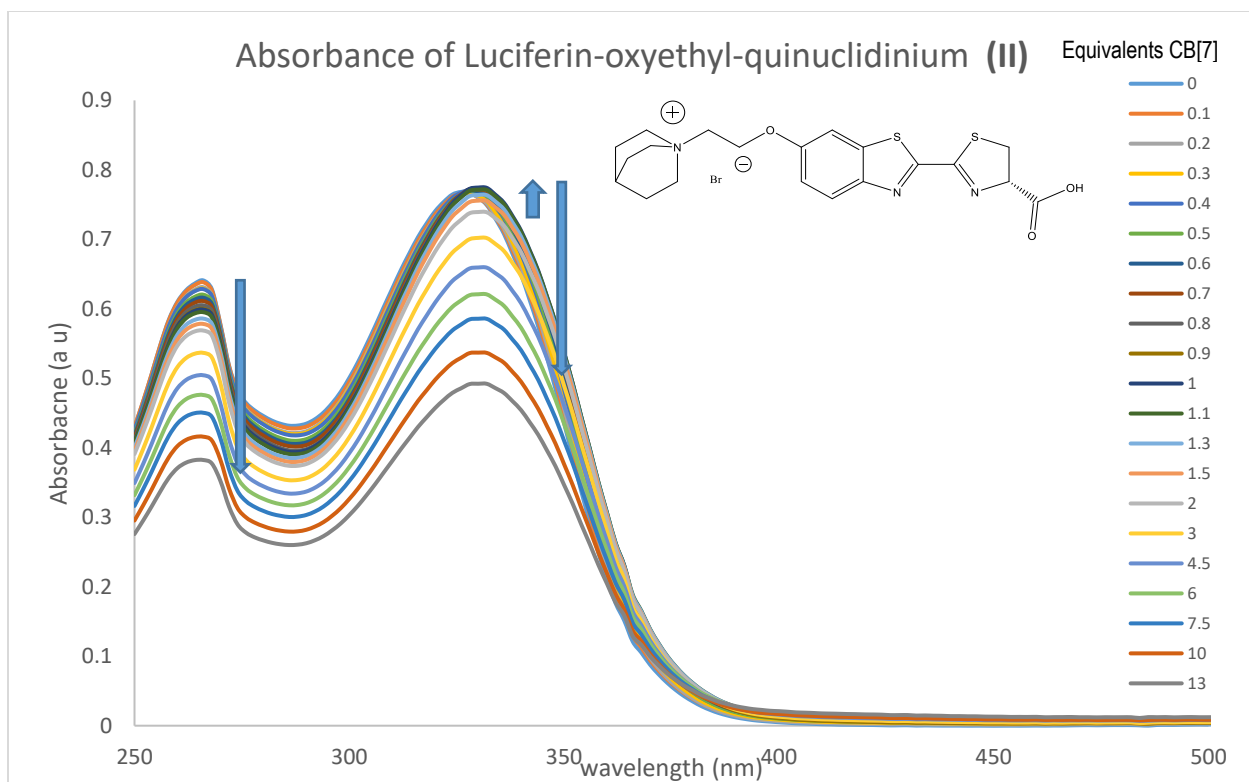
*The change in peak absorptivity was fitted using "Bindfit 0.5" freeware compensating for dilution and a 1:1 binding equation.*



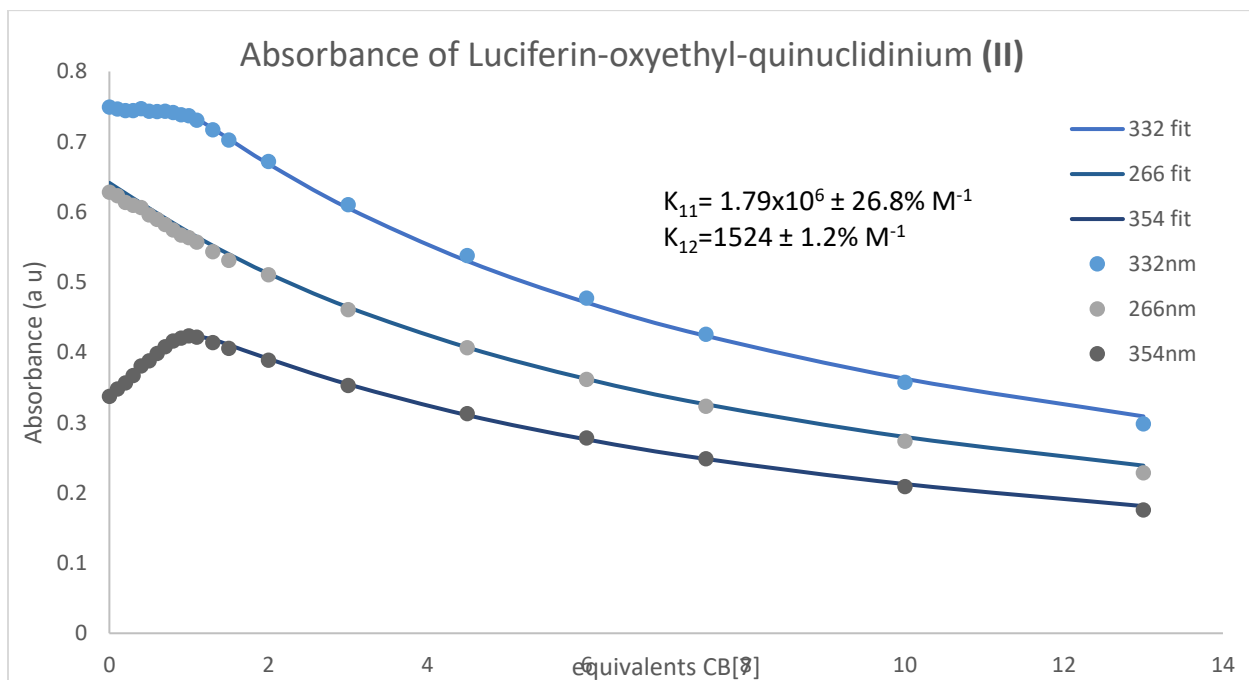
*The molar absorptivity of luciferin-alkyne decreased as CB[7] was titrated into the solution.*



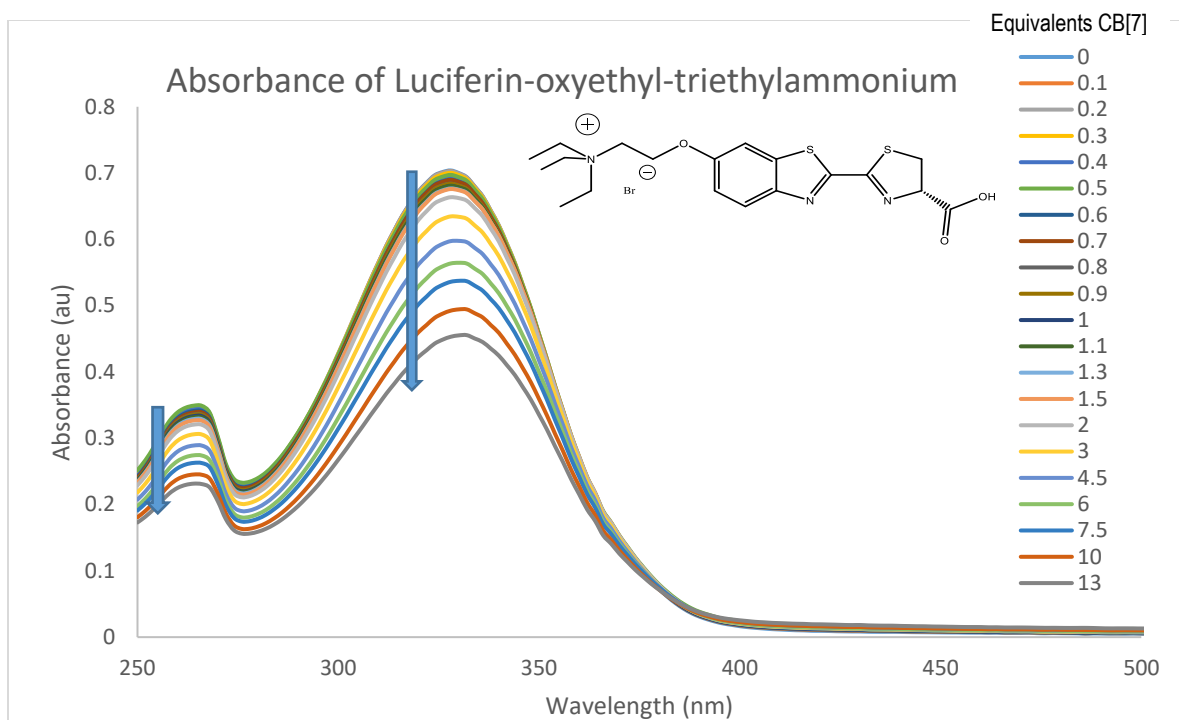
*The change in peak absorptivity was fitted using "Bindfit 0.5" freeware compensating for dilution and a 1:1 binding equation.*



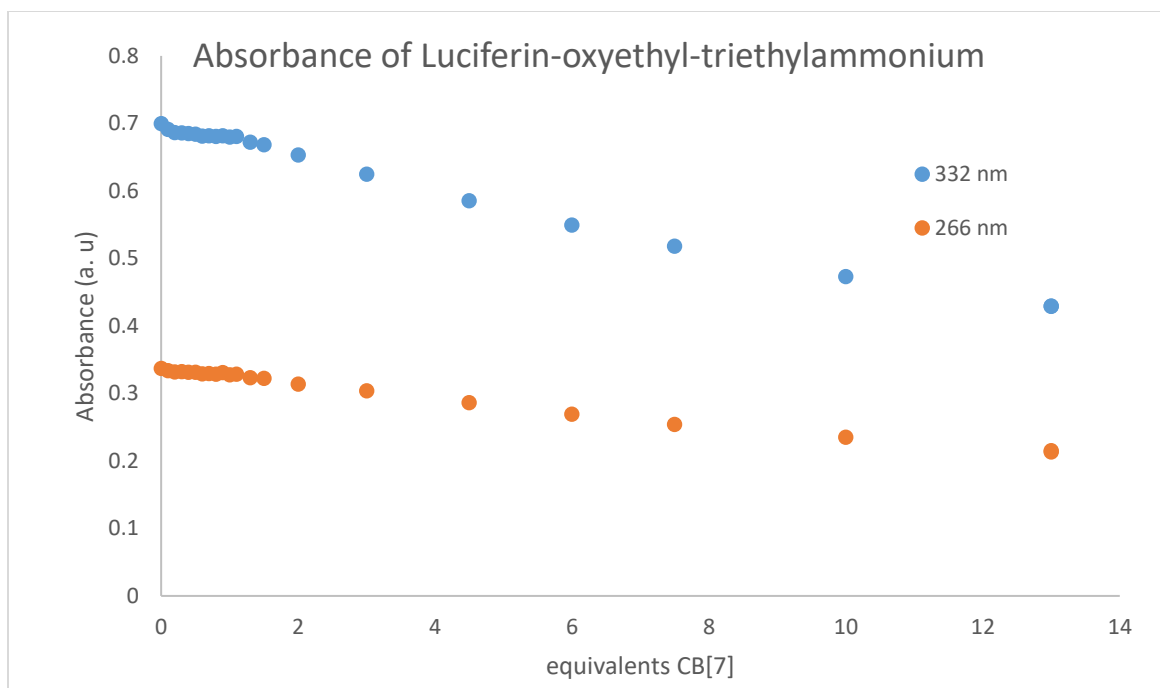
The 332 nm peak molar absorptivity of luciferin-oxyethyl-quinuclidinium (II) initially increased from 0-1 equivalents of CB[7] then decreased after the quinuclidinium binding site was saturated



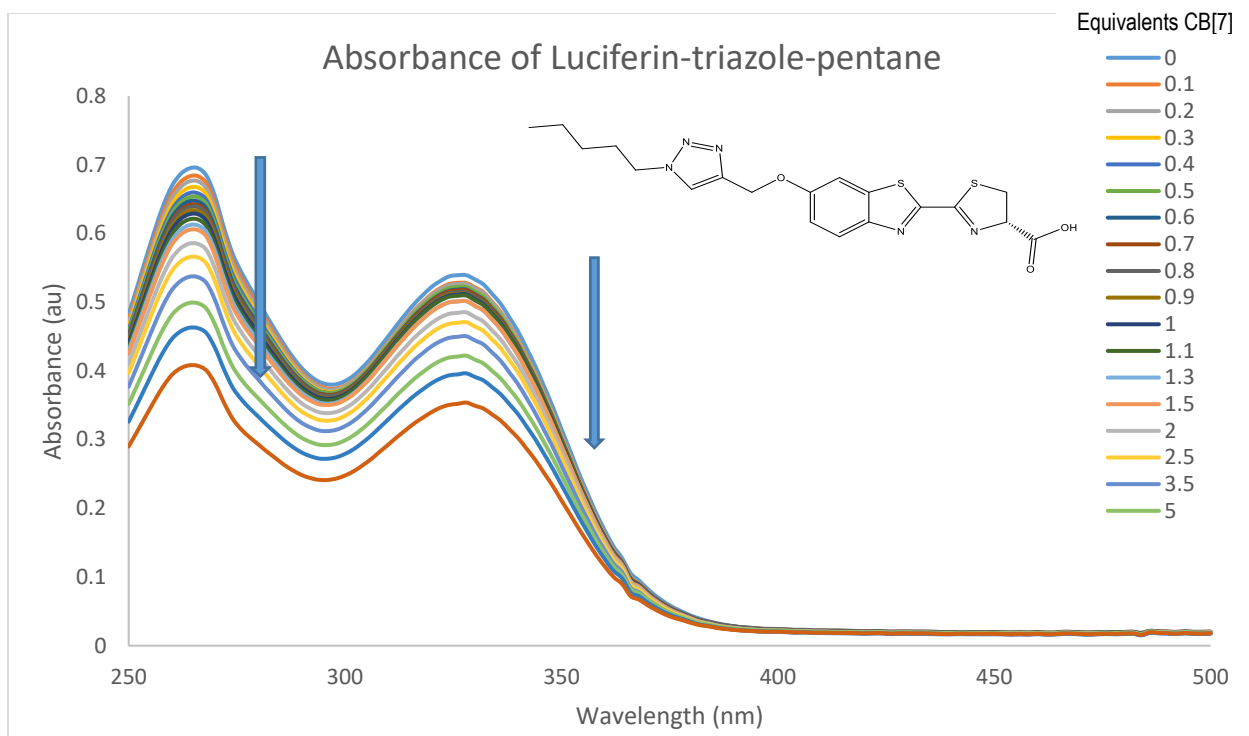
The change in peak absorptivity was fitted using "Bindfit 0.5" freeware compensating for dilution and a 1:2 binding equation. To assist with fitting, the wavelength where the greatest change was observed was all used to fit the binding events



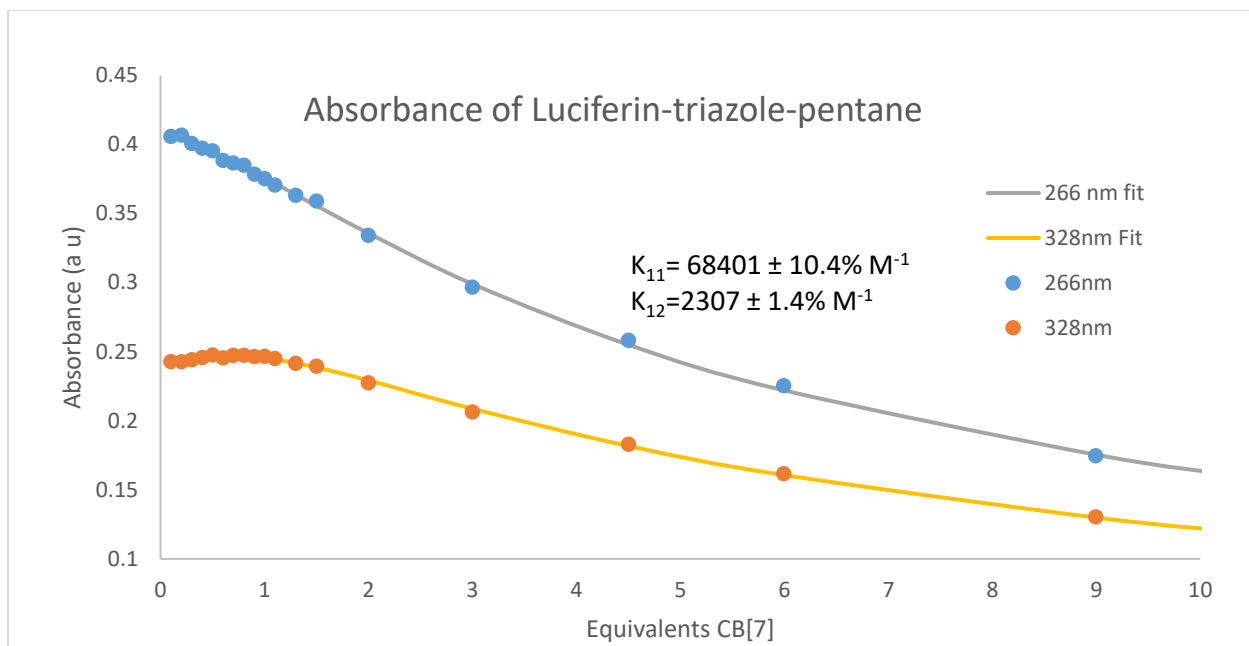
The molar absorptivity of luciferin-oxyethyl-triethylammonium decreased as CB[7] was titrated into the solution.



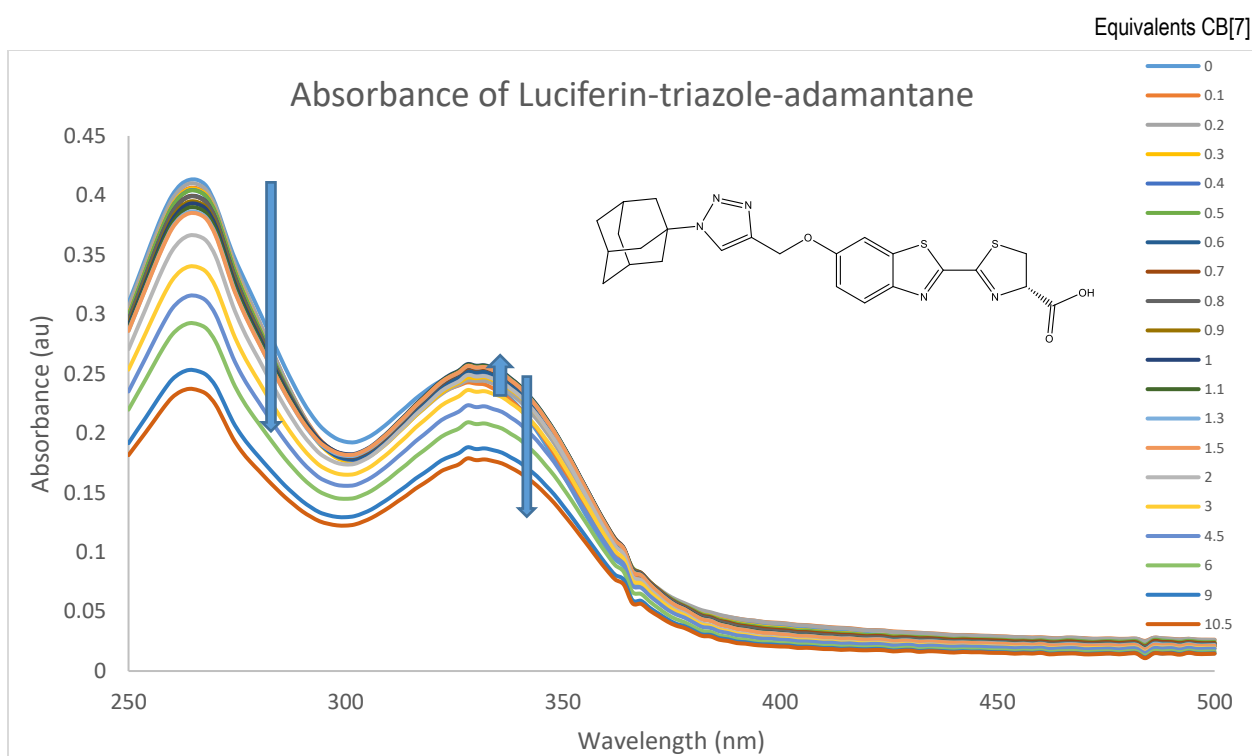
The peak absorptivity shows a distinct bimodal 1:2 change in absorptivity in which there is little change in absorptivity from 0-1 equivalent and a steady drop from 1-13 equivalents of CB[7]. Because of its little change between 0-1 equivalents this curve was hard to fit with realistic quantities, thus it is anticipated that binding first occurs at the ammonium then on the aromatic core of the luciferin.



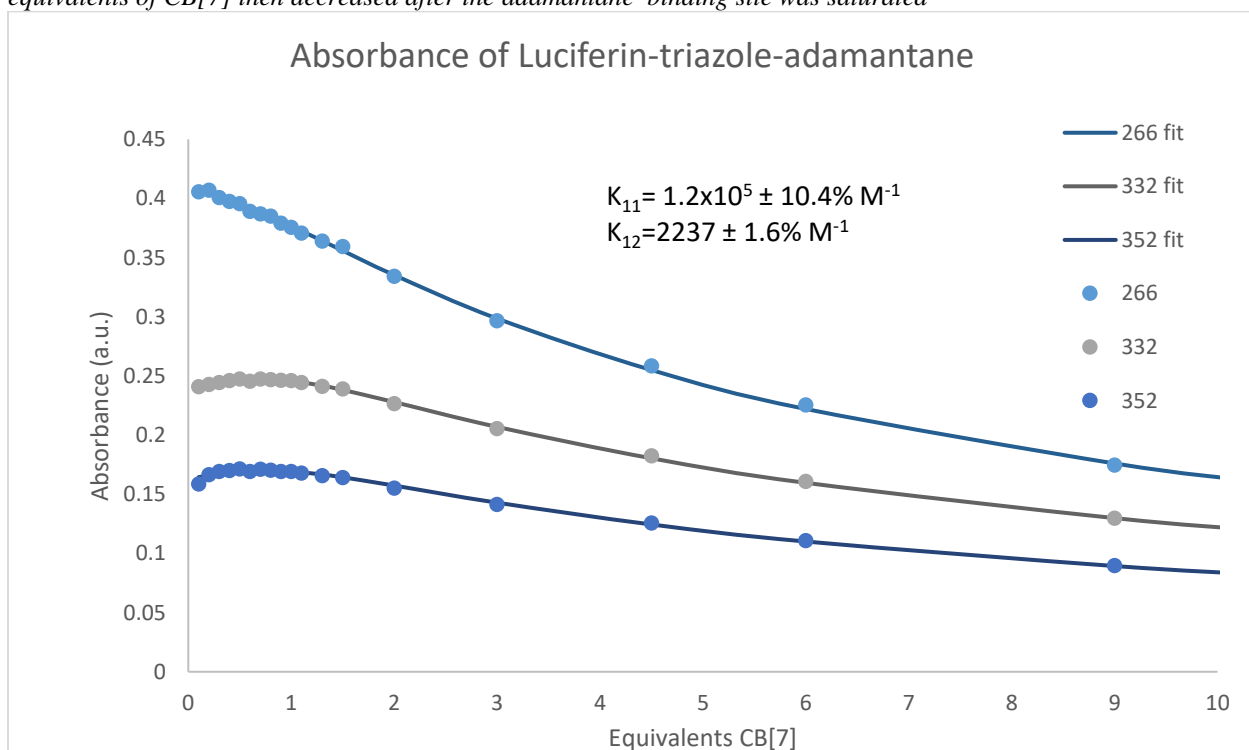
*The 328 nm peak molar absorptivity of luciferin-triazole-pentane initially increased from 0-1 equivalents of CB[7] then decreased after the pentane binding site was saturated*



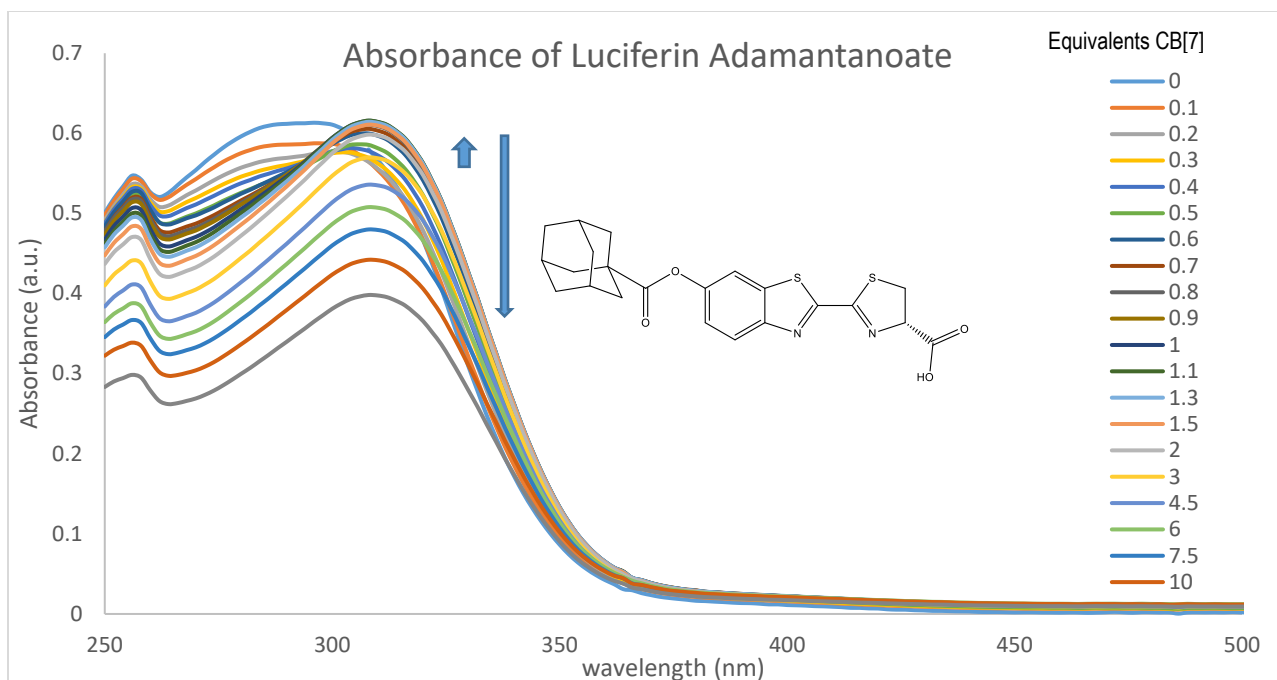
*The change in peak absorptivity was fitted using "Bindfit 0.5" freeware compensating for dilution and a 1:2 binding equation.*



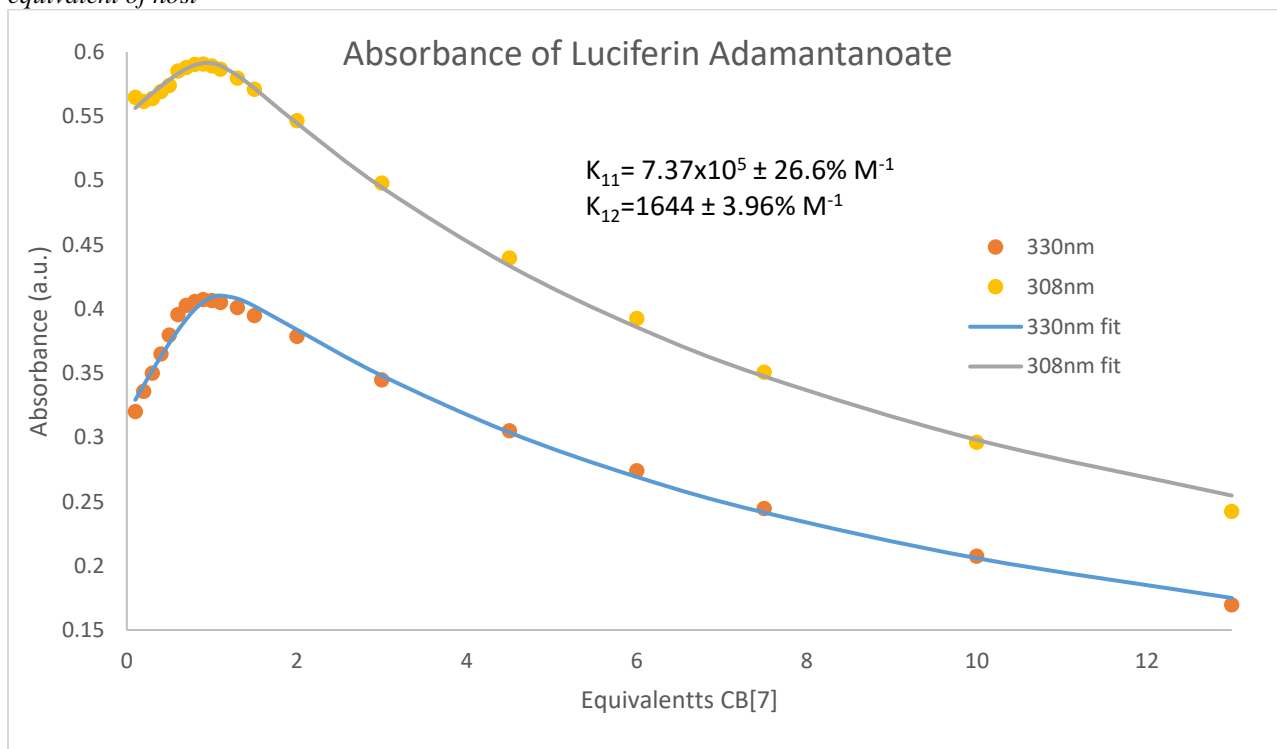
The 332 nm peak molar absorptivity of luciferin-triazole-adamantane initially increased from 0-1 equivalents of CB[7] then decreased after the adamantane binding site was saturated



The change in peak absorptivity was fitted using "Bindfit 0.5" freeware compensating for dilution and a 1:2 binding equation.



A peak at 308 increases from 0-1 equivalent CB[7] then the absorbance decreases dramatically after 1 equivalent of host



The change in peak absorptivity was fitted using "Bindfit 0.5" freeware compensating for dilution and a 1:2 binding equation.



## SI.4 NMR Spectra of Novel Species and CB[7]

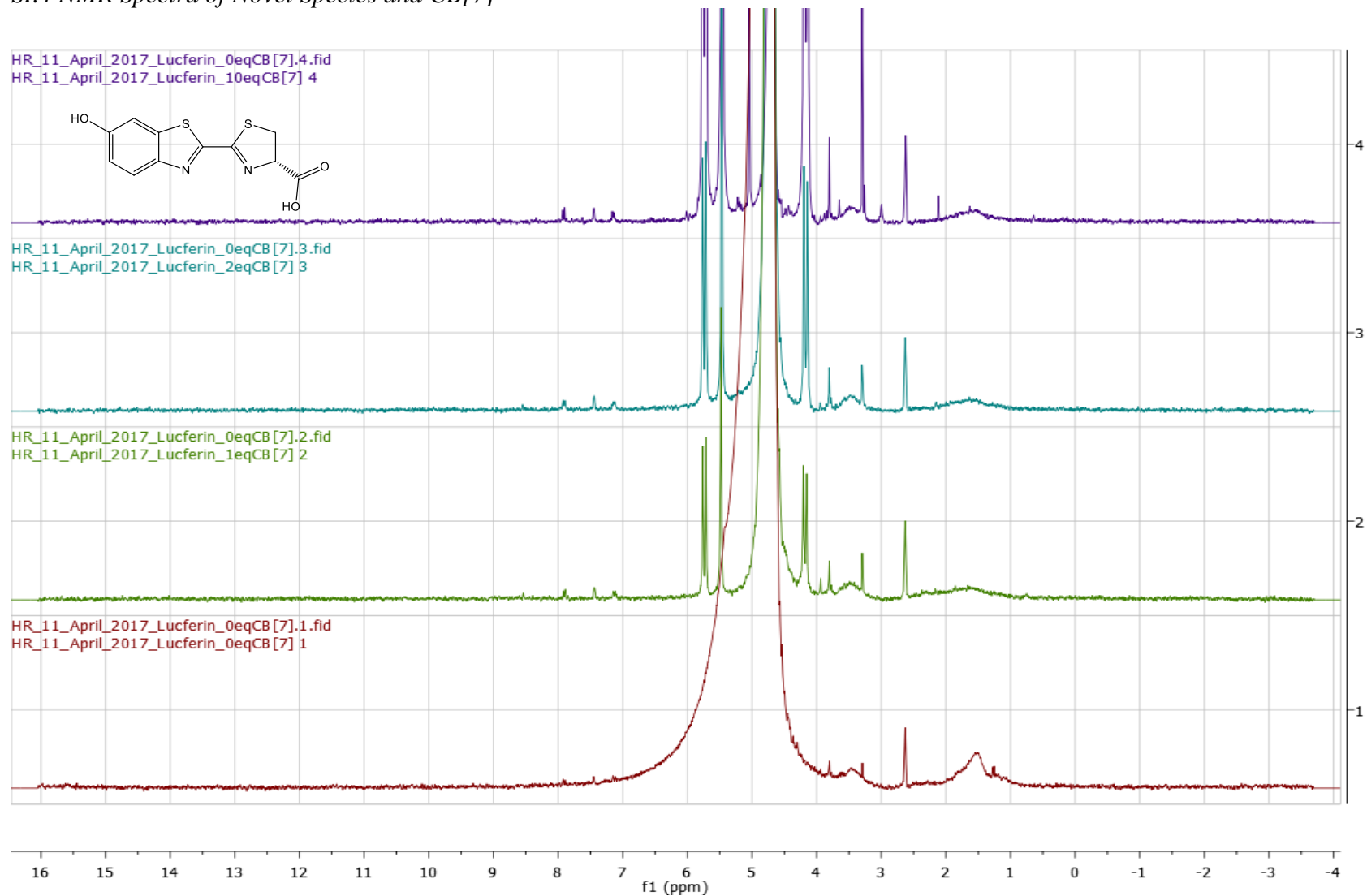


Figure: Raw NMR of luciferin in D<sub>2</sub>O (no peak-picking software used for processing): 1% d<sub>6</sub>-DMSO titrated with 0, 1, 2, 10 equivalents of CB[7] (increasing vertical displacement in the figure). Concentration of luciferin is 0.167 mmol.

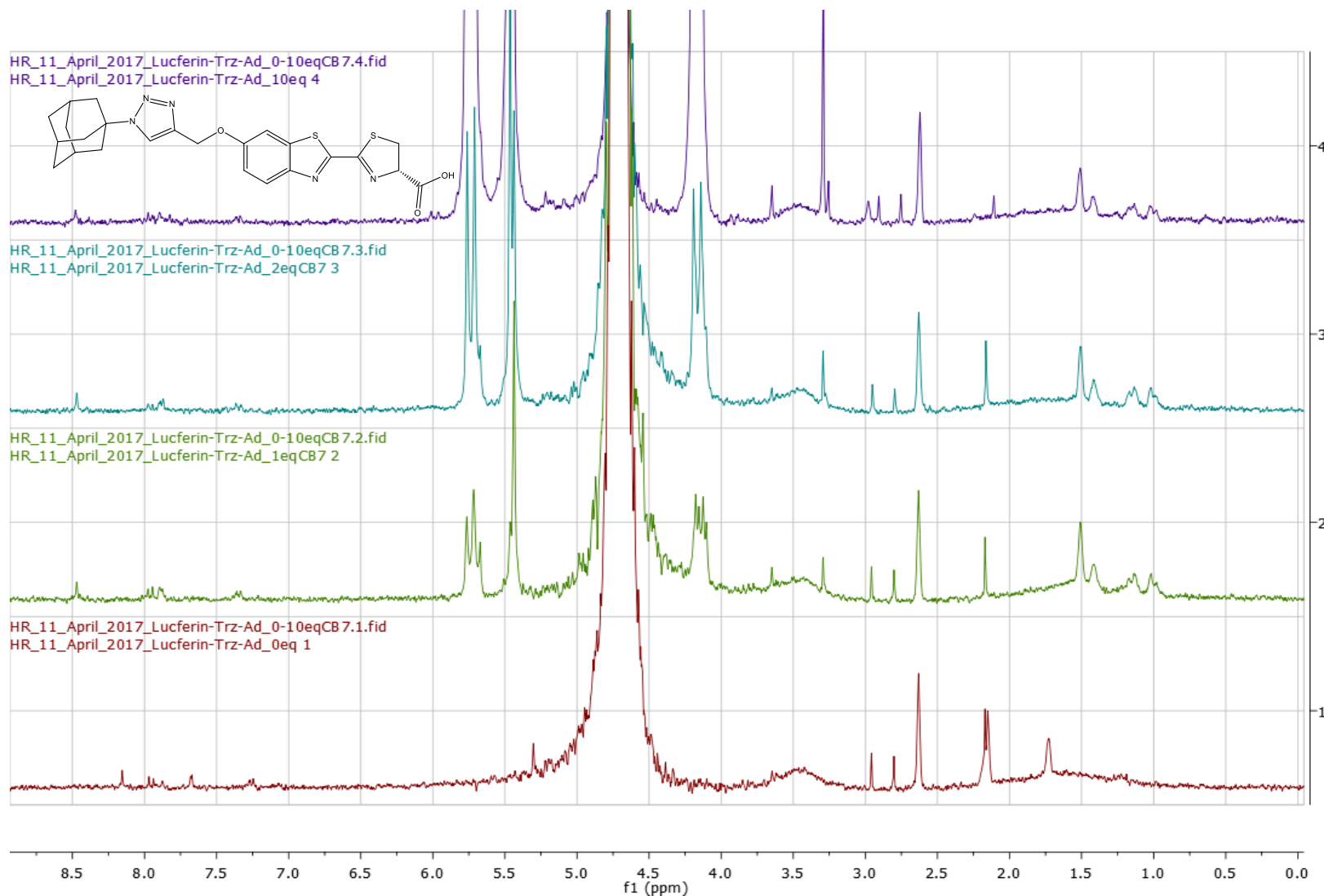


Figure: Raw NMR of luciferin-triazole-adamantane in  $D_2O$  (no peak-picking software used for processing): 1%  $d_6$ -DMSO titrated with 0, 1, 2, 10 equivalents of CB[7] (increasing vertical displacement in the figure). Concentration of luciferin-triazole-adamantane is 0.167 mmol.

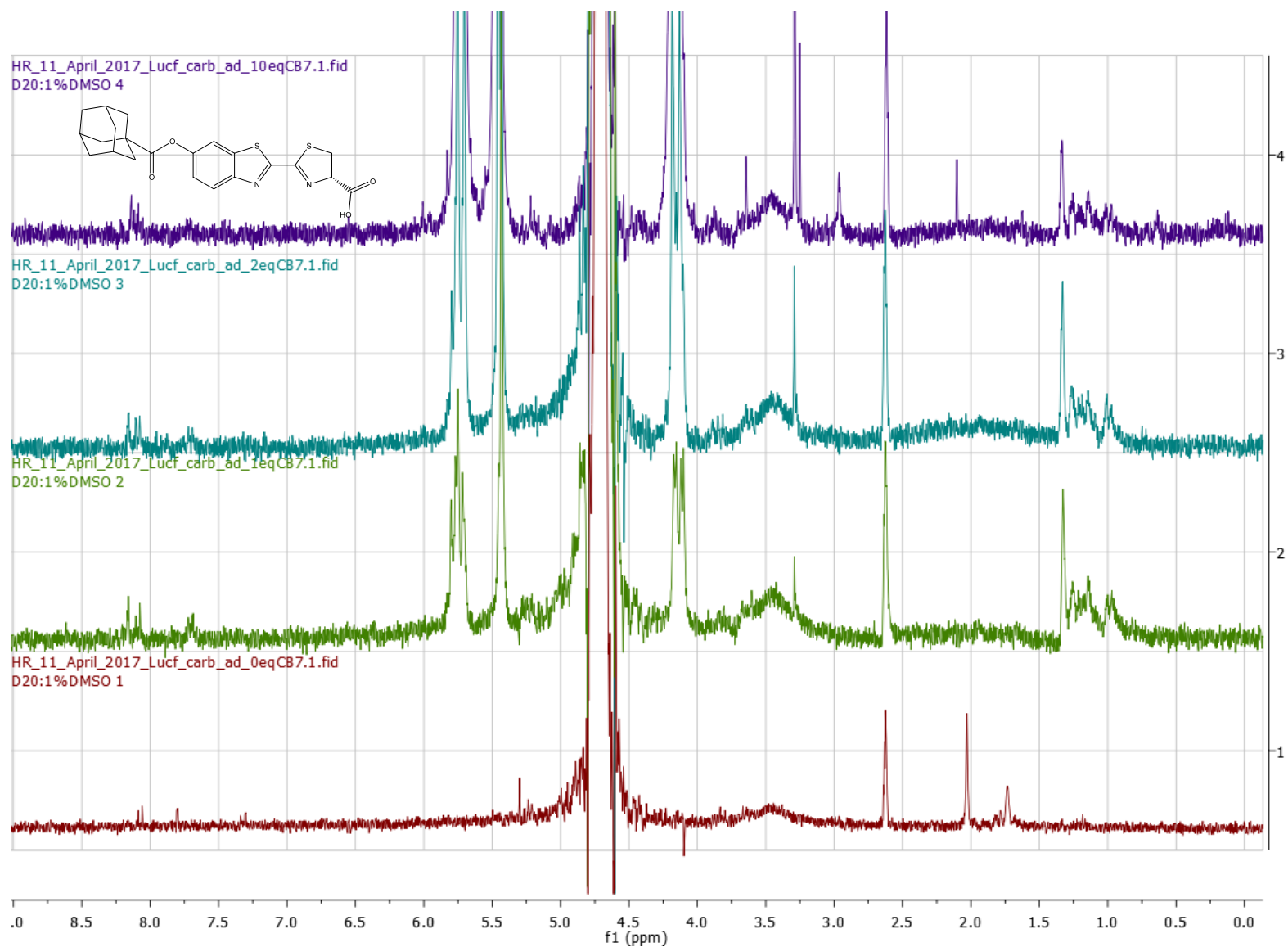
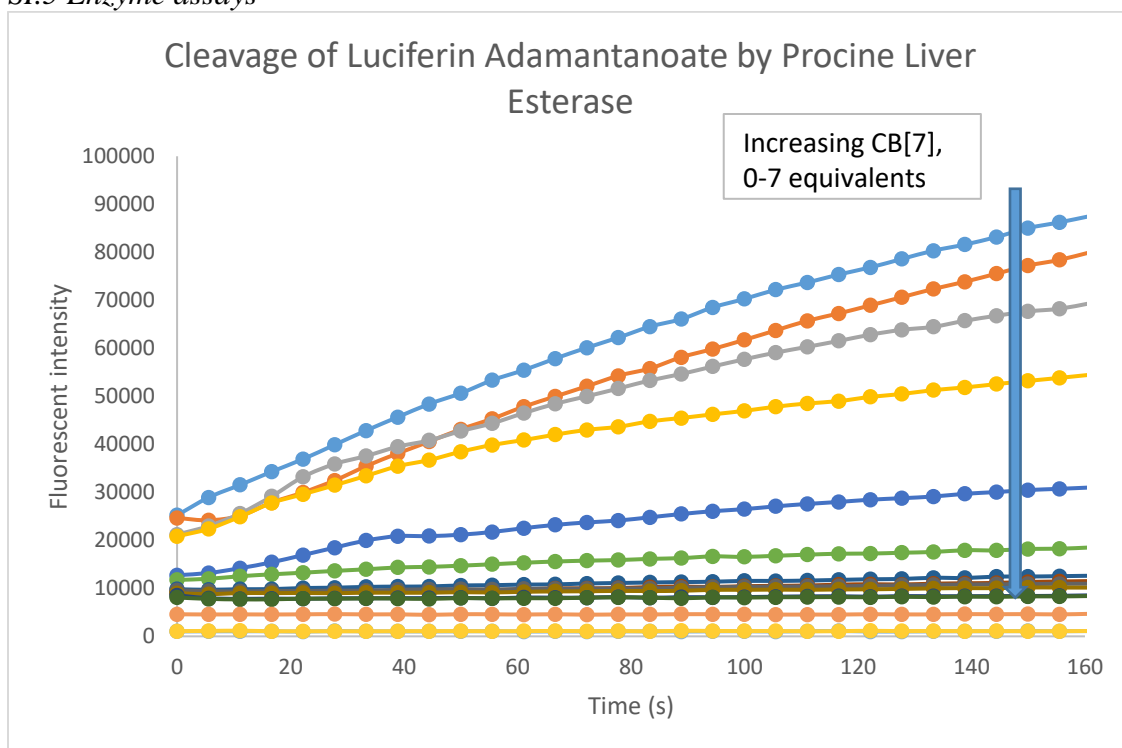
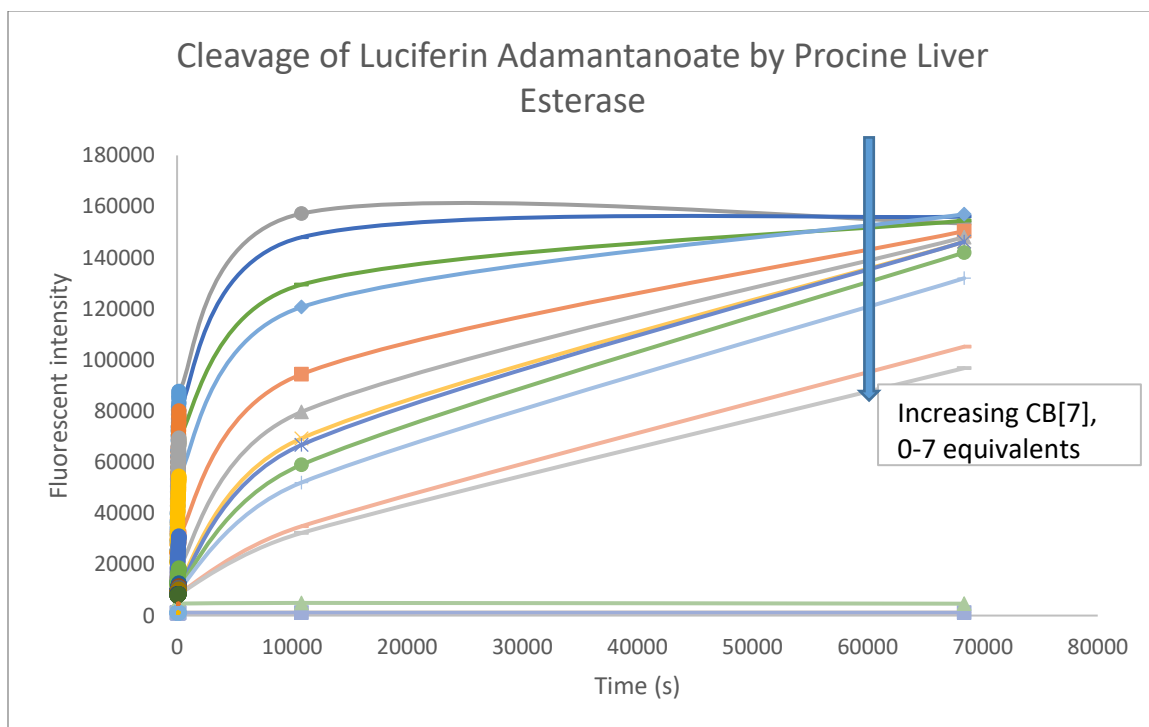


Figure: Raw NMR of luciferin-adamantanoate in D<sub>2</sub>O (no peak-picking software used for processing): 1% d<sub>6</sub>-DMSO titrated with 0, 1, 2, 10 equivalents of CB[7] (increasing vertical displacement in the figure). Concentration of luciferin-adamantanoate(**XII**) is 0.167 mmol

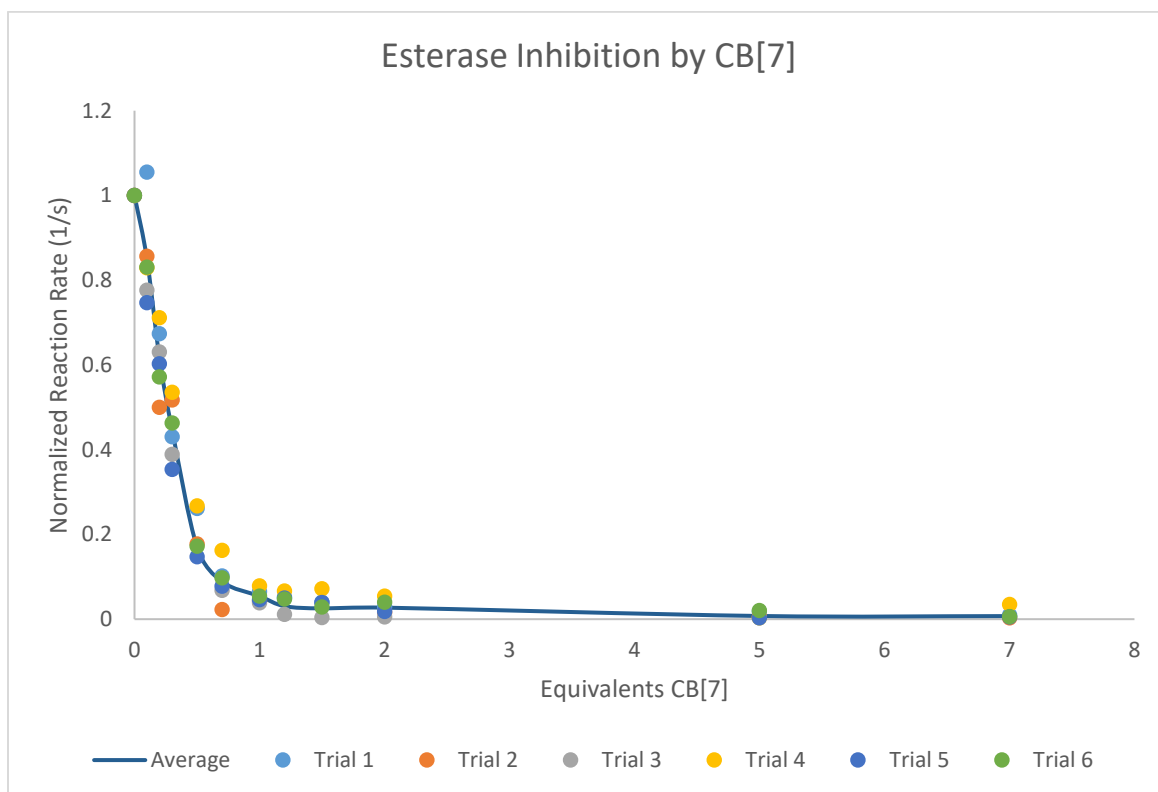
## SI.5 Enzyme assays



*Trial 1: Short term kinetics for analysis of reaction rate. Luciferin adamantanoate is cleaved to luciferin and this is monitored by fluorescence using a platereader.*

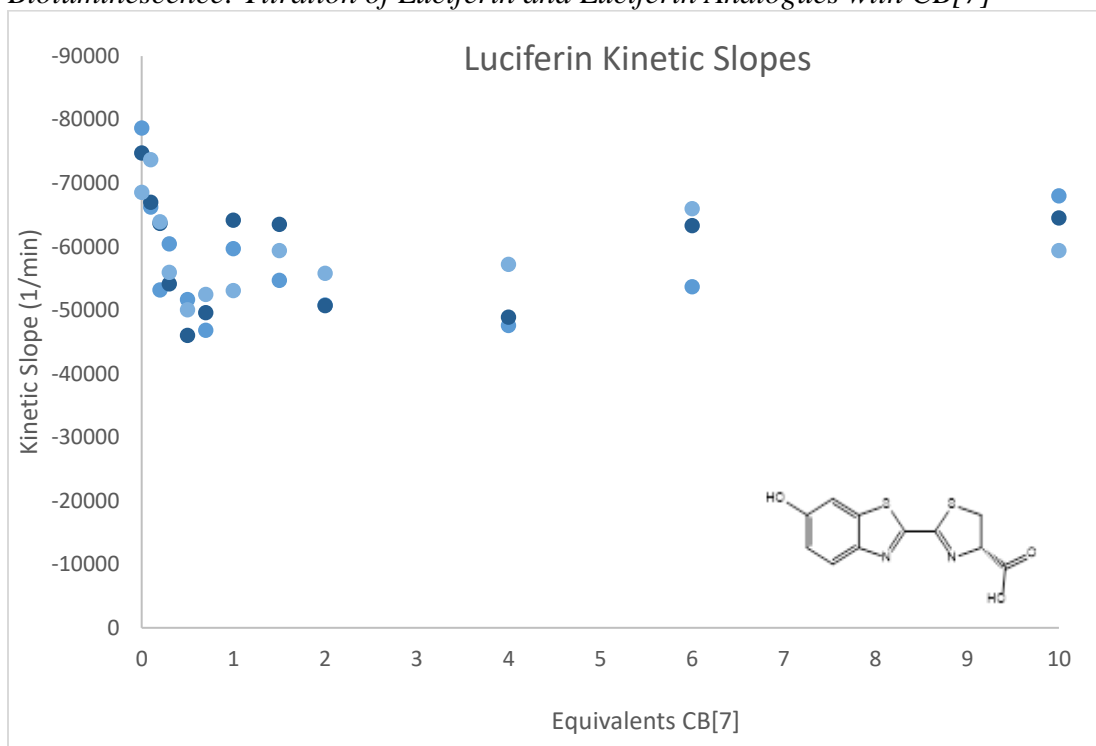


*Trial 1: Long term kinetics for analysis of stability of host-guest complex. Luciferin adamantanoate is cleaved to luciferin and this is monitored by fluorescence using a platereader. Plate was allowed to sit, covered, for 19 hours.*

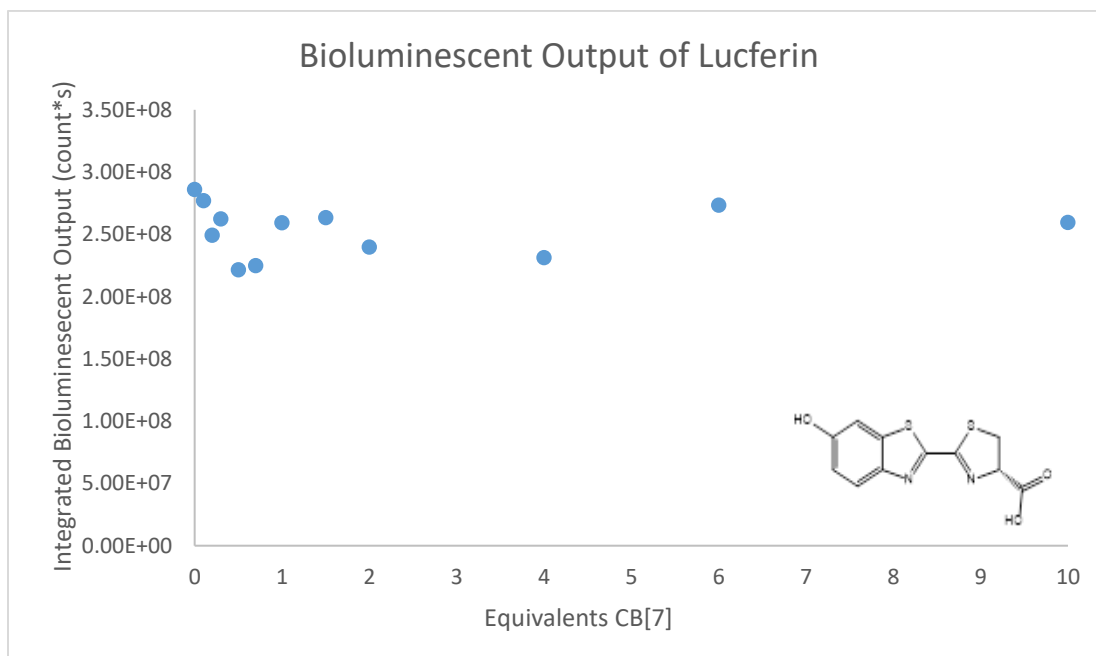


*Relative reaction rate of luciferin-adamantanoate cleavage by porcine liver esterase as the concentration of CB[7] increases in solution. Assay is described in section 3.4, page 43*

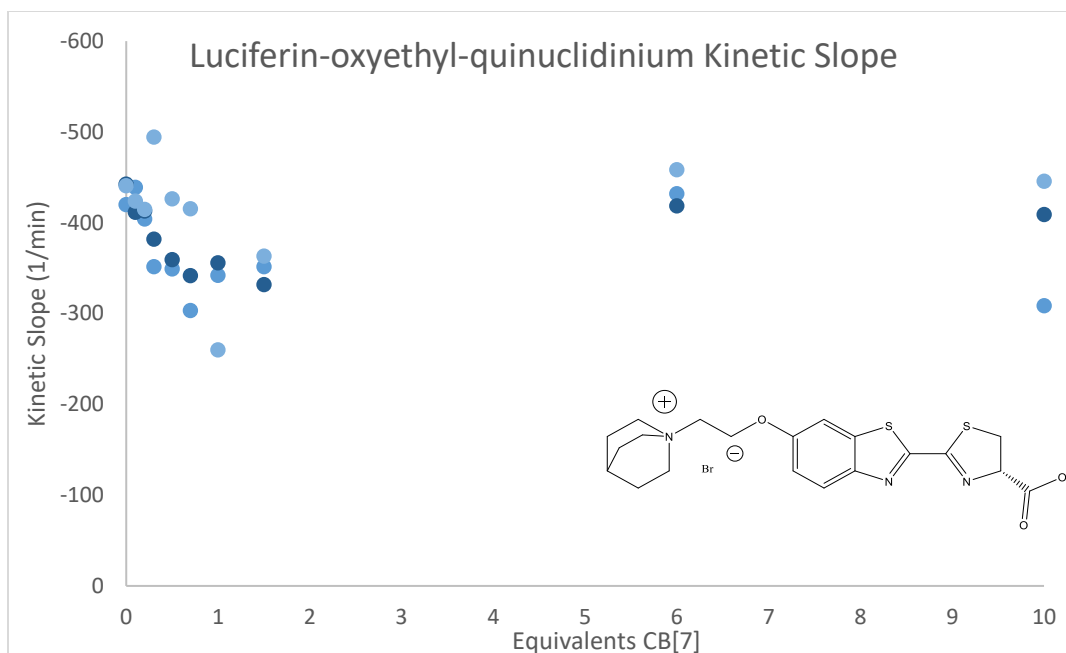
*Bioluminescence: Titration of Luciferin and Luciferin Analogues with CB[7]*



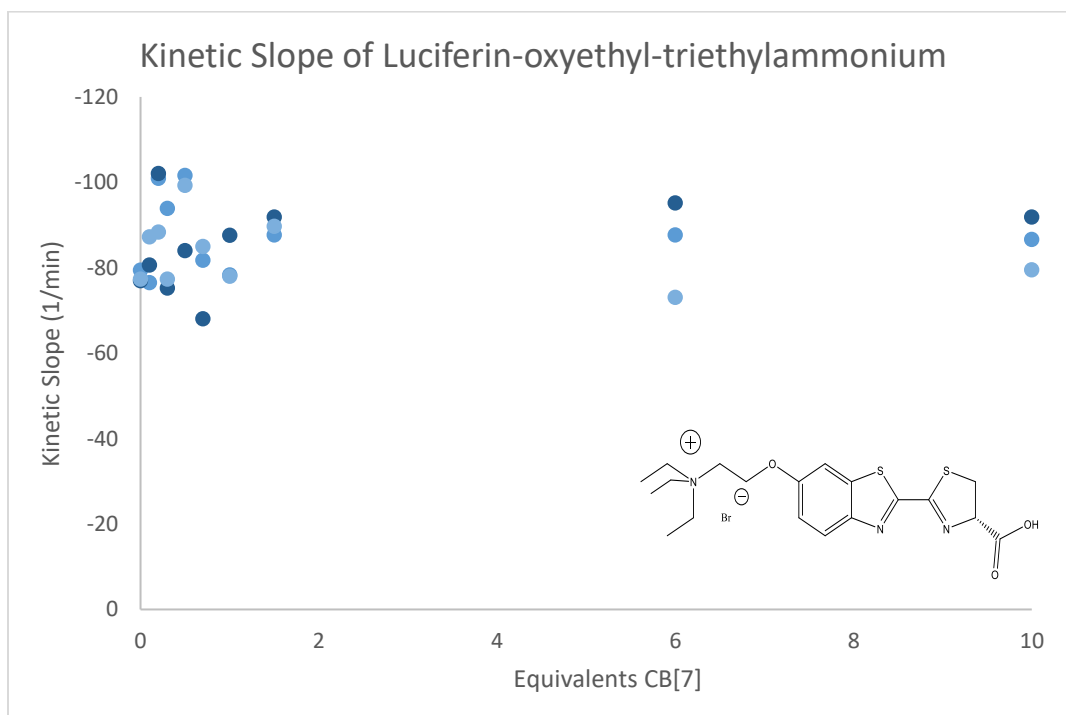
*Kinetic slopes across 3 trials of luciferin with luciferase as measured by bioluminescence over the first 10 minutes of the reaction. CB[7] was titrated into luciferin then ATP was added to start the reaction. Assay is described in section 3.4.*



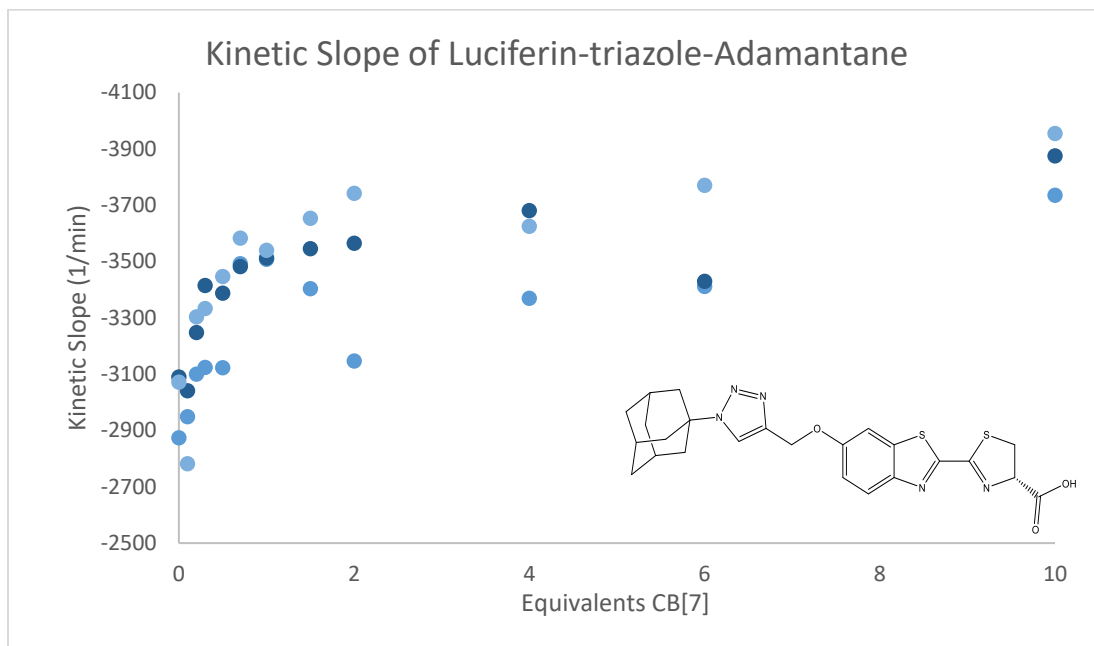
*Bioluminescent output of luciferin over the first 2 minutes of reaction time. There is no significant trend from the titration with CB[7]. Assay is described in section 3.4.*



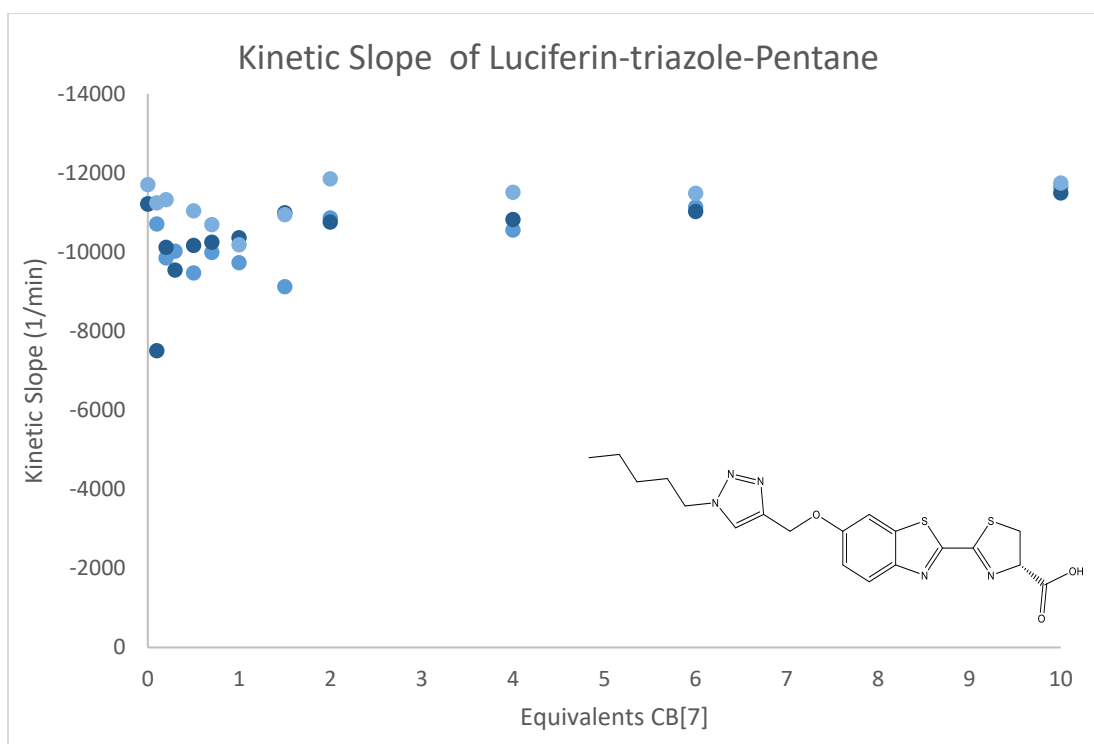
Kinetic slopes across 3 trials of luciferin-oxyethyl-quinuclidinium (**II**) with luciferase as measured by bioluminescence over the first 10 minutes of the reaction. CB[7] was titrated into luciferin-oxyethyl-quinuclidinium (**II**) then ATP was added to start the reaction. Assay is described in section 3.4.



Kinetic slopes across 3 trials of luciferin-oxyethyl-triethylammonium with luciferase as measured by bioluminescence over the first 10 minutes of the reaction. CB[7] was titrated into luciferin-oxyethyl-triethyl-ammonium then ATP was added to start the reaction. Assay is described in section 3.4.

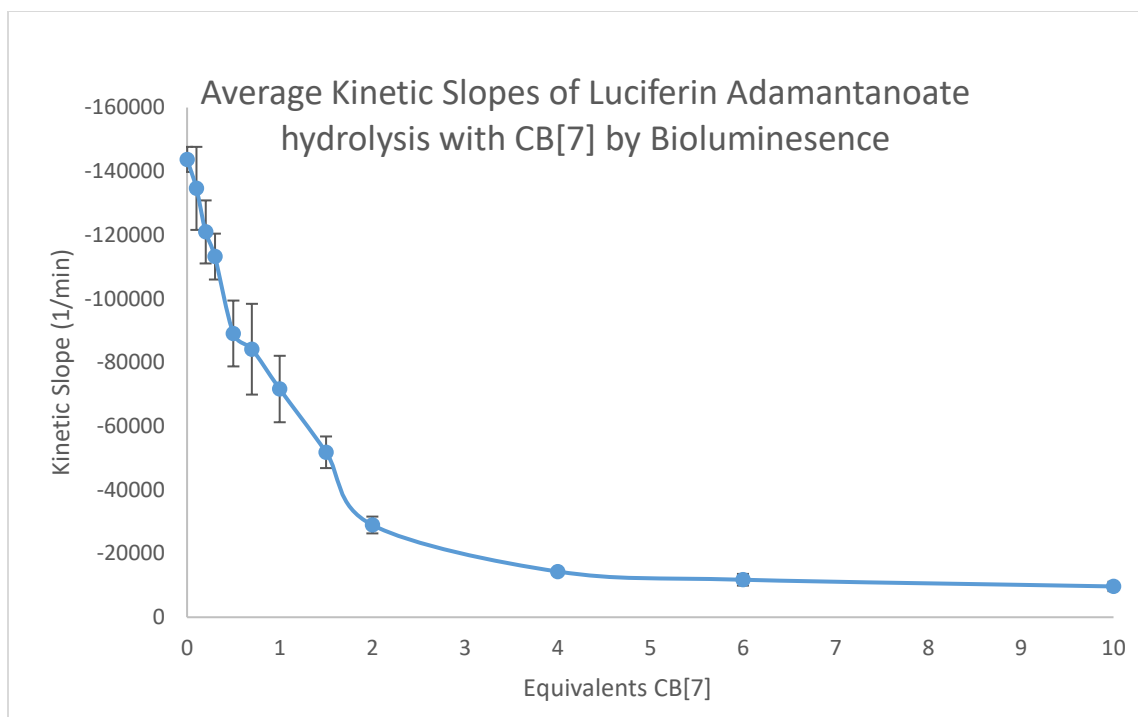


*Kinetic slopes across 3 trials of luciferin-triazole-adamantane with luciferase as measured by bioluminescence over the first 10 minutes of the reaction. CB[7] was titrated into luciferin-triazole-adamantane then ATP was added to start the reaction. Assay is described in section 3.4.*

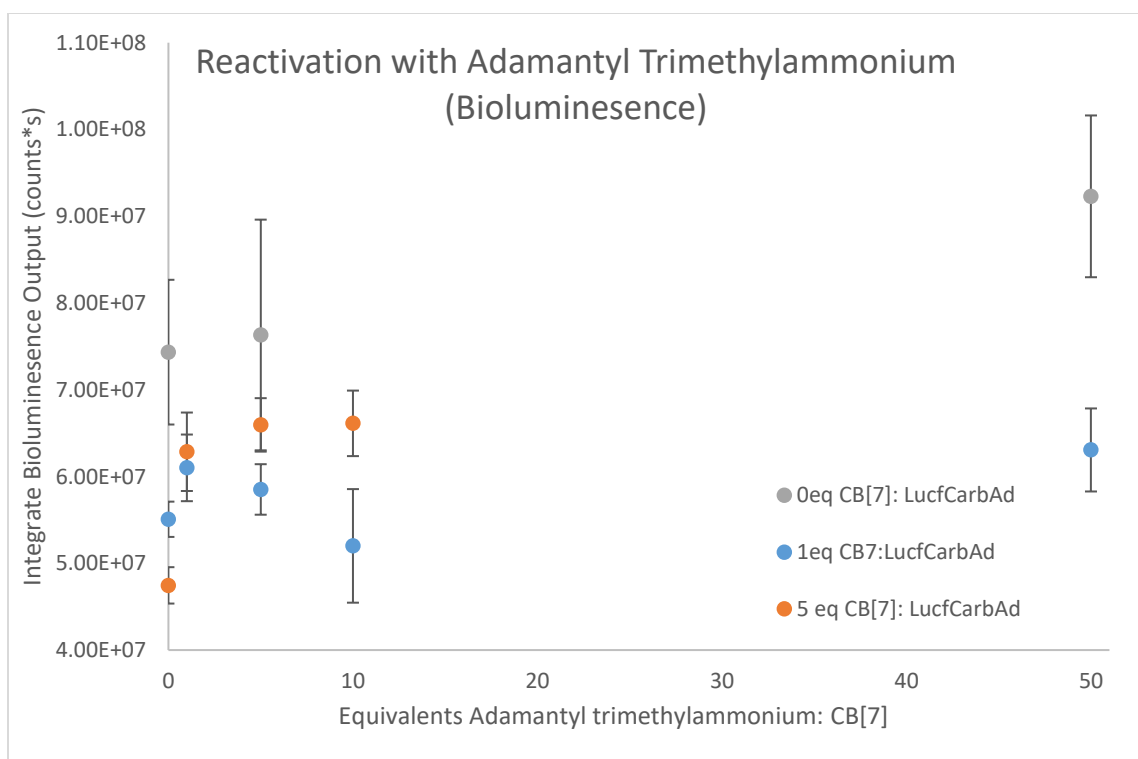


*Kinetic slopes across 3 trials of luciferin-triazole-pentane with luciferase as measured by bioluminescence over the first 10 minutes of the reaction. CB[7] was titrated into luciferin-triazole-pentane then ATP was added to start the reaction. Assay is described in section 3.4.*





As the concentration of CB[7] increases, there is a quick drop in porcine liver esterase activity as determined by the kinetic slope of the luciferin-luciferase reaction. Assay is described in section 3.4.



Integrated bioluminescence as a measure of dissociation of the luciferin-adamantanoate:CB[7] complex after addition of a strong CB[7] binder, adamantyl trimethylammonium. Assay is described in section 3.4.